THE MINOR PLANET BULLETIN

BULLETIN OF THE MINOR PLANETS SECTION OF THE ASSOCIATION OF LUNAR AND PLANETARY OBSERVERS

VOLUME 53, NUMBER 2, A.D. 2026 APRIL-JUNE 93.

ROTATION PERIOD AND LIGHTCURVE ANALYSIS OF 4510 SHAWNA

Alexandra Lombardi
King Kekaulike High School
121 Kula Hwy.
Makawao, HI 96768 USA
alexandralombardi1@icloud.com

James D. Armstrong
University of Hawaii Institute for Astronomy
34 Ohia Ku Street
Pukalani, HI 96768 USA

(Received: 2025 December 2)

Photometric observations of asteroid 4510 Shawna were obtained in October and November of 2024. We found a period of rotation P = 20.1 ± 0.04 h.

4510 Shawna (1930 XK) is a main-belt asteroid which is part of the Vesta family. It has a semi-major axis of 2.36 au and an eccentricity of 0.14. The diameter is estimated to be 6.8 km. It was discovered by Clyde W. Tombaugh on December 13, 1930, at Flagstaff observatory. This asteroid was named in honor of his granddaughter Shawna Willoughby.

CMOS photometric observations of 4510 Shawna were obtained using the Las Cumbres Observatory 0.4-meter network between 2024 October 20 and 2024 November 29. (See Table I.) Observations cover 1.54 rotations, based on the period we determined. The photometry and period analysis were performed using *TychoTracker Pro* (Tycho) Version 12.2. The *Tycho* program performs photometric analysis using standard differential techniques on provided images. The ATLAS catalog (Kostov and Boney, 2017; Tonry et al., 2018) was used as the source of reference stars for this asteroid. The program then uses the magnitude of the reference stars and the asteroid to create a light curve.

SiteId	EncId	MPC Code	# Sessions
coj	clma	Q58	7
cpt	aqwa	L09	12
elp	aqwa	V38	6
lsc	aqwa	W89	14
lsc	aqwb	W79	9
ogg	clma	T03	18
ogg	clma	T04	5
tfn	aqwa	Z14	1
tfn	aqwa	Z17	8
tfn	aqwa	Z21	16

Table I. The SiteId refers a unique identifier for ground-based observation stations. The same site can have different telescopes. EncId refers to a specific enclosure at an observatory and some enclosures can have more than one telescope. An MPC Code is a unique three-digit code provided by the Minor Planet Center that can be used to identify observatories. Each session consisted of roughly 4 images from the same telescope and a red filter was applied in every session.

After constructing the lightcurve, the program performs the least squared fit of modeled magnitudes to photometric magnitudes. The models are constructed with a user defined number of Fourier components. For our analysis we used 3 and 4 components. The program then lists the possible candidate periods found within the span of a user-defined period range and sampling frequency. The Periods and corresponding root mean squared error (RMSE) values are plotted as a periodogram. The best fit between the models and the observations is where the periodogram is a minimum. It is usually the case that a periodogram shows several local minima which are integer multiples of the lowest fit, i.e.

$$t = n * T(1)$$

Where t are the periods of the local minima, T is the fundamental (lowest) frequency, and n is an integer. Usually, the rotational period is the second harmonic (n=2).

Number	Name	yyyy mm/dd	Phase	L_{PAB}	B_{PAB}	Period (h)	P.E.	Amp	A.E	Grp
4510	Shawna	2024 10/20-011/29	15.8,23.7	18	4	20.10	0.04	0.1218	0.0306	401

Table II. Observing circumstances and results. The phase angle is given for the first and last date. L_{PAB} and B_{PAB} are the approximate phase angle bisector longitude/latitude at mid-date range (see Harris et al., 1984). Grp is the asteroid family/group (Warner et al., 2009).

We applied this analysis technique to our observations from 96 observing sessions (383 exposures) obtained using the Las Cumbres Observatory 0.4-meter network of telescopes. The observations were taken between 2024 October 29 and 2024 November 29. Through our analysis, the first three harmonics can be seen in the periodogram shown here. The results are summarized in Table II. We selected P = 20.1±0.04 hours, and A = 0.12±.05 mag. as the best fit to our measurements, with the resulting lightcurve presented here.

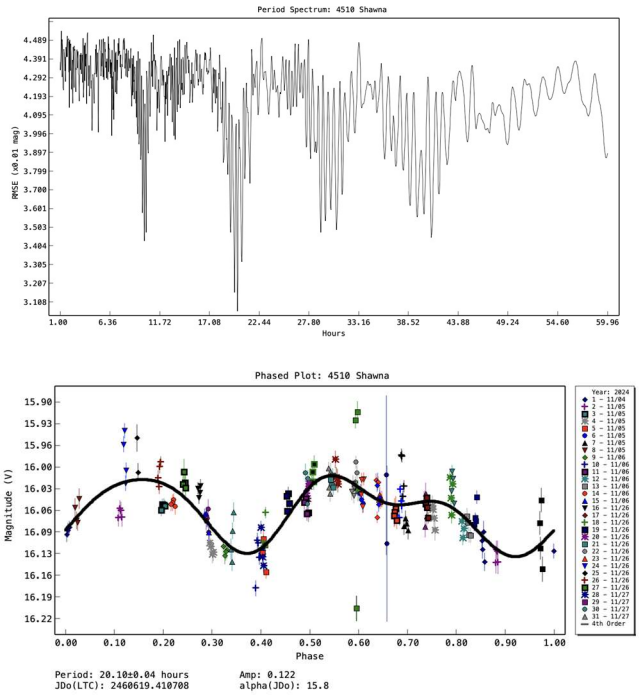

There have been at least two previous attempts at obtaining this asteroid's rotation rate (Berhend, 2017web, 2021web), but they vary from shorter periods (under 15 hours) to longer periods (over 40 hours).

Acknowledgements

Our thanks are extended to Daniel Parrott, author of *TychoTracker Pro*. This work makes use of observations from the Las Cumbres Observatory global telescope network. This work has developed from the University of Hawai'i HI STAR program, which is funded in part by the Department of the Air Force (AFRL) / Space Force (15 SpSS) and Las Cumbres Observatory. This work includes data from the Asteroid Terrestrial-impact Last Alert System (ATLAS) project. ATLAS is primarily funded to search for near earth asteroids through NASA grants NN12AR55G, 80NSSC18K0284, and 80NSSC18K1575; by products of the NEO search include images and catalogs from the survey area. The ATLAS science products have been made possible through the contributions of the University of Hawaii Institute for Astronomy, the Queen's University Belfast, the Space Telescope Science Institute, and the South African Astronomical Observatory. This work uses data obtained from the Asteroid Lightcurve Data Exchange Format (ALCDEF) database, which is supported by funding from NASA grant 80NSSC18K0851. We would like to thank Wayne Hawley for his help and guidance.

References

Behrend, R. (2017web, 2021web). Observatoire de Geneve web site. *https://www.astro.unige.ch/~behrend/page5cou.html#004583*

Harris, A.W.; Young, J.W.; Scaltriti, F.; Zappala, V. (1984). "Lightcurves and phase relations of the asteroids 82 Alkmene and 444 Gyptis." *Icarus* **57**, 251-258.

JPL (2023). Small-Body Database Lookup. *https://ssd.jpl.nasa.gov/tools/sbdb_lookup.html*

Kostov, A.; Bonev, T. (2017). "Transformation of Pan-STARRS1 gri to Stetson BVRI magnitudes. Photometry of small bodies observations." *Bulgarian Astron. J.* **28**, 3 (ArXiv:1706.06147v2).

Tonry, J.L.; Denneau, L.; Flewelling, H.; Heinze, A.N.; Onken, C.A.; Smartt, S.J.; Stadler, B.; Weiland, H.J.; Wolf, C. (2018). "The ATLAS All-Sky Stellar Reference Catalog." *Ap. J.* **867**, A105.

Warner, B.D.; Harris, A.W.; Pravec, P. (2009). "The Asteroid Lightcurve Database." *Icarus* **202**, 134-146. Updated 2023 Oct. 1. *http://www.MinorPlanet.info/php/lcdb.phpA105*

ROTATION PERIOD AND A NEW DENSE LIGHTCURVE OF 168 SIBYLLA

Frederick Pilcher
Organ Mesa Observatory (G50)
4438 Organ Mesa Loop
Las Cruces, NM 88011 USA
fpilcher35@gmail.com

Vladimir Benishek
Belgrade Astronomical Observatory
Volgina 7, 11060 Belgrade 38, SERBIA

(Received: 2025 November 18)

Photometric lightcurves of minor planet 168 Sibylla 2025 Aug. 26 - Nov. 9 show a synodic rotation period 47.016 ± 0.002 h, amplitude 0.18 ± 0.01 mag with an asymmetric and somewhat irregular bimodal lightcurve.

Authors Pilcher and Benishek agreed to collaborate to obtain a dense photometric lightcurve of 168 Sibylla with full phase coverage.

Observations by Pilcher were made at the Organ Mesa Observatory with a Meade 35-cm LX200 GPS Schmidt-Cassegrain, SBIG STL-1001E CCD, 30 second exposures, unguided, clear filter. Observations by Benishek were made at the Sopot Astronomical Observatory with a Meade 35-cm LX200GPS Schmidt-Cassegrain, SBIG ST-10 XME CCD, 20, 30, and 45 second exposures depending upon the brightness of the target, unfiltered, unguided.

Image measurement and lightcurve construction were with *MPO Canopus* software with calibration star magnitudes for solar colored stars from the CMC15 catalog reduced to the Cousins R band. Zero-point adjustments of a few × 0.01 magnitude were made for best fit. To reduce the number of data points on the lightcurve and make them easier to read, data points have been binned in sets of 3 with maximum time difference 5 minutes.

168 Sibylla. Warner et al. (2009) cite previous synodic period measurements of 168 Sibylla by di Martino et al. (1994), 23.82 hours; and by Pilcher et al. (2008), 47.009 hours. A sidereal period determined entirely from sparse data, by Durech et al. (2020) is 47.015 hours. A total of 25 sessions obtained 2025 Aug. 26 - Nov. 9 by the two authors combined provide a dense asymmetric and somewhat irregular bimodal lightcurve, with full phase coverage, and a synodic period of 47.016 ± 0.002 h, amplitude 0.18 ± 0.01 mag. This result is in excellent agreement with Pilcher et al. (2008) and Durech et al. (2020). The 23.82-hour period by di Martino et al. can now be rejected.

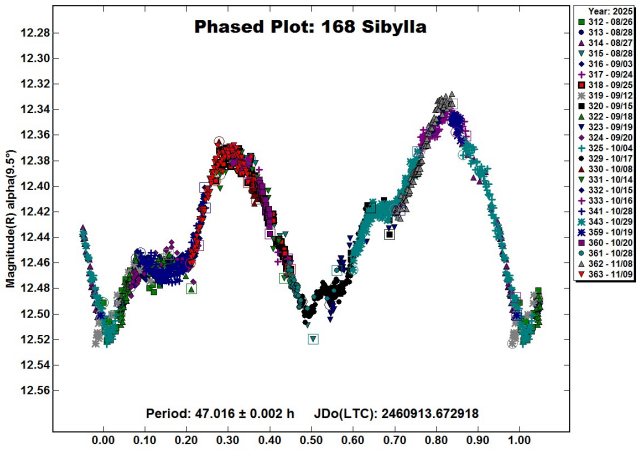

References

di Martino, M.; Blanco, C.; Riccioli, D.; de Sanctis, G. (1994). "Lightcurves and rotational periods of nine main belt asteroids." *Icarus* **107**, 269-275.

Durech, J.; Tonry, J.; Erasmus, N.; Denneau, L.; Henize, A.N.; Flewelling, H.; Vanco, R. (2020). "Asteroid models reconstructed from ATLAS photometry." *Astron. Astrophys.* **643**, A59.

Harris, A.W.; Young, J.W.; Scaltriti, F.; Zappala, V. (1984). "Lightcurves and phase relations of the asteroids 82 Alkmene and 444 Gyptis." *Icarus* **57**, 251-258.

Pilcher, F.; Benishek, V.; Brinsfield, J.W. (2008). "Period determination for 168 Sibylla: A collaboration triumph." *Minor Planet Bull.* **35**, 104-105.

Warner, B.D.; Harris, A.W.; Pravec, P. (2009). "The Asteroid Lightcurve Database." *Icarus* **202**, 134-146. Updated 2023 Oct. *https://minplanobs.org/MPInfo/php/lcdb.php*

Number	Name	2025/mm/dd	Phase	L_{PAB}	B_{PAB}	Period(h)	P.E	Amp	A.E.
168	Sibylla	08/26-11/09	* 9.6, 14.7	359	2	47.016	0.002	0.18	0.01

Table I. Observing circumstances and results. The phase angle is given for the first and last date, except that a * denotes a minimum was reached between these dates. L_{PAB} and B_{PAB} are the approximate phase angle bisector longitude and latitude at mid-date range (see Harris et al., 1984).

NEW LIGHTCURVES AND A TENTATIVE ROTATION PERIOD OF TUMBLING ASTEROID 571 DULCINEA

Frederick Pilcher
Organ Mesa Observatory (G50)
4438 Organ Mesa Loop
Las Cruces, NM 88011 USA
fpilcher35@gmail.com

Jesús Delgado Casal
Observatorio Nuevos Horizontes (Z73)
Camas (Sevilla - SPAIN) CP 41900

Esteban Reina Lorenz
Av. Can Marcel, 41
087863 Masquefa (Barcelona - SPAIN)

Petr Pravec
petr.pravec@asu.cas.cz

(Received: 2026 January 15)

We find for tumbling asteroid 571 Dulcinea a principal rotation period of 190 ± 1 hours with a second period too close to commensurate to be separately found. The full lightcurve amplitude is 0.7 magnitudes.

According to "The Asteroid Lightcurve Database," (Warner et al., 2009), only one paper on the rotational parameters of 571 Dulcinea has been previously published. Stephens (2011), on the basis of 18 sessions 2010 Nov. 2 - Dec. 4, found a principal period of 126.3 hours and included a lightcurve with great scatter between sessions. He added a note reported by P. Pravec: "A second period cannot be uniquely determined from the available data."

The observations by Pilcher to produce the results reported in this paper were made at the Organ Mesa Observatory with a Meade 35-cm LX200 GPS Schmidt-Cassegrain, SBIG STL-1001E CCD, 60 to 120 second exposures, unguided, clear filter. Observations by Delgado are with an 11-inch Celestron Schmidt-Cassegrain, Atik 4.14 EX CCD, 60 to 120 second exposures. Observations by Lorenz are with a Meade Classic 10-inch Schmidt-Cassegrain, ZWO ASI 294 MM Pro CMOS camera, 120 second exposures, Cousins R filter, images obtained using parallel guiding. For image measurement and lightcurve construction, the authors used *MPO Canopus* software with calibration star magnitudes for solar colored stars from the CMC15 catalog reduced to the Cousins R band.

Observing circumstances were especially favorable for northern hemisphere observers. Asteroid 571 Dulcinea was at declination near +31 degrees. Long nights enabled most of the sessions to be 7 to more than 10 hours duration. A fortuitous long spell of weather occurred in the southwest desert of the USA that was unusually clear even by the standards of the region. These many clear nights enabled first author Pilcher to obtain 50 sessions. With another 18 sessions by Delgado and Lorenz from Spain, the three observers combined obtained 68 sessions, with a total of 24874 measurable data points, in the interval 2025 Oct. 19 - 2026 Jan. 6.

Large amplitude tumbling was confirmed very early in the campaign, as no reasonable adjustment of zero points produced a good fit. Hence no attempt was made at adjustment. With the use of *MPO Canopus* software for single period examination, trial lightcurves for all possible periods between 50 hours and 550 hours were examined and a period spectrum plotted (Figure 1). A deep minimum occurs near 190 hours, and a single period lightcurve was plotted (Figure 2) to a period of 190 hours, amplitude near 0.7 magnitudes. There is a good fit in slopes of segments at corresponding phases in the cycle, but there are magnitude discords up to 0.3. These discords are much too great to be realistically explained by catalog errors and CCD response differences. They can only be caused by tumbling of the target. We also include raw plots for the intervals 2025-10-19 to 2025-11-05 (Figure 3), 2025-11-10 to 2025-12-02 (Figure 4), and 2025-12-07 to 2026-01-06 (Figure 5).

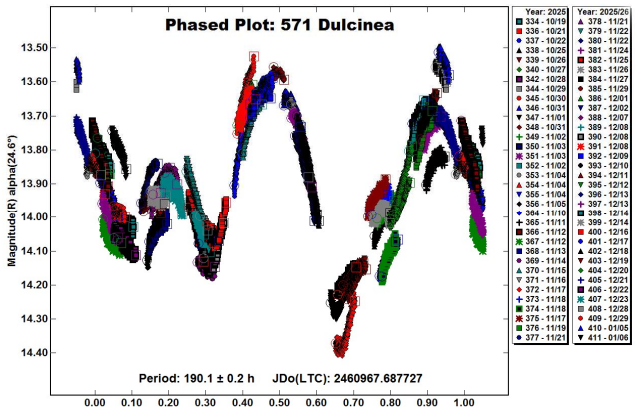

Figure 1. The single period lightcurve of 571 Dulcinea phased to 190 hours.

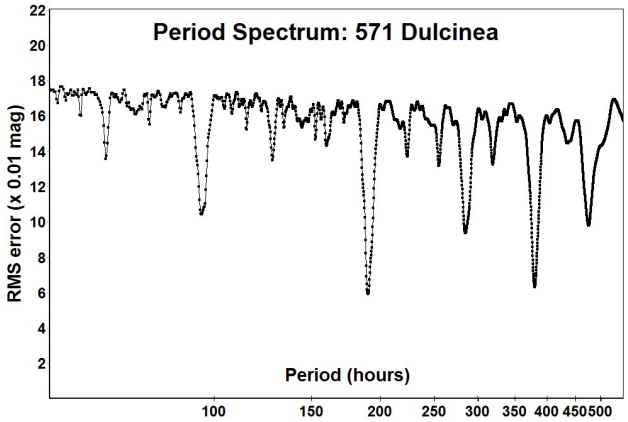

Figure 2. The period spectrum for 571 Dulcinea between 50 and 550 hours.

Number	Name	yyyy/mm/dd	Phase	L_{PAB}	B_{PAB}	Period(h)	P.E	Amp	A.E.
571	Dulcinea	2025/10/19-2026/01/06	*24.5 - 19.5	70	+7	190	1	0.7	0.1

Table I. Observing circumstances and results. The phase angle is given for the first and last date, unless a minimum (second value) was reached. L_{PAB} and B_{PAB} are the approximate phase angle bisector longitude and latitude at mid-date range (see Harris et al., 1984).

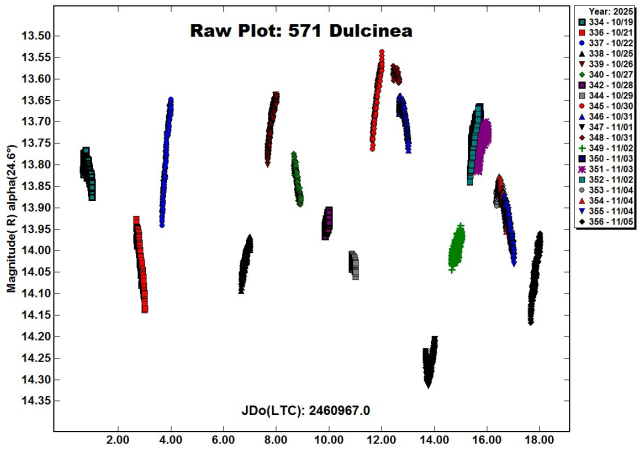

Figure 3. The raw lightcurve of 571 Dulcinea 2025 Oct. 19 to Nov. 5.

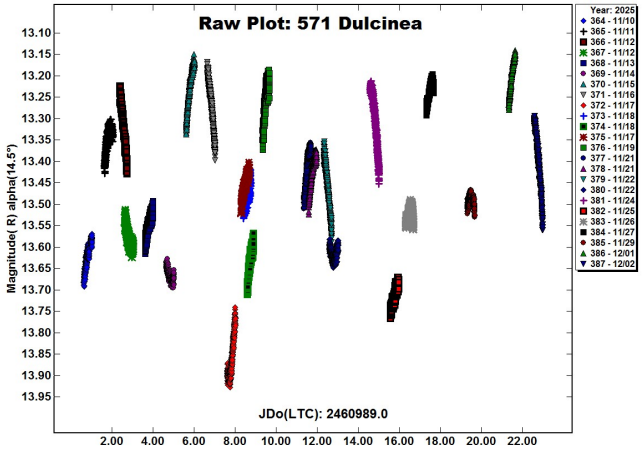

Figure 4. The raw lightcurve of 571 Dulcinea 2025 Nov. 10 to Dec. 2.

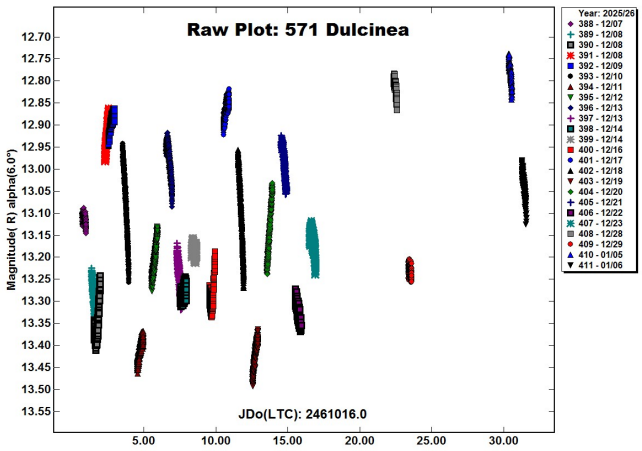

Figure 5. The raw lightcurve of 571 Dulcinea 2025 Dec. 7 to 2026 Jan. 6.

Co-author Pravec used custom software which includes terms for the sums and differences of primary rotation frequency f1 and tumbling frequency f2, as well as for the two separate frequencies, using the 2-period Fourier series method (Pravec et al., 2005, 2014). This analysis of the complete data set shows that (571) is clearly a tumbler, but there is only one predominating period detected: 189.9 h (realistic error about 1 h). The error of ± 0.2 hours quoted in Figure 2 is formal and a realistic error is ± 1 hours. The second period is not well resolved. However, the shape and character of the lightcurve suggest that the second period is actually very close to a commensurability with the main period. (It happens probably by chance only; there is probably no physical significance in the period commensurability.) In other words, the ratio P1/P2 seems to be close to n/m, where n and m are low integers. In such case, solution for P2 is degenerate and it cannot be formally resolved from the main period and its harmonics. And, the period 126.3 h suggested by Stephens (2011) is 2/3 of the main period, apparently also an effect of the period commensurability.

References

Harris, A.W.; Young, J.W.; Scaltriti, F.; Zappala, V. (1984). "Lightcurves and phase relations of the asteroids 82 Alkmene and 444 Gyptis." *Icarus* **57**, 251-258.

Pravec, P. Harris, A.W.; Scheirich, P.; Kušnirák, P.; Šarounová, L.; Hergenrother, C.W.; Mottola, S.; Hicks, M.D.; Masi, G.; Krugly, Yu N.; Shevchenko, V.G.; Nolan, M.C.; Howell, E.S.; Kaasalainen, M.; Galád, A.; Brown, P.; DeGraff, D.R.; Lambert, J.V.; Cooney, W.R.; Foglia, S. (2005). "Tumbling asteroids." *Icarus* **173**, 108-131.

Pravec, P.; Scheirich, P.; Ďurech, J.; Pollock, J.; Kušnirák, P.; Hornoch, K.; Galád, A.; Vokrouhlický, D.; Harris, A.W.; Jehin, E.; Manfroid, J.; Opitom, C.; Gillon, M.; Colas, F.; Oey, J.; Vraštil, J.; Reichart, D.; Ivarsen, K.; Haislip, J.; LaCluyze, A. (2014). "The tumbling spin state of (99942) Apophis." *Icarus* **233**, 48-60.

Stephens, R.D. (2011), "Asteroids observed from GMARS and Santana Observatories: 2010 October - December." *Minor Planet Bull.* **38**, 115.

Warner, B.D.; Harris, A.W.; Pravec, P. (2009). "The Asteroid Lightcurve Database." *Icarus* **202**, 134-146. Updated 2023 Oct. *http://www.minorplanet.info/lightcurvedatabase.html*

ROTATION PERIOD AND A NEW DENSE LIGHTCURVE OF 702 ALAUDA

Frederick Pilcher
Organ Mesa Observatory (G50)
4438 Organ Mesa Loop
Las Cruces, NM 88011 USA
fpilcher35@gmail.com

(Received: 2025 November 11)

Minor planet 702 Alauda has a synodic rotation period 16.706 ± 0.001 h, amplitude 0.12 ± 0.01 mag with a somewhat irregular and asymmetric bimodal lightcurve.

Observations to produce the results reported in this paper were made at the Organ Mesa Observatory with a Meade 35-cm LX200 GPS Schmidt-Cassegrain, SBIG STL-1001E CCD, 30 second exposures, unguided, clear filter. Image measurement and lightcurve construction were with *MPO Canopus* software with calibration star magnitudes for solar colored stars from the CMC15 catalog reduced to the Cousins R band. Zero-point adjustments of a few × 0.01 magnitude were made for best fit. To reduce the number of data points on the lightcurve and make them easier to read, data points have been binned in sets of 3 with maximum time difference 5 minutes.

702 Alauda. Many measurements of the rotation period of 702 Alauda have been reported in the literature (Warner et al., 2009). All of them are near 8.35 hours, or twice that value, 16.7 hours. Papers reporting the shorter period are by Harris and Young (1983), 8.36 hours; Fauerbach and Bennett (2005), 8.348 hours; Benishek and Protitch-Benishek (2009), 8.3589 hours; Alkema (2014), 8.3531 hours; and Polakis (2020), 8.333 hours. Papers reporting the longer period are by Behrend (2009web) 16.7044 hours; Behrend (2014web), 16.7027 hours; Behrend (2019web), 16.7072 hours; Polakis (2021), 16.65 hours; Colazo et al. (2022), 16.7 hours; and Behrend (2023web), 16.686 hours.

The goals of this investigation were to find which of these two possible periods is the correct one and continue observations for several weeks to obtain a rotation period whose value is both secure and accurate. Both goals were achieved. Observations on six nights 2025 Oct. 5 - Nov. 7 provide a good fit to a somewhat irregular and asymmetric bimodal lightcurve with period 16.706 ± 0.001 hours, amplitude 0.12 ± 0.01 magnitudes. The split halves version of the lightcurve phased to 16.706 hours shows that the asymmetry of the two halves greatly exceeds the scatter of data points. A period of 16.706 hours may be considered secure.

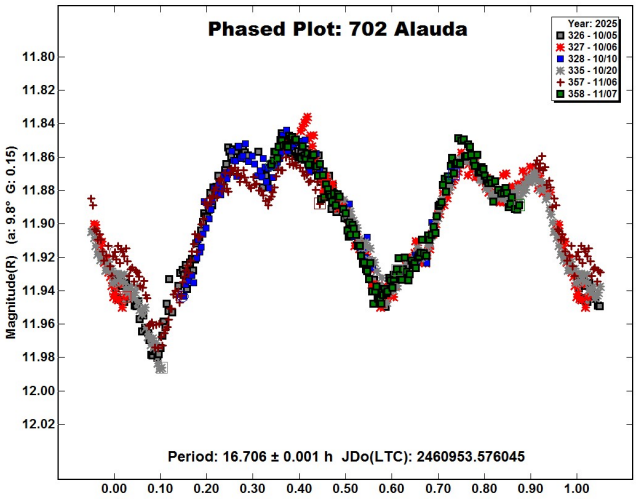

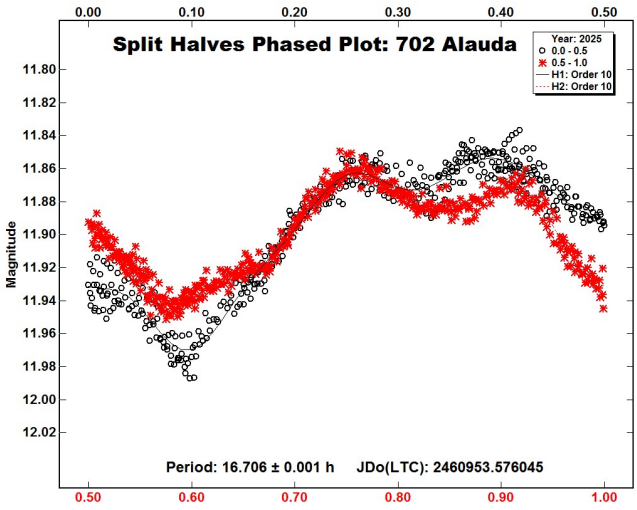

References

Alkema, M.S. (2014). "Asteroid lightcurve analysis at Elephant Head Observaory: 2013 October-December." *Minor Planet Bull.* **41**, 186-187.

Behrend, R. (2009, 2014, 2019, 2023). Observatoire de Geneve web site. *http://obswww.unige.ch/~behrend/page_cou.html*

Benishek, V.; Protitch-Benishek, V. (2008). "CCD photometry of seven asteroids at the Belgrade Astronomical Observatory." *Minor Planet Bull.* **35**, 28-30.

Number	Name	2025/mm/dd	Phase	L_{PAB}	B_{PAB}	Period(h)	P.E	Amp	A.E.
702	Alauda	10/05-11/07	* 9.8, 10.5	25	25	16.706	0.001	0.12	0.01

Table I. Observing circumstances and results. The phase angle is given for the first and last date, except that a * denotes a minimum was reached between these dates. L_{PAB} and B_{PAB} are the approximate phase angle bisector longitude and latitude at mid-date range (see Harris et al., 1984).

Colazo, M.; Monteleone, B.; Santos, F.; Morales, M.; García, A.; Suárez, N.; Altuna, L.; Caballero, M; Romero, F.; Speranza, T.; Bellocchio, E.; Santucho, M.; Fornari, C.; Melia, R.; Stechina, A.; Scotta, D.; Arias, N.; Chapman, A.; Ciancia, G.; Wilberger, A.; Anzola, M.; Mottino, A.; Colazo. C. (2022). "Asteroid photometry and lightcurve results for seven asteroids." *Minor Planet Bull.* **49**, 189-192.

Fauerbach, M.; Bennett, T. (2005). "Photometric lightcurve observations of 125 Liberatrix, 218 Bianca, 423 Diotima, 702 Alauda, 1963 Bezovec, and (5840) 1990 HF1." *Minor Planet Bull.* **32**, 80-81.

Harris, A.W.; Young, J.W. (1983). "Asteroid Rotation. IV." *Icarus* **54**, 59-109.

Harris, A.W.; Young, J.W.; Scaltriti, F.; Zappala, V. (1984). "Lightcurves and phase relations of the asteroids 82 Alkmene and 444 Gyptis." *Icarus* **57**, 251-258.

Polakis, T. (2020). "Photometric observations of twenty-three minor planets." *Minor Planet Bull.* **47**, 94-101.

Polakis, T. (2021). "Period determinations for twenty minor planets." *Minor Planet Bull.* **48**, 239-245.

Warner, B.D.; Harris, A.W.; Pravec, P. (2009). "The Asteroid Lightcurve Database." *Icarus* **202**, 134-146. Updated 2023 Oct. *https://minplanobs.org/MPInfo/php/lcdb.php*

PHOTOMETRIC OBSERVATIONS OF ASTEROIDS 2484 PARENAGO, 3807 PAGELS, AND 7631 VOKROUHLICKY

Alessandro Marchini, Riccardo Papini
Astronomical Observatory, University of Siena (K54)
Via Roma 56, 53100 - Siena, ITALY
marchini@unisi.it

Tommaso Iozia
Department of Information Engineering and Mathematics,
University of Siena, Siena, ITALY

(Received: 2026 January 15)

Photometric observations of three main-belt asteroids were conducted to verify or determine their synodic rotation periods. For 2484 Parenago, we found P = 3.430 ± 0.002 h with A = 0.38 ± 0.04 mag. For 3807 Pagels, we found P = 3.287 ± 0.001 h with A = 0.10 ± 0.02 mag. For 7631 Vokrouhlicky, we present a preliminary solution with P = 75.24 ± 0.24 h with A = 0.56 ± 0.05 mag.

CCD photometric observations of three main-belt asteroids were carried out in 2025 October-December at the Astronomical Observatory of the University of Siena (K54). We used a 0.30-m *f*/5.6 Maksutov-Cassegrain telescope and SBIG STL-6303E NABG CCD camera; the pixel scale was 2.30 arcsec when binned at 2×2 pixels. We used a Clear filter and 300 seconds of exposure time.

Data processing and analysis were done with *MPO Canopus* (Warner, 2018). All images were calibrated with dark and flat-field frames and the instrumental magnitudes converted to R magnitudes using solar-colored field stars from a version of the CMC-15 catalogue distributed with *MPO Canopus*. Table I shows the observing circumstances and results.

A search through the asteroid lightcurve database (LCDB; Warner et al., 2009) indicates that our result may be the first reported lightcurve observations and results for 7631 Vokrouhlicky.

2484 Parenago (1928 TK) was discovered by G.N. Neujmin at Simeis on 1928 October 7 and named in memory of Pavel Petrovich Parenago (1906-1960), a professor at Moscow University, a corresponding member of the U.S.S.R. Academy of Sciences and the founder of the Moscow school of stellar astronomy. It is an inner main-belt asteroid with a semi-major axis of 2.343 AU, eccentricity 0.254, inclination 1.201°, and an orbital period of 3.59 years. Its absolute magnitude is H = 13.27 (JPL, 2026). The NEOWISE satellite infrared radiometry survey (Meinzer et al., 2019) found a diameter D = 6.266 ± 0.249 km using an absolute magnitude H = 14.0 and a geometric albedo of p_V = 0.113.

Number	Name	2025/mm/dd	Phase	L_{PAB}	B_{PAB}	Period(h)	P.E.	Amp	A.E.	Grp
2484	Parenago	11/28-11/30	1.3,2.1	65	-1	3.430	0.002	0.38	0.04	MB-I
3807	Pagels	10/10-10/16	2.4,5.1	15	-4	3.287	0.001	0.10	0.02	FLO
7631	Vokrouhlicky	12/26-12/30	4.0,5.4	92	-4	75.24	0.24	0.56	0.05	MB-I

Table I. Observing circumstances and results. The phase angle is given for the first and last date. If preceded by an asterisk, the phase angle reached an extremum during the period. L_{PAB} and B_{PAB} are the approximate phase angle bisector longitude/latitude at mid-date range (see Harris et al., 1984). Grp is the asteroid family/group (Warner et al., 2009).

Observations were conducted over two nights and collected 168 data points. The period analysis confirms a rotational period of P = 3.430 ± 0.002 h with an amplitude A = 0.38 ± 0.04 mag, in agreement with the result found by the same authors in 2014 (Marchini et al., 2015) and the previously results published in the LCDB (Behrend, 2014web; Pravec et al., 2014web).

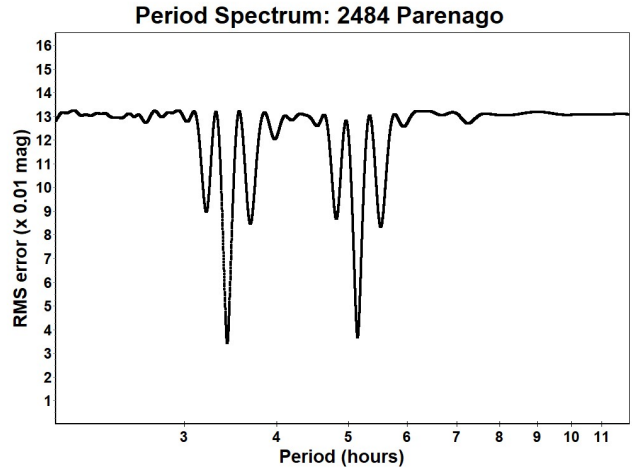

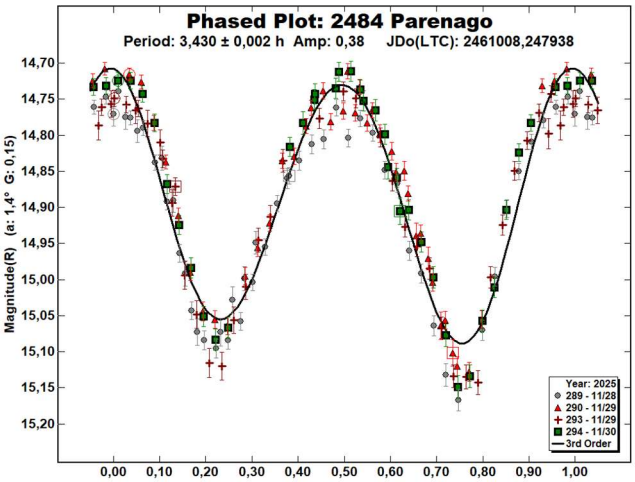

3807 Pagels (1981 SE1) was discovered on 1981 September 26 by B.A. Skiff and N.G. Thomas at the Anderson Mesa Station of the Lowell Observatory and is named in memory of Heinz R. Pagels (1939-1988), physicist, activist, educator, administrator, editor and author (among his numerous offices were the executive directorship of the New York Academy of Sciences and the presidency of the International League for Human Rights). It is a main-belt asteroid of the Flora family with a semi-major axis of 2.253 AU, eccentricity 0.168, inclination 4.299°, and an orbital period of 3.38 years. Its absolute magnitude is H = 13.16 (JPL, 2026). The NEOWISE satellite infrared radiometry survey (Mainzer et al., 2019) found a diameter D = 5.532 ± 0.183 km using an absolute magnitude H = 12.9 and a geometric albedo of p_V = 0.071.

Observations were conducted over three nights collecting 164 data points. The period analysis shows a rotational period of P = 3.287 ± 0.001 h with amplitude A = 0.10 ± 0.02 mag as the most likely solution, which is consistent with those published in the LCDB by Behrend (2001web) and Benishek (2022).

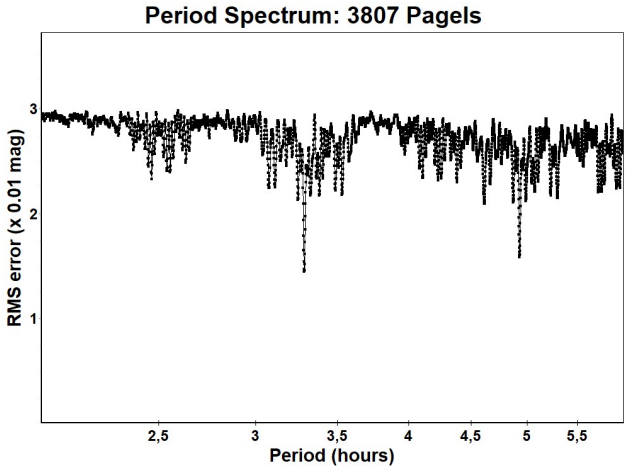

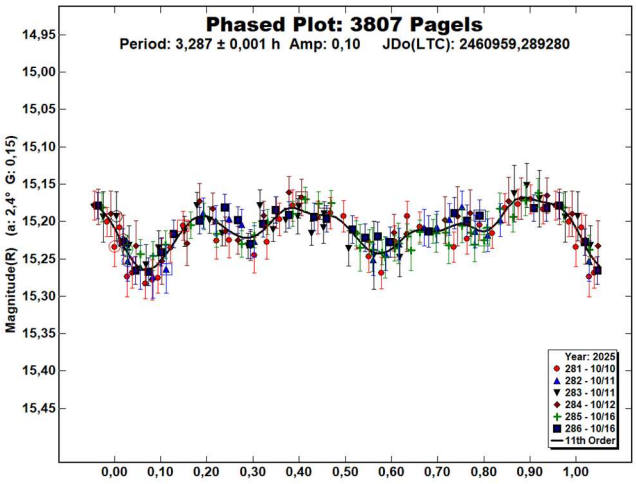

7631 Vokrouhlicky (1981 WH) was discovered on 1981 November 20 by E. Bowell at the Anderson Mesa Station of the Lowell Observatory; it is named in honor of David Vokrouhlický (b. 1966), a Czech physicist at Charles University, Prague, who has developed new physical models for the nongravitational forces acting on small minor planets and meteoroids. In particular, Vokrouhlický has studied the so-called Yarkovsky effect, which causes a slow orbital drift into main-belt resonances and is an important mechanism for transporting meteorites to Earth. It is an inner main-belt asteroid with a semi-major axis of 2.372 AU, eccentricity 0.283, inclination 4.032°, and an orbital period of 3.65 years. Its absolute magnitude is H = 14.14 (JPL, 2026). The NEOWISE satellite infrared radiometry survey (Mainzer et al., 2019) found a diameter D = 4.919 ± 0.200 km using an absolute magnitude H = 13.7 and a geometric albedo of p_V = 0.242.

Despite observing this asteroid for four nights and collecting 235 data points, we were unable to cover the entire rotation due to bad weather. The unphased light curve (Raw Plot) suggests that it is a very slow rotator with bimodal behaviour. We present a preliminary solution with a rotational period of P = 75.24 ± 0.24 h with amplitude A = 0.56 ± 0.05 mag, which is consistent with the period analysis and the phased plot. However, due to the large number of gaps in the phase curve, the actual period may differ considerably from that identified in this study. Further observations at future oppositions are strongly recommended.

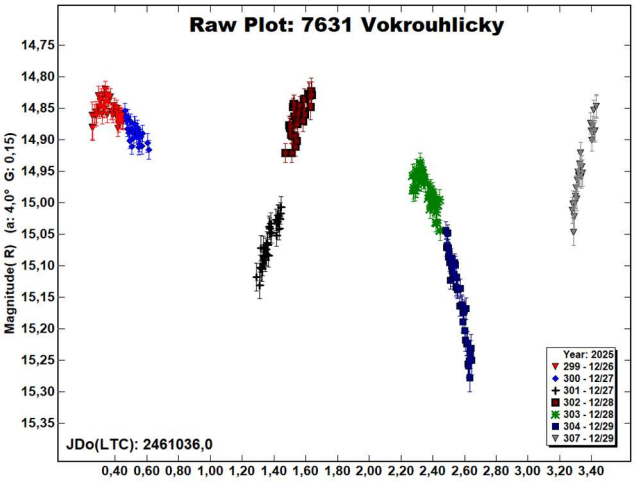

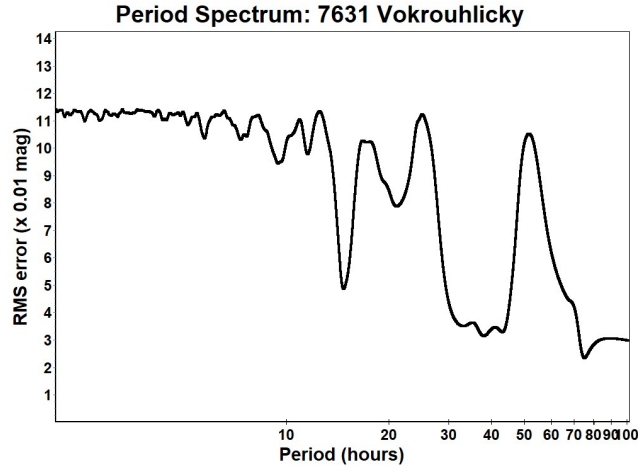

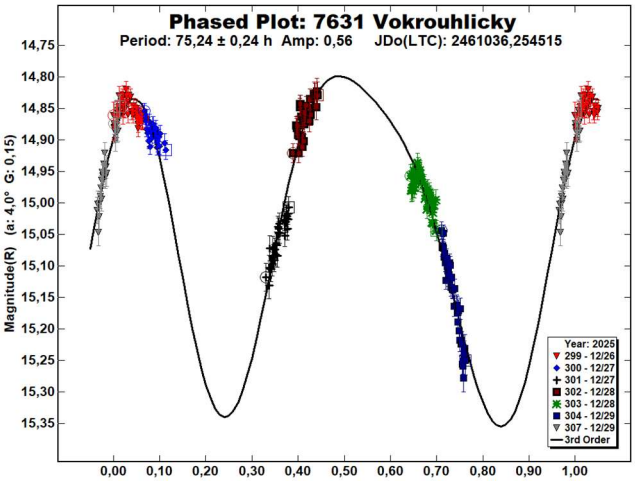

Acknowledgements

Tommaso Iozia is a student of the course in Mathematics at the University of Siena. He collaborated in images acquisition and further light curve and period analysis on the collected data. He is also preparing a bachelor's thesis in Mathematics, exploring the most used algorithms for period analysis on astronomical time series data. For these reasons, he deservedly appears as an author.

References

Behrend, R. (2001web, 2014web). Observatoire de Geneve web site. *http://obswww.unige.ch/~behrend/page_cou.html*

Benishek, V. (2022) "CCD Photometry of 29 Asteroids at Sopot Astronomical Observatory: 2020 July-2021 September" *Minor Planet Bull.* **49**, 38-44.

Harris, A.W.; Young, J.W.; Scaltriti, F.; Zappala, V. (1984). "Lightcurves and phase relations of the asteroids 82 Alkmene and 444 Gyptis." *Icarus* **57**, 251-258.

JPL (2026). Small Body Database Search Engine. *https://ssd.jpl.nasa.gov*

Mainzer, A.K.; Bauer, J.M.; Cutri, R.M.; Grav, T.; Kramer, E.A.; Masiero, J.R.; Sonnett, S.; Wright, E.L. (2019). "NEOWISE Diameters and Albedos V2.0" *NASA Planetary Data System, https://doi.org/10.26033/18S3-2Z54*.

Marchini, A.; Papini, R.; Salvaggio, F. (2015) "Rotation Period Determination for 2484 Parenago." *Minor Planet Bull.* **42**, 40.

Pravec, P.; Wolf, M.; Sarounova, L. (2014web). Ondrejov Asteroid Photometry Project web site. *http://www.asu.cas.cz/~ppravec/neo.htm*

Warner, B.D.; Harris, A.W.; Pravec, P. (2009). "The Asteroid Lightcurve Database." *Icarus* **202**, 134-146. Updated 2023 Oct. *https://minplanobs.org/mpinfo/php/lcdb.php*

Warner, B.D. (2018). MPO Software, *MPO Canopus* v10.7.7.0. Bdw Publishing. *http://bdwpublishing.com/*

LIGHTCURVE AND ROTATION PERIOD ANALYSIS OF 1984 FEDYNSKIJ, 2451 DOLLFUS AND 4583 LUGO

Wayne Hawley
Old Orchard Observatory (Z09)
Somerset, UK
hawley.wayne@gmail.com

Stephen M Brincat
Flarestar Observatory (171)
San Ġwann, MALTA

Charles Galdies
Znith Observatory, Institute of Earth Systems
Naxxar, MALTA

Tim Haymes
Southside Observatory (Y98)
Steeple Aston, UK

Mohammad Odeh
Al Khatim Observatory (M44)
Abu Dhabi, UAE

Paul C. Leyland
Tacande Observatory (J22)
La Palma, SPAIN

Patrick Wiggins
University of Utah (718)
Utah, USA

Emmanuel Kardasis
Pelagia-Eleni Observatory (247)
Athens, GREECE

Brian Scott
Calne Observatory (247)
Calne, UK

Kent DeGroff
Whiskey Creek Observatory (V19)
New Mexico, USA

Jean-Francois Gout
Tree Gate Farm Observatory (W05)
Mississippi, USA

(Received: 2025 December 12 Revised: 2025 December 18)

Photometric observations of asteroid 1984 Fedynskij, 2451 Dollfus and 4583 Lugo were obtained during 2025 Aug-Sep. Photometry and period determination were carried out with *TychoTracker Pro* Version 12.6.1. (*TT*). The photometric analysis was performed using standard differential techniques on images with the comparison stars employed selected by *TT* to be within the colour range of +0.50 < (B-V) < +0.90.

The Asteroid Terrestrial-impact Last Alert System (ATLAS) catalog (Tonry et al., 2015; Kostov and Bonev, 2017) was used as the source of reference stars. *TT*'s period determination operates by finding model light curves based on a user-defined number of Fourier components which best fit the asteroid photometric data. The program lists the candidate periods found within a user-defined period range and sampling frequency, based on minimizing Root Mean Square Errors (RMSE), between the modelled and photometric magnitudes. The candidate periods are listed in increasing RMSE value and the entire suite of RMSE values is plotted as a "periodogram" for quality control. In these periodograms the object yielded a clear 'best-fit' period solution having well defined minima as shown in the following figures. Periodograms often exhibit several possible candidate periods, in which case an examination of the rotational phase plot for each of these is then conducted looking for a credible lightcurve. Where the object shape is the dominant factor in producing the observed magnitude changes, (typically having lightcurve amplitudes of >0.2 mag), the rotational phase plot often has two peaks and two troughs (bimodal) and this is usually chosen as the most likely for such asteroids. In this paper no attempt is made to find an absolute magnitude and a value of $G = 0.15$ has been used throughout the calculations. Time-series magnitude estimates from different nights and observing locations using a variety of imaging equipment were offset in magnitude to bring them into alignment when producing the raw and rotational-phase plots. The same offset was used for each instance of an individual imaging setup. When this paper is accepted for publication all the observations will be loaded into the Asteroid Lightcurve Data Exchange Format (ALCDEF) database.

The results are summarized in Table I below. Column 3 gives the span of dates over which the observations were made. Column 4 is the range of phase angles for each date range, if this is preceded by an asterisk this means the asteroid passed through minimum phase angle during the observing period. Columns 5 and 6 give the range of values for the Phase Angle Bisector (PAB) longitude and latitude respectively, for the mid date of the observation set. Column 7 gives the period and Column 8 the minimum possible formal error in hours given by *TT*. Columns 9 and 10 give the amplitude and its associated uncertainty in magnitude. Dips in the results from the period analysis have been checked to see if they are monomodal or bimodal and a bimodal period has been chosen for the best-fit result. Information given for the object is taken from the NASA Jet Propulsion Laboratory (JPL) Small-Body Database Lookup webpage (2023).

1984 Fedynskij is an outer main-belt asteroid that was discovered on 1926 Oct. 10 by S.I. Belyavskij at Simeis. The lightcurve period and amplitude results reported here are based on a total of 289 exposures obtained during 2025 Aug-Sep. Our analysis found a synodic rotation period of 8.14 ± 0.005 h and peak-to-peak amplitude of 0.373 ± 0.026 mag. This period agrees with earlier results from Durech et al. (2020) and Dose (2025).

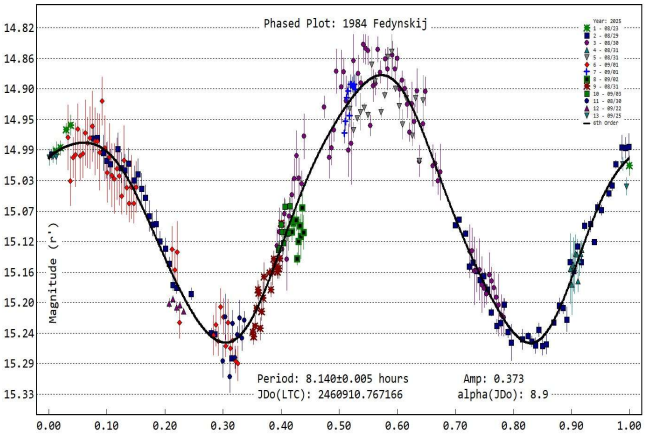

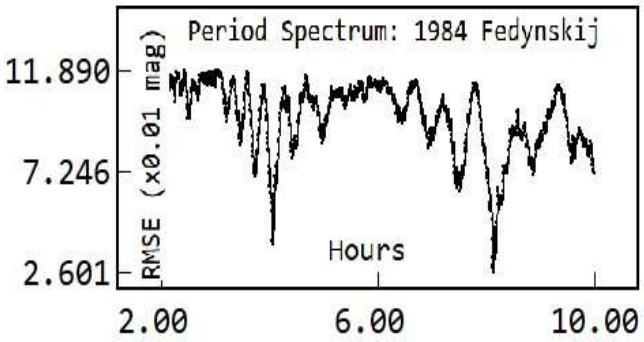

2451 Dollfus is an outer main-belt asteroid that was discovered 1980 September 2 by E. Bowell at the Anderson Mesa station of the Lowell Observatory. The lightcurve period and amplitude results reported here are based on a total of 537 exposures obtained during 2025 August-September. Our analysis found a synodic rotation period of 137.7 ± 0.09 h and peak-to-peak amplitude of 0.453 ± 0.03 mag. Currently, the ALCDEF database reports two possible periods: Behrend (2007web) 48 hours and Durech et al. (2020) 138.32 hours, with the 48 hours being retained for the default value. Our results suggest that the ~138 hours period should be retained.

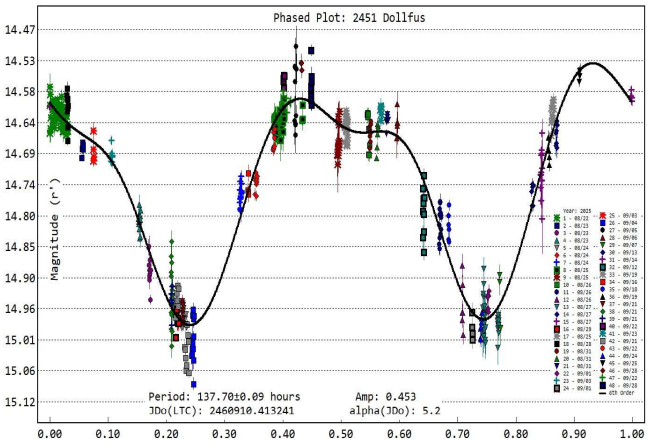

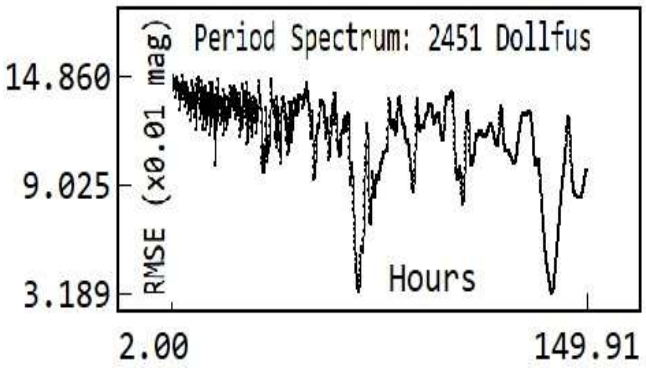

4583 Lugo is an inner main-belt asteroid that was discovered on 1989 Sep. 01 at Arecibo Observatory. One previously reported period by Behrend (2021) of 12h was found in the LCDB. The lightcurve period and amplitude results reported here are based on a total of 446 exposures obtained during 2025 August-September. Our analysis found a synodic rotation period of 39.77 ± 0.03 h and peak-to-peak amplitude of 0.399 ± 0.03 mag. One earlier rotation period was found in the LCDB (Behrend, 2021; 12h).

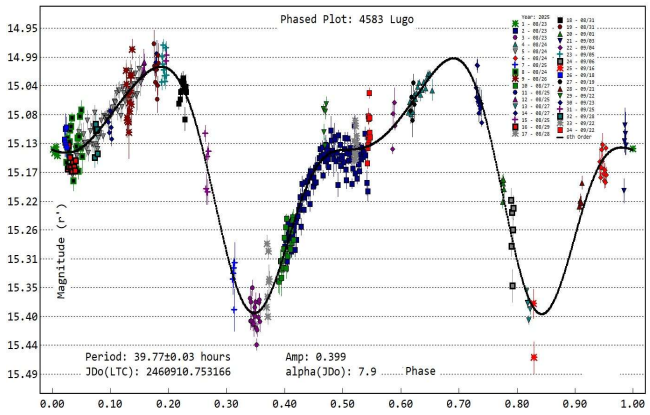

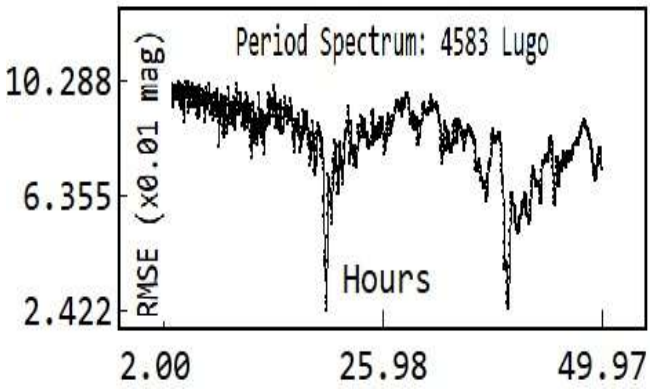

Acknowledgements

Our thanks are extended to Daniel Parrott, author of *Tycho Tracker Pro*. This work has made use of data from the Asteroid Terrestrial-impact Last Alert System (ATLAS) project. ATLAS is primarily funded to search for near earth asteroids through NASA grants NN12AR55G, 80NSSC18K0284, and 80NSSC18K1575; byproducts of the NEO search include images and catalogs from the survey area. The ATLAS science products have been made possible through the contributions of the University of Hawaii Institute for Astronomy, the Queen's University Belfast, the Space Telescope Science Institute, and the South African Astronomical Observatory. The ATLAS Catalog makes use of the formulae to convert Pan-STARRS gri to BVRI (Kostov and Bonev, 2017).

Number	Name	yyyy mm/dd	Phase	L_{PAB}	B_{PAB}	Period (h)	P.E.	Amp	A.E.	Grp
1984	Fedynskij	2025 08/23-09/25	*3.8, 8.9	351	2	8.14	0.01	0.373	0.03	9106
2451	Dollfus	2025 08/23-09/28	*0.9,12.3	340	2	137.70	0.09	0.453	0.03	9106
4583	Lugo	2025 08/23-09/28	*0.2,13.5	342	0	39.77	0.03	0.399	0.03	9104

Table I. Observing circumstances and results. The phase angle is given for the first and last date. If preceded by an asterisk, the phase angle reached a minimum during the period. L_{PAB} and B_{PAB} are the approximate phase angle bisector longitude/latitude at mid-date range (see Harris et al., 1984). Grp is the asteroid family/group (Warner et al., 2009).

Observatory	Telescope (m)	Camera	Filter	Object (sessions)
Old Orchard Observatory (Z09), Hawley	0.35m SCT f/6.7	SX694 Trius Pro	SR	1984 (4) 2451 (12) 4583 (10)
University of Utah (718), Wiggins	0.35m SCT f/5.5	ST-10XME (3x3)	C	1984 (4)
Pelagia-Eleni (247), Kardasis	0.35m SCT f/8	ASI 183MM Pro	L	1984 (1) 2451 (13) 4583 (10)
Tree Gate Farm (W05), Gout	0.28-m C11 f/1.9	ASI2600MM	C	1984 (2) 2451 (2) 4583 (5)
Whiskey Creek Observatory (V19), DeGroff	0.457m Newt f/4.2	QHY 268M	C	1984 (1) 2451 (2) 4583 (2)
Calne Observatory (247), Scott	0.28 f/8 SCT	SX-H674	L	1984 (1) 2451 (1)
Flarestar Observatory (171), Brincat	0.25m SCT f/6.3	G2-1600	C	2451 (9)
Al Khatim Observatory (M44), Odeh	0.36m SCT f/7.7	ASI 2600MM Pro	C	2451 (6) 4583 (4)
Znith Observatory Galdies	0.2m SCT	G2-1600	C	2451 (1)
Southside Observatory (Y98), Haymes	0.28m SCT f/5.8	QHY 174-GPS	C	1984 (4) 2451 (2) 4583 (2)
Tacande Observatory (J22), Leyland	0.4m Dilworth f/6.5	SX814 Trius Pro	C	4583 (1)

Table II. List of observers and equipment. The number in parentheses in the last column is the number of sessions for the given object.

References

Behrend, R. (2007web). Observatoire de Geneve web site. *https://www.astro.unige.ch/~behrend/page4cou.html#002451*

Behrend, R. (2021web). Observatoire de Geneve web site. *https://www.astro.unige.ch/~behrend/page4cou.html#004583*

Dose, E.V. (2025). "Lightcurves of eight asteroids." *Minor Planet Bulletin* **52**, 27-31.

Durech, J.; Tonry, J.; Erasmus, N.; Denneau, L.; Heinze, A.N.; Flewelling, H.; Vanco, R. (2020). "Asteroid models reconstructed from ATLAS photometry." *A&A* **643**, A59.

Harris, A.W.; Young, J.W.; Scaltriti, F.; Zappala, V. (1984). "Lightcurves and phase relations of the asteroids 82 Alkmene and 444 Gyptis." *Icarus* **57**, 251-258.

JPL (2023). Small-Body Database Lookup. *https://ssd.jpl.nasa.gov/tools/sbdb_lookup.html*

Kostov, A.; Bonev, T. (2017). "Transformation of Pan-STARRS1 gri to Stetson BVRI magnitudes. Photometry of small bodies observations." *Bulgarian Astron. J.* **28**, 3 (ArXiv:1706.06147v2).

Tonry, J.L.; Denneau, L.; Flewelling, H.; Heinze, A.N.; Onken, C.A.; Smartt, S.J.; Stadler, B.; Weiland, H.J.; Wolf, C. (2018). "The ATLAS All-Sky Stellar Reference Catalog." *Ap. J.* **867**, A105.

Warner, B.D.; Harris, A.W.; Pravec, P. (2009). "The Asteroid Lightcurve Database." *Icarus* **202**, 134-146. Updated 2023 Oct 1. *https://minplanobs.org/mpinfo/php/lcdb.php*

Warner, B.D., ed. (2021). Asteroid Lightcurve Data Exchange Format (ALCDEF) Database Bundle V1.0, urn:nasa:pds:gbo.ast.alcdef-database::1.0. NASA Planetary Data System. *https://doi.org/10.26033/b8cw-s522*

PHOTOMETRY OF KNOWN BINARY ASTEROID 26471 TRACYBECKER

Tom Polakis
Command Module Observatory
121 W. Alameda Dr.
Tempe, AZ 85282 USA
tpolakis@cox.net

(Received: 2025 December 18 Revised: 2026 January 29)

Photometric measurements were made for binary asteroid 26471 Tracybecker using CCD observations made during 2025 September and October. Mutual events were detected, and rotation and orbital periods were determined. All the data have been submitted to the ALCDEF database.

CCD photometric observations of the main-belt asteroid 26471 Tracybecker were performed at Command Module Observatory (MPC V02) in Tempe, AZ. The purpose of the observations was to determine if mutual events occur at a different position angle bisector from previous work.

Images were taken at V02 using a 0.32-m f/6.7 Modified Dall-Kirkham telescope, SBIG STXL-6303 CCD camera, and a 'clear' glass filter. Exposure time for the images was 2 minutes. The image scale after 2×2 binning was 1.76 arcsec/pixel. Table I shows the observing circumstances and results. All of the images of these asteroids were obtained in 2024 September and October. Images taken at V02 were calibrated using a dozen bias, dark, and flat frames. Flat-field images were made using an electroluminescent panel. Image calibration and alignment was performed using *MaxIm DL* (Diffraction Limited, 2017) software.

The data reduction and period analysis were done using *MPO Canopus* (Warner, 2023). In these fields, the asteroid and three to five comparison stars were measured. Comparison stars were selected with colors within the range of 0.5 < B-V < 0.95 to correspond with color ranges of asteroids. In order to reduce the internal scatter in the data, the brightest stars of appropriate color that had peak ADU counts below the range where chip response becomes nonlinear were selected. *MPO Canopus* plots instrumental vs. catalog magnitudes for solar-colored stars, which is useful for selecting comp stars of suitable color and brightness.

The clear-filtered images were reduced to Sloan r′ to minimize error with respect to a color term. Comparison star magnitudes were obtained from the ATLAS catalog (Tonry et al., 2018), which is incorporated directly into *Tycho*. The ATLAS catalog derives Sloan griz magnitudes using a number of available catalogs. The consistency of the ATLAS comp star magnitudes and color-indices allowed the separate nightly runs to be linked often with no zero-point offset required or shifts of only a few hundredths of a magnitude in a series.

Data reduction for V02 images used a 9-pixel (16 arcsec) diameter measuring aperture for asteroids and comp stars. It was typically necessary to employ star subtraction to remove contamination by field stars.

For the asteroid described here, the RMS scatter on the phased lightcurves is noted, which gives an indication of the overall data quality including errors from the calibration of the frames, measurement of the comp stars, the asteroid itself, and the period-fit. Period determination was done using the *MPO Canopus* Fourier-type FALC fitting method (Harris et al., 1989). The phased lightcurve shows the maximum at phase zero. Magnitudes in these plots are apparent and scaled by *MPO Canopus* to the first night.

The Asteroid Lightcurve Database (LCDB; Warner et al. (2009) was consulted to locate previously published results. All the new data for these asteroids can be found in the ALCDEF database.

26471 Tracybecker was discovered in 2000 by the Lincoln Laboratory Near-Earth Asteroid Research Team at Socorro. It was named after planetary scientist, Tracy M. Becker, who is affiliated with the Southwest Research Institute. The asteroid's orbit has an eccentricity of 0.15, and the opposition of 2025 September was favorably near perihelion.

The asteroid's rotation period of 2.687 ± 0.001 h was determined by Warner (2008), but its binary nature was discovered in 2010 (Warner et al., 2010), in which rotation and orbital periods are published as 2.68679 ± 0.000003 h and 39.28 ± 0.01 h, respectively. A set of further observations by Warner (2013) resulted in a rotation period of 2.6829 ± 0.0002 h, and an orbital period of 39.61 ± 0.05 h, with the mutual event barely detectable. Later analyses authored by Skiff et al. (2019) and Colazo et al. (2021) did not show detection of the presence of mutual events. Table II provides position angle bisectors for each of these sets of observations, and indicates whether mutual events were captured.

The asteroid was observed at V02 on nine nights, during which time 932 images were gathered. A synodic rotation period of 2.6870 ± 0.0001 h was computed. RMS error on the fit is 0.033 mag.

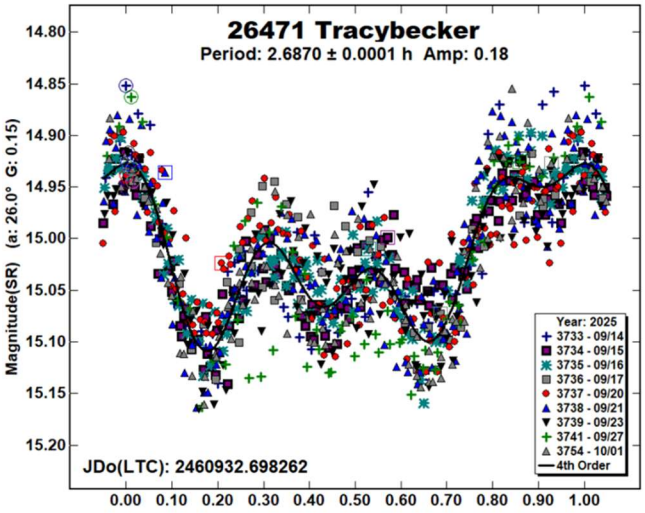

Number	Name	yy/mm/dd	Phase	L_{PAB}	B_{PAB}	Period(h)	P.E.	Amp	A.E.	Grp
26471	Tracybecker	25/09/14-10/01	26.0,25.6	357	32	2.6870 39.29	0.0001 0.02	0.19	0.03	HUN

Table I. Observing circumstances and results. The phase angle is given for the first and last date. If preceded by an asterisk, the phase angle reached an extrema during the period. L_{PAB} and B_{PAB} are the approximate phase angle bisector longitude/latitude at mid-date range (see Harris et al., 1984). Grp is the asteroid family/group (Warner et al., 2009).

Mutual events were detected on three of the nine nights. The resulting orbital period is 39.29 ± 0.02 h.

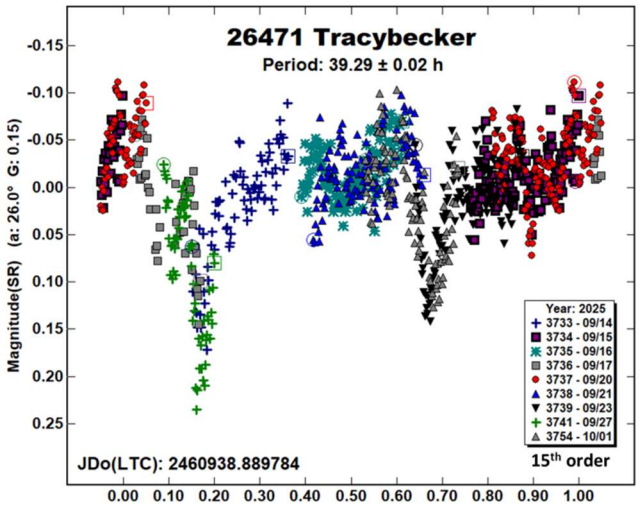

References

Colazo, M.; Duffard, R.; Weidmann, W. (2021). "The determination of asteroid H and G phase function parameters using Gaia DR2." *Monthly Notices of the Royal Astronomical Society* **504**, 761.

Diffraction Limited (2017). *MaxIm DL* software. *https://diffractionlimited.com/product/maxim-dl/*

Harris, A.W.; Young, J.W.; Bowell, E.; Martin, L.J.; Millis, R.L.; Poutanen, M.; Scaltriti, F.; Zappala, V.; Schober, H.J.; Debehogne, H.; Zeigler, K.W. (1989). "Photoelectric Observations of Asteroids 3, 24, 60, 261, and 863." *Icarus* **77**, 171-186.

Skiff, B.A.; McLelland, K.P.; Sanborn, J.J.; Pravec, P.; Koehn, B.W. (2019). "Lowell Observatory Near-Earth Asteroid Photometric Survey (NEAPS): Paper 4." *Minor Planet Bull.* **46**, 458.

Tonry, J.L.; Denneau, L.; Flewelling, H.; Heinze, A.N.; Onken, C.A.; Smartt, S.J.; Stalder, B.; Weiland, H.J.; Wolf, C. (2018). "The ATLAS all-sky stellar reference catalog." *Astrophys. J.* **867**, 105.

Warner, B.D. (2008). "Asteroid Lightcurve Analysis at the Palmer Divide Observatory: December 2007 - March 2008." *Minor Planet Bull.* **35**, 95.

Warner, B.D.; Harris, A.W.; Pravec, P. (2009). "The Asteroid Lightcurve Database." *Icarus* **202**, 134-146. Updated 2023 Oct. *http://www.minorplanet.info/lightcurvedatabase.html*

Warner, B.D.; Pravec, P.; Kusnirak, P; and 27 co-authors (2010). "A Trio of Hungaria Binary Asteroids." *Minor Planet Bull.* **37**, 70.

Warner, B.D. (2013). "Seeing Double Old and New: Observations and Lightcurve Analysis at the Palmer Divide Observatory of Six Binary Asteroids." *Minor Planet Bull.* **40**, 94.

Warner, B.D. (2023). *MPO Canopus* software. *http://bdwpublishing.com*

Author	yy/mm/dd	L_{PAB}	B_{PAB}	Mutual Events?
Warner 2008	2008-02-11	122.1	-17.3	N
Warner 2010	2009-07-15	322.4	21.4	Y
Warner 2013	2012-12-11	74.5	6.7	Y
Pravec 2016	2016-01-06	127.0	-14.6	N
Skiff 2019	2019-03-19	177.2	-27.3	N
This work	2025-09-20	357.4	32.5	Y
Future opp.	2027-03-23	182.2	-27.4	
Future opp.	2028-12-17	85.2	1.8	
Future opp.	2030-06-02	249.3	-10.5	
Future opp.	2032-02-03	135.3	-20.0	
Future opp.	2033-10-02	9.2	31.6	

Table II. Position angle bisectors and detection of mutual events compared to prior observations, and five future oppositions. Dates are the mid-date range.

LIGHTCURVES, SYNODIC ROTATION PERIOD, PHASE CURVE, SPECTRAL CLASSIFICATION AND COLOR INDEX V-R OF TROJAN ASTEROID (2893) PEIROOS

Alexander Taube
Universidad Nacional de La Plata
Facultad de Ciencias Astronómicas y Geofísicas (FCAGLP)
La Plata, ARGENTINA
alextaube92@fcaglp.unlp.edu.ar

Mario Daniel Melita
Instituto de Astronomía y Física del Espacio (IAFE)
Caba, ARGENTINA
Universidad Nacional de Hurlingham (UNAHUR)
Hurlingham (Buenos Aires), ARGENTINA
Universidad Nacional de La Plata
Facultad de Ciencias Astronómicas y Geofísicas (FCAGLP)
La Plata, ARGENTINA

Eduardo Luis Tello Huanca
Instituto de Astronomía y Física del Espacio (IAFE)
Caba, ARGENTINA
Universidad Nacional de La Plata
Facultad de Ciencias Astronómicas y Geofísicas (FCAGLP)
La Plata, ARGENTINA

Eugenia Noel Gomes
Instituto de Astronomía y Física del Espacio (IAFE)
Caba, ARGENTINA
Universidad Nacional de La Plata
Facultad de Ciencias Astronómicas y Geofísicas (FCAGLP)
La Plata, ARGENTINA

(Received: 2025 December 8 Revised: 2026 January 13)

We present an updated estimate for the synodic rotation period (P) and the lightcurve amplitudes for each observation epoch of the Jupiter Trojan asteroid 2893 Peiroos (preliminary designation 1975 QD). We compared the spectral slope of 2893 Peiroos with that associated to a classical D-type asteroid, reaffirming its taxonomic classification. The color index V-R was also updated for the observation epochs 2011.5 and 2023.8 and the estimates were used to analyze its compatibility with the D spectral class inside the L5 Trojan population.

2893 Peiroos (1975 QD) is a Jupiter Trojan asteroid situated in the L_5 Lagrange cloud (Stephens and Warner, 2019). It was discovered on 1975 August 30 by the Felix Aguilar Observatory (CASLEO) (Minor Planet Center Database, 2025). The asteroid has an estimated diameter of 86 km (Mainzer et al., 2019). Its orbit has a semi-major axis of 5.138 AU, an eccentricity of 0.0763 and an inclination of 14.67º. Its absolute magnitude is 9.00 (Jet Propulsion Laboratory, 2025 May 5).

We report photometric observations of 2893 Peiroos from six nights, distributed across 2011 August 3, 4 and 7 and 2023 November 5, 6 and 7. Observations were made remotely from the Complejo Astronómico El Leoncito (CASLEO) (San Juan, Argentina, MPC code 829) through the 2.15m Jorge Sahade telescope and a Roper VersArray CCD Camera in Reducer Focal Mode with a binning of 2 × 2. The images from 2011 August were registered through an R filter while the images from 2023 November were captured with a V Filter, in both cases with a 180-second exposure time. These reports bring the observation interval to more than 12 years, i.e. approximately the orbital period of the Jupiter Trojan asteroids. The previous known interval of 4 and a half years is augmented for almost 8 years.

The images were analyzed and reduced through the *Image Reduction and Analysis Facility* (IRAF). To visualize and manipulate the images we used the *Smithsonian Astrophysical Observatory Deep Space Nine* (DS9) program. As a result of the photometric reduction, we obtained the differential magnitude of 2893 Peiroos for each observation with respect to a comparison star selected for each opposition. The brightness measured in the oppositions of 2011 August was corrected by the color index V-R from Chatelain et al. (2016). We retrieved the mean brightness of each comparison star in the magbands G, G_{BP} and G_{RP} from the *Gaia Early Data Release 3* (EDR3) catalog, using digitized images displayed in the *Aladin* software. By means of a third-degree polynomial transformation provided by the EDR3 catalog we computed the V-band magnitude of the comparison stars in the Johnson-Cousins photometric System, and so the standard apparent magnitude of 2893 Peiroos was obtained as:

$$m_{Peiroos} = (m_{Peiroos,\ inst} - m_{star,\ inst}) + m_{star,cat} \quad (1)$$

In Equation (1) $m_{Peiroos}$ is its standard V-band apparent magnitude, $m_{Peiroos,\ inst}$ is its instrumental magnitude (corrected by the aforementioned V-R color index whether necessary), $m_{star,\ inst}$ is the V-band instrumental magnitude of the comparison star and $m_{star,\ cat}$ is its standard V-band magnitude.

The V-band apparent standard magnitude, the solar phase angle, and the phase angle bisector longitude (L_{PAB}) and latitude (B_{PAB}) for the approximate mid date from the oppositions between the years 2015 and 2020 were retrieved from *ALCDEF* database. These data were combined with our own data to estimate the rotational parameters and to model its shape. To compute the reduced magnitude and the geocentric and heliocentric distance of the asteroid, we used the values provided by the JPL *Horizons* System. With the respective ephemerides (cartesian coordinates of the Earth and of 2893 Peiroos with respect to the Sun) we computed the asteroidal position vectors from the Earth and the Sun at an approximate mid-date for each night. The absolute magnitude was computed with the three-parameter H, G_1, G_2 photometric phase function from Penttilä et al. (2016). H is the mean absolute magnitude, and G_1, G_2 are parameters that describe the general shape of the phase function. To compute them we used the online calculator by Penttilä et al. (2016). The parameters were estimated by a minimum squared method through which the phase function was fitted. To fit the phase function, we adopted the linear unconstrained fit from Muinonen et al. (2010) (see Figure 1). To compare models with a different number of parameters, we needed to penalize the (weighted) sum of squared errors (SSE) with the number of parameters p. In Penttilä et al. (2016) this is performed using the Bayesian Information criterion (BIC). The smaller the value of the BIC, the more preferred the model. For 2893 Peiroos, the model which satisfies this condition is the one-dimensional H(D), in which only the parameter H is fitted and the values adopted for G_1, G_2 correspond to the means associated to the D taxonomic class. Our corresponding values are: H=9.2114, G1=0.9617 and G2=0.01645. These parameters are broadly consistent with those reported by Mahlke et al. (2021) (H=9.229, G1=0.856, G2=0.050), and especially the magnitude parameter H is coherent with a D spectral type. From the linear unconstrained fit k=-0.03294 is the photometric slope, WRMS=0.4314 is the weighted root mean square and the BIC=-37.18.

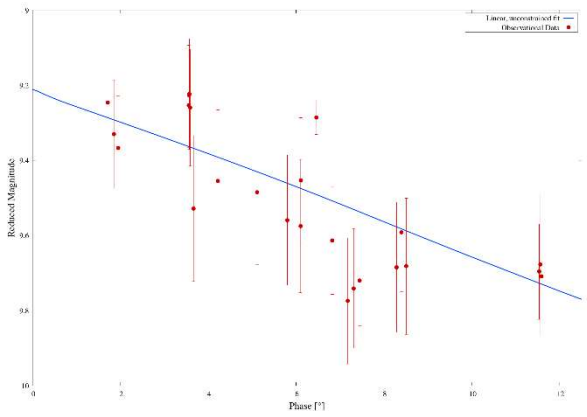

Figure 1: Linear, unconstrained fit (Muinonen et al., 2010) of the reduced mean magnitude versus the three-parameter (H, G1, G2) photometric phase function (Penttilä et al., 2016) in each opposition. The red filled circles represent the mean reduced magnitudes computed for the approximated solar phase angles and the blue curve represents the corresponding fit.

The phase curve shown in Figure 1 is characteristic of a Trojan asteroid, with an approximately linear slope up to ~ 1°, at which point a break occurs and a smooth opposition effect is observed for smaller phase angles. Due to its steep slope extending to phase angles greater than 10º and considering the low albedo of 2893 Peiroos, the presence of exposed regolith could be inferred on its surface (Oszkiewicz et al., 2012). With the absolute magnitude parameter H and the geometric albedo p_v=0.048 in the V band reported by the WISE mission, we estimated empirically the effective diameter of the object D_{eff}=87.22 km. This value is consistent with the estimates previously reported in ALCDEF: D_{eff}=87.46 km (Tedesco et al., 2004), D_{eff}=86.88 km (Mainzer et al., 2011), D_{eff}=86.76 km (Usui et al., 2011), and D_{eff}=86.884 km (Mainzer et al., 2019).

We also estimated the color index V-R independently for the epochs 2011.6 and 2023.8 with our own data (apparent standard magnitude lightcurves computed in the R-band or V-band with Equation (1)). For the epoch 2011.6 we combined two lightcurves computed both in the R and V bands for the same oppositions. For the epoch 2023.8 we combined four lightcurves in the V-band with one lightcurve in the R-band. Individual V-R color indices were computed by subtracting, for each V-band point, the nearest data point in rotational phase from one of the R-band lightcurves, as expressed in Equation (2):

$$V\text{-}R = m_{Peiroos,\,V} - m_{Peiroos,\,R} \quad (2)$$

The global V-R color indices were obtained independently for our two observation epochs (2011.6 and 2023.8) by averaging the corresponding individual measurements, and the associated error was calculated as 2 × (SEM), being (SEM) the standard error of the mean. Our estimates, together with the color index reported by Chatelain et al. (2016), are shown in Table I.

Epoch	V-R	(V-R) Error
2011.6	0.425	0.069
2023.8	0.364	0.083
Chatelain et al. (2016)	0.470	0.040

Table I: Our color index V-R estimates derived for the epochs 2011.6 and 2023.8 are shown, together with the value reported by Chatelain et al. (2016).

For period analysis we generated one periodogram per observation epoch through the Phase Dispersion Minimization technique (Stellingwerf, 1978), allowing for a local estimation of the synodic period. These periodograms are shown in Figure 2. We searched for a synodic period between 2 h and 12 h with a time step equal to 0.002 h. Our sample comprised the absolute magnitudes corresponding to each observation given in Julian Date (JD). The mean synodic period was computed as the unweighted arithmetic mean of the individual epoch measurements, with the associated uncertainty computed as the standard error of the mean in order to reflect the dispersion among epochs. The resulting estimate is P = 8.948 ± 0.003 h. This mean value is in excellent agreement with the individual epoch estimates, with differences falling within the combined uncertainties and the expected synodic variations due to changing viewing geometry. It lies at 0.2σ for 2011.6, 0.15σ for 2015.9, 0.19σ for 2016.9, 0.22σ for 2017.9, 0.07σ for 2019.1, 0.04σ for 2020.3 and 0.23σ for 2023.8.

The previous values of the rotation period reported in ALCDEF are: 1) P = 8.99 ± 0.01 h (Stephens, 2016), 2) P = 8.951 ± 0.002 h (Stephens, 2017), 3) P = 8.936 ± 0.004 h (Stephens and Warner, 2018), 4) P = 8.945 ± 0.001 h (Stephens and Warner, 2019), 5) P = 8.946 ± 0.002 h (Stephens and Warner, 2020) and 6) P = 8.949 ± 0.005 h (McNeill et al., 2021). See Table II of observing circumstances and results. According to the quoted errors the difference of our period estimate (P = 8.948 ± 0.003 h), quantified using a z-score function, is statistically consistent (within the 95% confidence interval) with 2), 4), 5) and 6), lying at 0.83σ for 2), 0.95σ for 4), 0.55σ for 5) and 0.17σ for 6). However, the period difference with respect to 1) and 3), given by 4.02σ and 2.4σ respectively, is not considered statistically consistent.

We computed the V-band reduced magnitude lightcurves and phased them, for each observation epoch, according to the local specific period estimated by the PDM technique. Subsequently, a 4th-order Fourier series was fitted to the phased data in order to derive the lightcurve peak-to-peak amplitudes and its associated uncertainty. The epoch-specific periods estimated by the PDM technique and the lightcurve amplitudes are shown in Table II. The folded lightcurves are shown in Figure 3.

The differing amplitudes derived from the Fourier fit across different epochs indicate that 2893 Peiroos was observed at different viewing geometries (i.e, changing aspect angles). The lightcurves from all the epochs are dominated by a bimodal shape. The regularity of the lightcurves, combined with amplitudes reaching up to Δm ~ 0.41 mag, indicates a non-spherical shape, consistent with a triaxial ellipsoid elongation.

In a complementary analysis, we noted that the blueshift in our color index V-R estimates between the epochs of 2011.6 and 2023.8 (Table I) can be related to an increase of the solar phase angle (between ~ 2º in 2011.6 and ~12º in 2023.8, as seen in Figure 1). According to Colazo et al. (2025), from the analysis of an ATLAS survey sample they concluded that both a blueshift or a redshift are observed for phase angles below 5º (toward higher values), without any clear preference. However, within the range 10º-30º redshift cases prevail, consistent with the fact that the effects that generate this behaviour are noticeable at higher phase angles (Colazo et al., 2025). In contrast, Álvarez-Candal (2024) showed that for phase angles below 4.5º intrinsically red objects tend to become bluer towards higher values and vice versa. However, for phase angles greater than 5º, intrinsically red objects tend to become redder, consistent with the traditional *phase coloring* (Alvarez-Candal, 2024). The blueshift for higher phase angles that we observe is

Number	Name	yyyy mm/dd	Phase	L_{PAB}	B_{PAB}	Period(h)	P.E.	Amp	A.E.	Obs.
2893	Peiroos	2011 08/03-08/07	1.7, 2.0	315	-7	8.94	0.04	0.30	0.04	CASLEO
2893	Peiroos	2015 09/09-09/11	7.5, 7.2	89	-7	8.96	0.08	0.29	0.05	CS3
2893	Peiroos	2016 12/12-12/28	6.4, 3.7	116	2	8.95	0.01	0.35	0.07	CS3
2893	Peiroos	2017 12/26-12/28	8.5, 8.3	145	8	8.93	0.08	0.39	0.03	CS3
2893	Peiroos	2019 02/12-02/19	6.8, 5.8	176	15	8.95	0.03	0.34	0.04	CS3
2893	Peiroos	2020 04/18-04/22	3.6	211	16	8.95	0.05	0.29	0.02	CS3
2893	Peiroos	2023 11/05-11/07	11.5, 11.6	328	-11	8.950	0.008	0.41	0.03	CASLEO

Table II. Observing circumstances and results. The phase angle is given for the first and last date. If preceded by an asterisk, the phase angle reached an extrema during the period. L_{PAB} and B_{PAB} are the approximate phase angle bisector longitude/latitude at mid-date range (see Harris et al., 1984). Amplitude error (A.E.) is calculated as √2 x (lightcurve RMS residual). Obs. is the observatory involved. CS3: Center for Solar System Studies, CASLEO: Complejo Astronómico El Leoncito (Warner et al., 2009).

atypical since 2893 Peiroos is considered an intrinsically red object, especially for being a D spectral type. Some variability in color index between epochs could also be related to aspect-angle changes or mild surface heterogeneity, as reported in previous works (e.g Szabó et al., 2004; Cellino et al., 1989).

We corroborated the D-type taxonomy of 2893 Peiroos by extracting its featureless, reddish spectrum from the *Gaia Data Release 3* (DR3) catalog and comparing it with the templates retrieved from Bus-De Meo's spectral classification. From Figure 4 we observe that the spectral slope of (2893) Peiroos is stepper than that typically associated with a classical D-type, lying within its dispersion although towards its redder boundary.

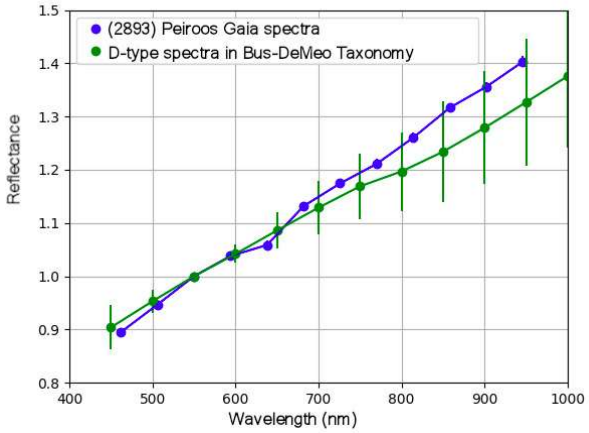

Figure 4: Spectral slope of 2893 Peiroos (blue curve) and of a classical D-type from the Bus-DeMeo spectral classification (green curve).

Finally, to evaluate the compatibility of 2893 Peiroos with the D-type spectral class inside the L5 Trojan cloud we compared its weighted mean V-R color index X_P = 0.400 (computed with our own values from Table I) with the V-R global mean color index μ_D = 0.463 from the sample of 32 D-type Jupiter Trojans from the L5 Lagrange cloud reported by Chatelain et al. (2016). For each asteroid in the sample, we computed the individual weighted mean V-R color index and the standard uncertainty, and then derived μ_D and the sample dispersion σ_D = 0.025. Subsequently, we compared the weighted mean color of 2893 Peiroos $\bar{X}_P$ and its global uncertainty $\sigma_{\bar{X}P}$ = 0.027 to the sample distribution through a z-score defined as:

$$z = \frac{\bar{X}_P - \mu_D}{\sqrt{\sigma^2_D + \sigma^2_{\bar{X}P}}} \quad (3)$$

We obtained z ~ -1.72. That means that $\bar{X}_P$ lies at approximately 1.72 composite standard deviations from μ_D towards the blue-ward wing (lower V-R) of the D-type Trojan distribution, remaining formally compatible with it.

It is interesting to note that, although the spectrum of 2893 Peiroos presents a redder reflectance slope than the corresponding to a classical D-type asteroid, our color index analysis places it on the blue side of the D-type L5 Trojan sample analyzed by Chatelain et al. (2016).

Acknowledgments

We acknowledge funding from CONICET PIP 2169/2023.

References

Alvarez-Candal, A. (2024). "A discussion on estimating small bodies taxonomies using phase curves results." *Planetary and Space Science* **251**.

Cellino, A.; Zappala, V.; Farinella, P. (1989). "Asteroid shapes and lightcurve morphology." *Icarus* **78**, 298-310.

Chatelain, J.; Henry, T.; French, L.; Winters, J.; Trilling, D. (2016). "Photometric colors of the brightest members of the Jupiter L5 Trojan cloud." *Icarus* **271**, 158-169.

Colazo, M.; Oszkiewicz, D.; Alvarez-Candal, A.; Pożniak, P.; Bartczak, P.; Podlewska-Gaca, E. (2025). "Asteroid phase curves and phase coloring effect using the ATLAS survey data." *Icarus* **436**.

Gaia Collaboration, DPAC. (2020). Photometric relations [Chapter Section CU5: Photometric processing]. ESA Gaia Archive. *https://gea.esac.esa.int/archive/documentation/GEDR3/Data_processing/chap_cu5pho/cu5pho_sec_photSystem/cu5pho_ssec_photRelations.html*

Jet Propulsion Laboratory (2025). Small-Body Database Lookup: (2893) Peiroos. *https://ssd.jpl.nasa.gov/tools/sbdb_lookup.html#sstr=peiroos&view=OPDA*

Mahlke, M.; Carry, B.; Denneau, L. (2021). "Asteroid phase curves from ATLAS dual-band photometry." *Icarus* **354**, A114094.

Mainzer, A.; Grav, T.; Masiero, J.; Hand, E.; Bauer, J.; Tholen, D.; McMillan, R.S.; Spahr, T.; Cutri, R.M.; Wright, E.; Watkins, J.; Mo, W.; Maleszewski, C. (2011). "NEOWISE studies of spectrophotometrically classified asteroids: preliminary results." *The Astrophysical Journal* **741**, A90.

Mainzer, A.; Bauer, J.; Cutri, R.; Grav, T.; Kramer, E.; Masiero, J.; Sonnett, S.; Wright, E.; Eds. (2019). "NEOWISE Diameters and AlbedosV2.0", urn:nasa:pds:neowise_diameters_albedos::2.0. *NASA Planetary Data System*.

McNeill, A.; Erasmus, N.; Trilling, D.E.; Emery, J.P.; Tonry, J.L.; Denneau, L.; Flewelling, H.; Heinze, A.; Stalder, B.; Weiland, H.J. (2021). "Comparison of the Physical Properties of the L4 and L5 Trojan Asteroids from ATLAS Data." *The Planetary Science Journal* **2**, A6.

Muinonen, K.; Belskaya, I.N.; Cellino, A.; Delbò, M.; Levasseur-Regourd, A.; Penttilä, A.; Tedesco, E.F. (2010). "A three-parameter magnitude phase function for asteroids." *Icarus* **209** 542-555.

Oszkiewicz, D.A.; Bowell, E.; Wasserman, L.H.; Muinonen, K.; Penttilä, A.; Pieniluoma, T.; Trilling, D.E.; Thomas, C.A. (2012). "Asteroid taxonomic signatures from photometric phase curves." *Icarus* **219**, 283-296.

Penttilä, A.; Shevchenko, V.G.; Wilkman, O.V.; Muinonen, K. (2016). "H, G1, G2 photometric phase function extended to low-accuracy data." *Planetary and Space Science* **123**, 117-125.

Stellingwerf, R.F. (1978). "Period determination using Phase Dispersion Minimization.". *The Astrophysical Journal* **224**, 953-960

Stephens, R.D. (2016). "A report from the L5 Trojan camp - lightcurves of Jovian Trojan asteroids from the Center for Solar System Studies." *The Minor Planet Bulletin* **43**, 265-270.

Stephens, R.D. (2017). "Lightcurve Analysis of Trojan Asteroids at the Center of Solar System Studies." *The Minor Planet Bulletin* **44**, 123-125.

Stephens, R.D.; Warner, B. (2018). "Lightcurve Analysis of L5 Trojan asteroids at the Center for Solar System Studies: 2017 September to December." *The Minor Planet Bulletin* **45**, 124-128.

Stephens, R.D.; Warner, B. (2019). "Lightcurve Analysis of L5 Trojan asteroids at the Center for Solar System Studies: 2019 January to March." *The Minor Planet Bulletin* **46**, 315-317.

Stephens, R.D.; Warner, B. (2020). "Lightcurve Analysis of L5 Trojan asteroids at the Center for Solar System Studies: 2020 April to June." *The Minor Planet Bulletin* **47**, 285-289.

Szabó, G.M.; Ivezić, Ž.; Jurić, M.; Lupton, R. Kiss, L.L. (2004). "Colour variability of asteroids in the Sloan Digital Sky Survey Moving Object Catalog." *Monthly Notices of the Royal Astronomical Society* **348**, 987-998.

Tedesco, E.F.; Noah, P.V.; Noah, M.; Price, S.D. (2004), "IRAS Minor Planet Survey V6.0." *NASA Planetary Data System*, ID: IRAS-A-FPA-3-RDR-IMPS-V6.0.

Usui, F.; Kuroda, D.; Müller, T.G.; Hasegawa, S.; Ishiguro, M.; Ootsubo, T.; Ishihara, D.; Kataza, H.; Takita, S.; Oyabu, S.; Ueno, M.; Matsuhara, H.; Onaka, T. (2011). "Asteroid Catalog Using Akari: AKARI/IRC Mid-Infrared Asteroid Survey." *Publications of the Astronomical Society of Japan* **63**, A5, 1117-1138.

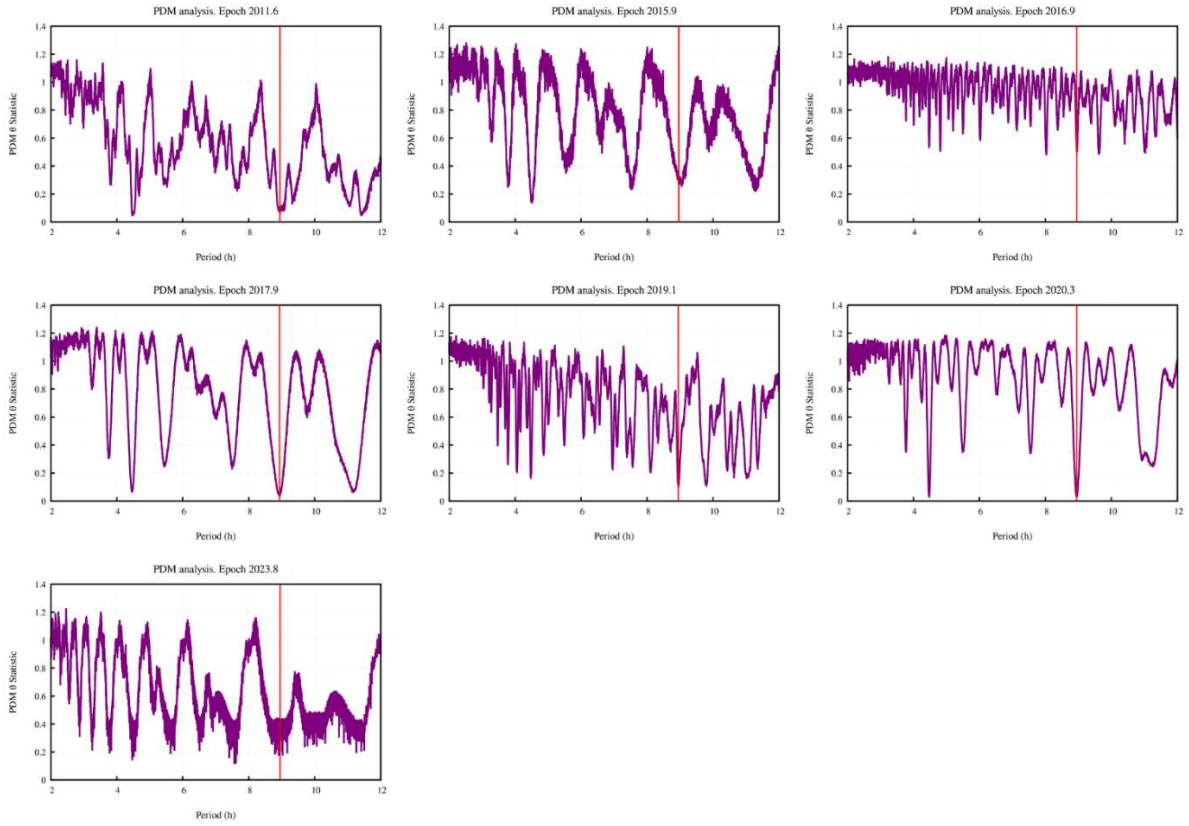

Figure 2: Phase Dispersion Minimization analysis of 2893 Peiroos for each observation epoch. The red vertical line indicates the most probable estimate of the synodic period which minimizes the statistic function and was therefore used for the local lightcurve phasing and Fourier fit.

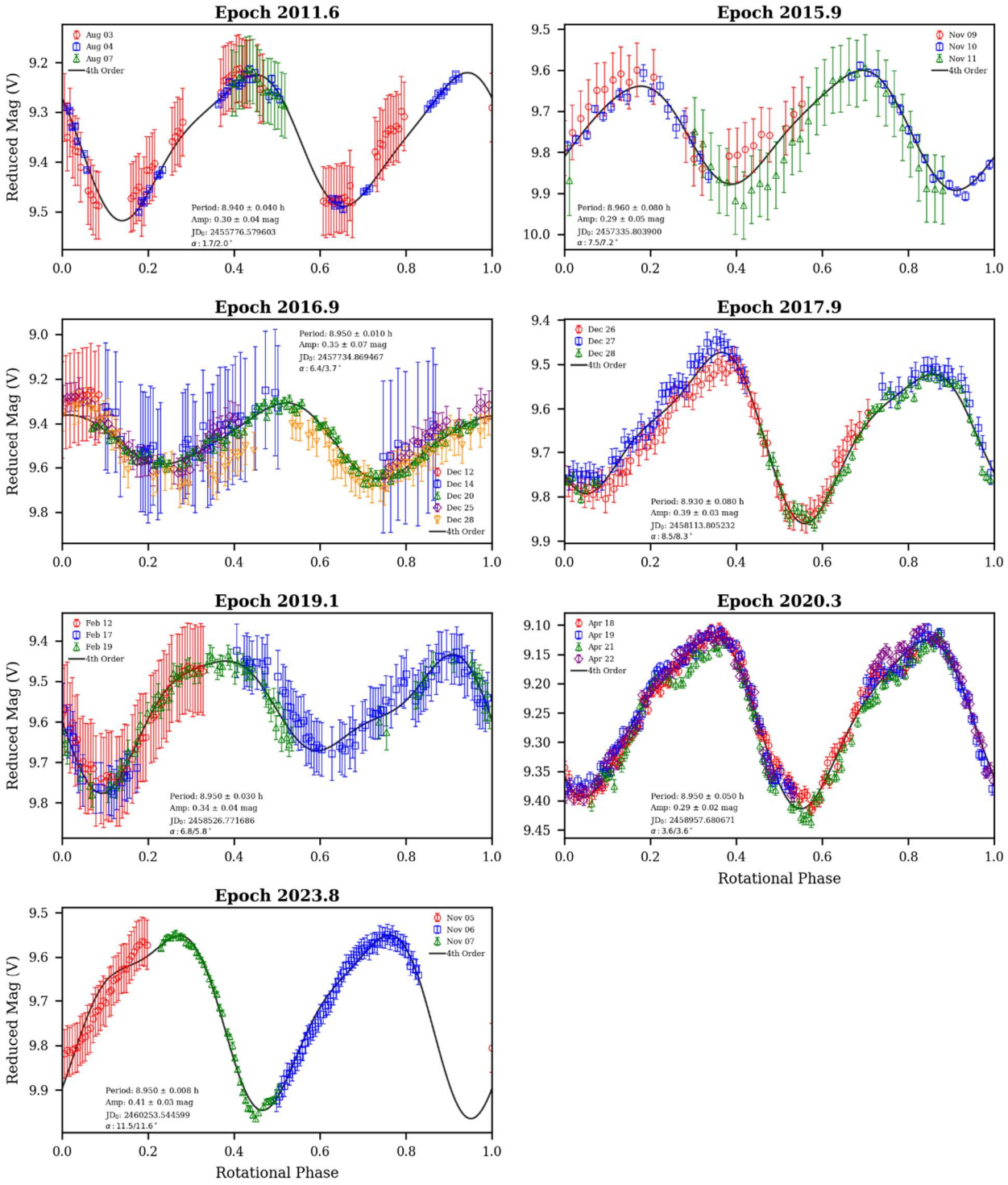

Figure 3: V-band reduced magnitude lightcurves folded for each observation epoch. Inside the plot area the following information is added: the synodic period estimated by the PDM technique, the peak-to-peak amplitude of the Fourier model lightcurve, the Julian Date of the first data point, and the solar phase angle for the first and last date.

LIGHTCURVE AND ROTATION PERIOD ANALYSIS OF 8556 JANA

Wayne Hawley
Old Orchard Observatory (Z09)
Somerset, UK
hawley.wayne@gmail.com

Mohammad Odeh
Al Khatim Observatory (M44)
Abu Dhabi, UAE

Emmanuel Kardasis
Pelagia-Eleni Observatory (247)
Attica, GREECE

Brian Scott
Calne Observatory (247)
Wiltshire, UK

Kent DeGroff
Whiskey Creek Observatory (V19)
New Mexico, USA

Jean-Francois Gout
Tree Gate Farm Observatory (W05)
Mississippi, USA

Tim Haymes
Southside Observatory (Y98)
Oxfordshire, UK

James D. Armstrong
Univ. of Hawaii Institute for Astronomy (L09) (Q59) (T04) (W89)
Hawaii, USA

(Received: 2026 January 13)

Photometric observations of asteroid 8556 Jana were obtained 2025 September-November. For 8556 Jana, we found P = 35.52 ± 0.01 h, A = 0.5354 ± 0.0364 magnitudes. A search of the LCDB and Minor Planet Bulletin found no earlier periods reported

Minor planet 8556 Jana is a main belt outer asteroid it was discovered on 1995 July 07 by Z. Moravec at Klet. Our photometric observations of 8556 Jana were made from 2025 September 08 and 2025 November 25. Photometry and period determination were carried out with *TychoTracker Pro* Version 12.6.1. (*TT*). The photometric analysis was performed using standard differential techniques on images with the comparison stars employed selected by *TT* to be within the colour range of +0.50 < (B-V) < +0.90.

The Asteroid Terrestrial-impact Last Alert System (ATLAS) catalog (Tonry et al, 2018; Kostov and Bonev, 2017) was used as the source of reference stars. *TT*'s period determination operates by finding model lightcurves based on a user-defined number of Fourier components which best fit the asteroid photometric data. The program lists the candidate periods found within a user-defined period range and sampling frequency, based on minimizing Root Mean Square Errors (RMSE), between the modelled and photometric magnitudes. The candidate periods are listed in increasing RMSE value and the entire suite of RMSE values is plotted as a "periodogram" for quality control. In these periodograms the object yielded a clear 'best-fit' period solution having well defined minima as shown in the following figures. Periodograms often exhibit several possible candidate periods, in which case an examination of the rotational phase plot for each of these is then conducted looking for a credible lightcurve. Where the object shape is the dominant factor in producing the observed magnitude changes, (typically having lightcurve amplitudes of >0.2 mag), the rotational phase plot often has two peaks and two troughs (bimodal) and this is usually chosen as the most likely for such asteroids.

In this paper no attempt is made to find an absolute magnitude and a value of G = 0.15 has been used throughout the calculations. Time-series magnitude estimates from different nights and observing locations using a variety of imaging equipment were offset in magnitude to bring them into alignment when producing the raw and rotational-phase plots. The same offset was used for each instance of an individual imaging setup. When this paper is accepted for publication all the observations will be loaded into the Asteroid Lightcurve Data Exchange Format (ALCDEF) database.

The lightcurve period and amplitude results reported here are based on a total of 773 exposures obtained during 2025 September to November. Our analysis found a synodic rotation period 35.52 ± 0.01 h, and peak-to-peak amplitude of 0.5354 ± 0.0364 mag. These results are summarized in Table 1 below. Column 3 gives the span of dates over which the observations were made. Column 4 is the range of phase angles for each date range, if this is preceded by an asterisk this means the asteroid passed through minimum phase angle during the observing period. Columns 5 and 6 give the range of values for the Phase Angle Bisector (PAB) longitude and latitude respectively, for the mid date of the observation set. Column 7 gives the period and Column 8 the minimum possible formal error in hours given by TT. Columns 9 and 10 give the amplitude and its associated uncertainty in magnitude. Dips in the results from the period analysis have been checked to see if they are monomodal or bimodal and a bimodal period has been chosen for the best-fit result. Information given for the object is taken from the NASA Jet Propulsion Laboratory (JPL) Small-Body Database Lookup webpage (2023).

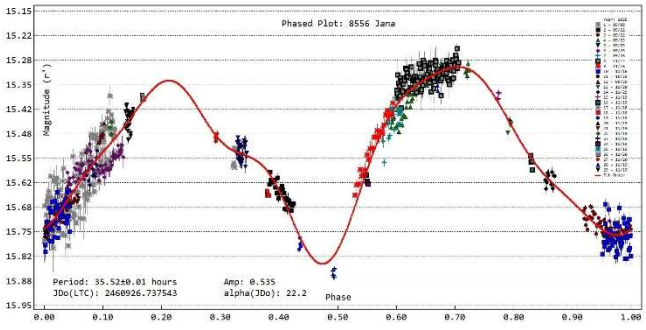

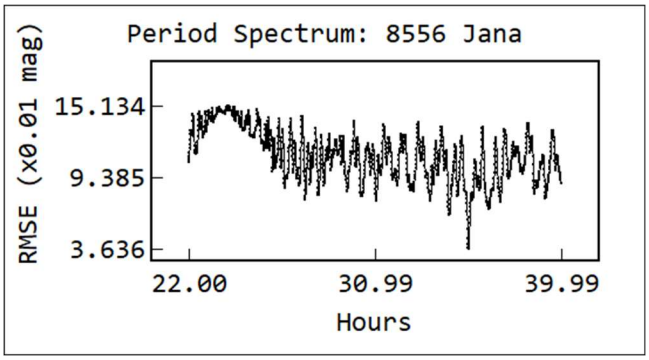

Number	Name	yyyy mm/dd	Phase	L_{PAB}	B_{PAB}	Period (h)	P.E.	Amp	A.E.	Grp
8556	Jana	2025 09/08-11/25	*8.6,22.2	24	-7	32.52	0.01	0.5354	0.36	9106

Table I. Observing circumstances and results. The phase angle is given for the first and last date. If preceded by an asterisk, the phase angle reached a minimum during the period. L_{PAB} and B_{PAB} are the approximate phase angle bisector longitude/latitude at mid-date range (see Harris et al., 1984). Grp is the asteroid family/group (Warner et al., 2009).

Acknowledgements

Our thanks are extended to Daniel Parrott, author of *Tycho Tracker Pro*. This work has made use of data from the Asteroid Terrestrial-impact Last Alert System (ATLAS) project. ATLAS is primarily funded to search for near earth asteroids through NASA grants NN12AR55G, 80NSSC18K0284, and 80NSSC18K1575; byproducts of the NEO search include images and catalogs from the survey area. The ATLAS science products have been made possible through the contributions of the University of Hawaii Institute for Astronomy, the Queen's University Belfast, the Space Telescope Science Institute, and the South African Astronomical Observatory. The ATLAS Catalog makes use of the formulae to convert Pan-STARRS gri to BVRI (Kostov and Bonev, 2017). This paper is based on observations made with the Las Cumbres Observatory's education network telescopes that were upgraded through generous support from the Gordon and Betty Moore Foundation.

This work makes use of observations from the Las Cumbres Observatory global telescope network.

References

Harris, A.W.; Young, J.W.; Scaltriti, F.; Zappala, V. (1984). "Lightcurves and phase relations of the asteroids 82 Alkmene and 444 Gyptis." *Icarus* **57**, 251-258.

JPL (2023). Small-Body Database Lookup. *https://ssd.jpl.nasa.gov/tools/sbdb_lookup.html*

Kostov, A.; Bonev, T. (2017). "Transformation of Pan-STARRS1 gri to Stetson BVRI magnitudes. Photometry of small bodies observations." *Bulgarian Astron. J.* **28**, 3 (ArXiv:1706.06147v2)

Tonry, J.L.; Denneau, L.; Flewelling, H.; Heinze, A.N.; Onken, C.A.; Smartt, S.J.; Stadler, B.; Weiland, H.J.; Wolf, C. (2018). "The ATLAS All-Sky Stellar Reference Catalog." *Ap. J.* **867**, A105.

Warner, B.D.; Harris, A.W.; Pravec, P. (2009). "The Asteroid Lightcurve Database." *Icarus* **202**, 134-146. Updated 2023 Oct 1. *https://minplanobs.org/mpinfo/php/lcdb.php*

Observatory	Telescope (m)	Camera	Filter	Object (sessions)
Old Orchard Observatory (Z09), Hawley	0.35 f/6.7	SX694 Trius Pro (2×2)	SR	8556 (8)
Pelagia-Eleni Observatory (247), Kardasis	0.35 f/8	ASI 183 MM Pro (1×1)	V	8556 (1)
Tree Gate Farm Observatory (W05), Gout	0.28 f/1.9	ASI 2600 MM Pro (1×1)	C	8556 (1)
Whiskey Creek Observatory (V19), DeGroff	0.457m Newt f/4.2	QHY 268M (2x2)	C	8556 (1)
Calne Observatory (247), Scott	0.28 f/7 SCT	SXH674 (2x2)	L	8556 (1)
Al Khatim Observatory (M44), Odeh	0.36 f/7.7	ASI 2600 MM Pro (2x2)	C	8556 (2)
Southside Observatory (Y98), Haymes	0.28 f/5.8	QHY 174-GPS (1×1)	C	8556 (1)
Siding Spring LCO Clamshell #2 (Q59), Armstrong	0.35 *f*/3	QHY 600 CMOS (1×1)	SR	8556 (2)
Sutherland LCO Aqawan A #1 (L09), Armstrong	0.35 f/3	QHY 600 CMOS (1×1)	SR	8556 (6)
Cerro Tololo LCO Aqawan A #1 (W89), Armstrong	0.35 *f*/3	QHY 600 CMOS (1×1)	SR	8556 (5)
Haleakala LCO Clamshell #1 (T04), Armstrong	0.35 *f*/3	QHY 600 CMOS (1×1)	SR	8556 (1)

Table II. List of observers and equipment. The number in parentheses in the last column is the number of sessions for the given object.

LIGHTCURVE AND ROTATION PERIOD ANALYSIS OF 2387 XI'AN

Wayne Hawley
Old Orchard Observatory (Z09)
Fiddington, UK
hawley.wayne@gmail.com

Jean-Francois Gout
Tree Gate Farm Observatory (W05)
Mississippi, USA

Kent DeGroff
Whiskey Creek Observatory (V19)
New Mexico, USA

Jean Genebriera
Astropriorat Observatory (M02)
Catalonia, SPAIN

Mohammad Odeh
Al Khatim Observatory (M44)
Abu Dhabi, UAE

(Received: 2025 December 24)

Photometric observations of asteroid 2387 Xi'an were obtained during 2025 August. We found P = 4.2971 ± 0.001 h, A = 0.2087 ± 0.0215 magnitudes. Two earlier results were found in the Lightcurve Database, Waszczak et al. (2015) and Durech et al. (2020).

Minor planet 2387 Xi'an is a member of the Brangäne family that was discovered on 1975 March17 by Purple Mountain Observatory at Nanking. Our photometric observations of 2387 Xi'an were made from 2025 November 14 to 25. Photometry and period determination were carried out with *TychoTracker Pro* Version 12.6.1. (*TT*). The photometric analysis was performed using standard differential techniques on images with the comparison stars employed selected by *TT* to be within the colour range of +0.50 < (B-V) < +0.90.

The Asteroid Terrestrial-impact Last Alert System (ATLAS) catalog (Tonry et al., 2015; Kostov and Bonev, 2017) was used as the source of reference stars. *TT*'s period determination operates by finding model lightcurves based on a user-defined number of Fourier components which best fit the asteroid photometric data. The program lists the candidate periods found within a user-defined period range and sampling frequency, based on minimizing Root Mean Square Errors (RMSE), between the modelled and photometric magnitudes. The candidate periods are listed in increasing RMSE value and the entire suite of RMSE values is plotted as a "periodogram" for quality control. In these periodograms the object yielded a clear 'best-fit' period solution having well defined minima as shown in the following figures. Periodograms often exhibit several possible candidate periods, in which case an examination of the rotational phase plot for each of these is then conducted looking for a credible lightcurve. Where the object shape is the dominant factor in producing the observed magnitude changes, (typically having lightcurve amplitudes of >0.2 mag), the rotational phase plot often has two peaks and two troughs (bimodal) and this is usually chosen as the most likely for such asteroids.

In this paper no attempt is made to find an absolute magnitude and a value of G = 0.15 has been used throughout the calculations. Time-series magnitude estimates from different nights and observing locations using a variety of imaging equipment were offset in magnitude to bring them into alignment when producing the raw and rotational-phase plots. The same offset was used for each instance of an individual imaging setup. When this paper is accepted for publication all the observations will be loaded into the Asteroid Lightcurve Data Exchange Format (ALCDEF) database.

The lightcurve period and amplitude results reported here are based on a total of 264 exposures obtained during 2025 November. Our analysis found a synodic rotation period of 4.2971 ± 0.001 h and peak-to-peak amplitude of 0.2087 ± 0.0215 mag. These results are summarized in Table 1 below. Column 3 gives the span of dates over which the observations were made. Column 4 is the range of phase angles for each date range, if this is preceded by an asterisk this means the asteroid passed through minimum phase angle during the observing period. Columns 5 and 6 give the range of values for the Phase Angle Bisector (PAB) longitude and latitude respectively, for the mid date of the observation set. Column 7 gives the period and Column 8 the minimum possible formal error in hours given by TT. Columns 9 and 10 give the amplitude and its associated uncertainty in magnitude. Dips in the results from the period analysis have been checked to see if they are monomodal or bimodal and a bimodal period has been chosen for the best-fit result. Information given for the object is taken from the NASA Jet Propulsion Laboratory (JPL) Small-Body Database Lookup webpage (2023).

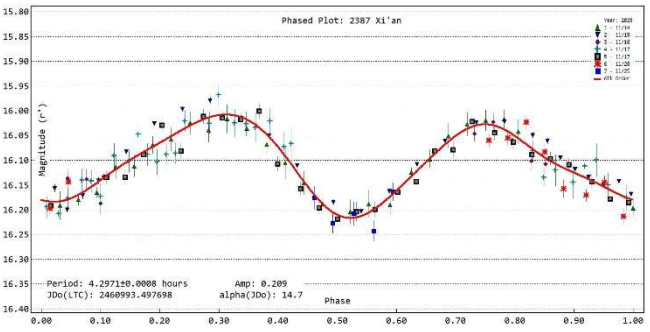

Number	Name	yyyy mm/dd	Phase	L_{PAB}	B_{PAB}	Period (h)	P.E.	Amp	A.E.	Grp
2387	Xi'an	2025 11/04-11/25	14.7,17.0	10	-6	4.2971	0.001	0.2087	0.022	606

Table I. Observing circumstances and results. The phase angle is given for the first and last date. If preceded by an asterisk, the phase angle reached a minimum during the period. L_{PAB} and B_{PAB} are the approximate phase angle bisector longitude/latitude at mid-date range (see Harris et al., 1984). Grp is the asteroid family/group (Warner et al., 2009).

Observatory	Telescope (m)	Camera	Filter	Object (sessions)
Old Orchard Observatory (Z09), Hawley	0.35 f/6.7	SX694 Trius Pro (2×2)	SR	2387 (3)
Tree Gate Farm Observatory (Q59), Gout	0.28 f/1.9	ASI 2600 MM Pro (1×1)	C	2387 (1)
Whiskey Creek Observatory (V19), DeGroff	0.457 Newt f/4.2	QHY 268M (2x2)	C	2387(1)
Al Khatim Observatory (M44), Odeh	0.36 f/7.7	ASI 2600 MM Pro (2x2)	C	2387 (1)
Astropriorat Observatory (M02), Genebriera	0.406 RC f/8	C4-16000EC CMOS (1×1)	V-Bessel	2387 (1)

Table II. List of observers and equipment. The number in parentheses in the last column is the number of sessions for the given object.

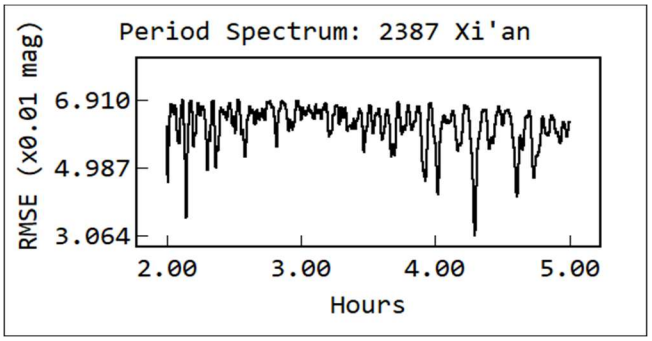

Acknowledgements

Our thanks are extended to Daniel Parrott, author of *Tycho Tracker Pro*. This work has made use of data from the Asteroid Terrestrial-impact Last Alert System (ATLAS) project. ATLAS is primarily funded to search for near earth asteroids through NASA grants NN12AR55G, 80NSSC18K0284, and 80NSSC18K1575; byproducts of the NEO search include images and catalogs from the survey area. The ATLAS science products have been made possible through the contributions of the University of Hawaii Institute for Astronomy, the Queen's University Belfast, the Space Telescope Science Institute, and the South African Astronomical Observatory. The ATLAS Catalog makes use of the formulae to convert Pan-STARRS gri to BVRI (Kostov and Bonev, 2017).

References

Durech, J.; Tonry, J.; Erasmus, N.; Denneau, L.; Heinze, A.N.; Flewelling, H.; Vanco, R. (2020). "Asteroid models reconstructed from ATLAS photometry." *A&A* **643**, A59.

Harris, A.W.; Young, J.W.; Scaltriti, F.; Zappala, V. (1984). "Lightcurves and phase relations of the asteroids 82 Alkmene and 444 Gyptis." *Icarus* **57**, 251-258.

JPL (2023). Small-Body Database Lookup. *https://ssd.jpl.nasa.gov/tools/sbdb_lookup.html*

Kostov, A.; Bonev, T. (2017). "Transformation of Pan-STARRS1 gri to Stetson BVRI magnitudes. Photometry of small bodies observations." *Bulgarian Astron. J.* **28**, 3 (ArXiv:1706.06147v2).

Tonry, J.L.; Denneau, L.; Flewelling, H.; Heinze, A.N.; Onken, C.A.; Smartt, S.J.; Stadler, B.; Weiland, H.J.; Wolf, C. (2018). "The ATLAS All-Sky Stellar Reference Catalog." *Ap. J.* **867**, A105.

Warner, B.D.; Harris, A.W.; Pravec, P. (2009). "The Asteroid Lightcurve Database." *Icarus* **202**, 134-146. Updated 2023 Oct 1. *https://minplanobs.org/mpinfo/php/lcdb.php*

Waszczak, A.; Chang, C.-K.; Ofek, E.O.; Laher, R.; Masci, F.; Levitan, D.; Surace, J.; Cheng, Y.-C.; Ip, W.-H.; Kinoshita, D.; Helou, G.; Prince, T.A.; Kulkarni, S. (2015). "Asteroid Light Curves from the Palomar Transient Factory Survey: Rotation Periods and Phase Functions from Sparse Photometry." *Astron. J.* **150**, A75.

LIGHTCURVE AND ROTATION PERIOD ANALYSIS OF 2990 TRIMBERGER

Wayne Hawley
Old Orchard Observatory (Z09)
Somerset, UK
hawley.wayne@gmail.com

Patrick Wiggins
University of Utah (718)
Utah, USA

Jean-Francois Gout
Tree Gate Farm Observatory (W05)
Mississippi, USA

Kent DeGroff
Whiskey Creek Observatory (V19)
New Mexico, USA

(Received: 2025 December 24)

Photometric observations of asteroid 2990 Trimberger were obtained during 2025 December. We found P = 7.787 ± 0.003 h, A = 0.898 ± 0.064 magnitudes. This agrees with the previously published result by Erasmus et al. (2020).

Minor planet 2990 Trimberger is a main-belt asteroid and member of the Nysa family that was discovered on 1981March 02 by S.J. Bus at Siding Spring. Our CCD photometric observations of 2990 Trimberger were made between 2025 December 10 and 2025 December 17. Photometry and period determination were carried out with *TychoTracker Pro* Version 12.6.1. (*TT*). The photometric analysis was performed using standard differential techniques on images with the comparison stars employed selected by *TT* to be within the colour range of +0.50 < (B-V) < +0.90.

The Asteroid Terrestrial-impact Last Alert System (ATLAS) catalog (Tonry et al., 2015; Kostov and Bonev, 2017) was used as the source of reference stars. *TT*'s period determination operates by finding model lightcurves based on a user-defined number of Fourier components which best fit the asteroid photometric data. The program lists the candidate periods found within a user-defined period range and sampling frequency, based on minimizing Root Mean Square Errors (RMSE), between the modelled and photometric magnitudes. The candidate periods are listed in increasing RMSE value and the entire suite of RMSE values is plotted as a "periodogram" for quality control. In these periodograms the object yielded a clear 'best-fit' period solution having well defined minima as shown in the following figures. Periodograms often exhibit several possible candidate periods, in which case an examination of the rotational phase plot for each of these is then conducted looking for a credible lightcurve. Where the object shape is the dominant factor in producing the observed magnitude changes, (typically having lightcurve amplitudes of >0.2 mag), the rotational phase plot often has two peaks and two troughs (bimodal) and this is usually chosen as the most likely for such asteroids.

In this paper no attempt is made to find an absolute magnitude and a value of G = 0.15 has been used throughout the calculations. Time-series magnitude estimates from different nights and observing locations using a variety of imaging equipment were offset in magnitude to bring them into alignment when producing the raw and rotational-phase plots. The same offset was used for each instance of an individual imaging setup. When this paper is accepted for publication all the observations will be loaded into the Asteroid Lightcurve Data Exchange Format (ALCDEF) database.

The lightcurve period and amplitude results reported here are based on a total of 186 exposures obtained during 2025 December. Our analysis found a synodic rotation period of 7.787 ± 0.003 h and peak-to-peak amplitude of 0.898 ± 0.064 mag. These results are summarized in Table 1 below. Column 3 gives the span of dates over which the observations were made. Column 4 is the range of phase angles for each date range, if this is preceded by an asterisk this means the asteroid passed through minimum phase angle during the observing period. Columns 5 and 6 give the range of values for the Phase Angle Bisector (PAB) longitude and latitude respectively, for the mid date of the observation set. Column 7 gives the period and Column 8 the minimum possible formal error in hours given by *TT*. Columns 9 and 10 give the amplitude and its associated uncertainty in magnitude. Dips in the results from the period analysis have been checked to see if they are monomodal or bimodal and a bimodal period has been chosen for the best-fit result. Information given for the object is taken from the NASA Jet Propulsion Laboratory (JPL) Small-Body Database Lookup webpage (2023).

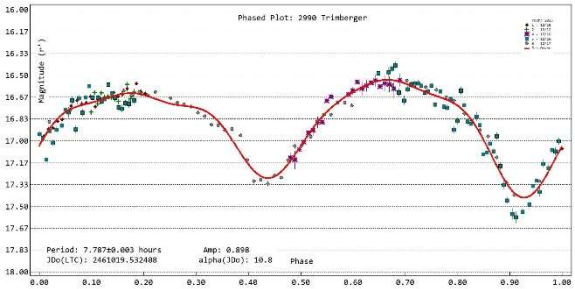

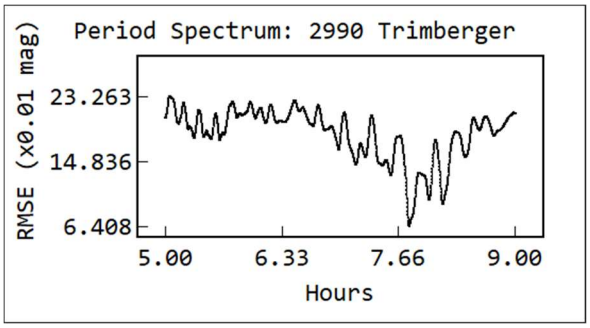

Number	Name	yyyy mm/dd	Phase	L_{PAB}	B_{PAB}	Period (h)	P.E.	Amp	A.E.	Grp
2990	Trimberger	2025 12/10-12/17	10.8,14.1	58	-3	7.787	0.003	0.898	0.06	405

Table I. Observing circumstances and results. The phase angle is given for the first and last date. If preceded by an asterisk, the phase angle reached a minimum during the period. L_{PAB} and B_{PAB} are the approximate phase angle bisector longitude/latitude at mid-date range (see Harris et al., 1984). Grp is the asteroid family/group (Warner et al., 2009).

Observatory	Telescope (m)	Camera	Filter	Object (sessions)
Old Orchard House Observatory (Z09), Hawley	0.35 *f*/6.7	SX694 Trius Pro (2 x 2)	SR	2990 (2)
University of Utah (718), Wiggins	0.35 f/5.5	SBIG ST-10XME (3 x 3)	C	2990 (1)
Tree Gate Farm Observatory (W05), Gout	0.28 *f*/1.9	ASI 2600 MM (1x1)	C	2990 (2)
Whiskey Creek Observatory (V19), DeGroff	0.46 *f*/4.2	QHY 268M (2x2)	C	2990 (1)

Table II. List of observers and equipment. The number in parentheses in the last column is the number of sessions for the given object.

Acknowledgements

Our thanks are extended to Daniel Parrott, author of *Tycho Tracker Pro*. This work has made use of data from the Asteroid Terrestrial-impact Last Alert System (ATLAS) project. ATLAS is primarily funded to search for near earth asteroids through NASA grants NN12AR55G, 80NSSC18K0284, and 80NSSC18K1575; byproducts of the NEO search include images and catalogs from the survey area. The ATLAS science products have been made possible through the contributions of the University of Hawaii Institute for Astronomy, the Queen's University Belfast, the Space Telescope Science Institute, and the South African Astronomical Observatory. The ATLAS Catalog makes use of the formulae to convert Pan-STARRS gri to BVRI (Kostov and Bonev, 2017).

References

Erasmus, N.; Navarro-Meza, S.; McNeill, A.; Trilling, D.E.; Sickafoose, A.A.; Denneau, L.; Flewelling, H.; Heinze, A.; Tonry, J.L. (2020). "Investigating Taxonomic Diversity within Asteroid Families through ATLAS Dual-Band Photometry" *The Astrophysical Journal Supplement Series* **247**, 7pp.

Harris, A.W.; Young, J.W.; Scaltriti, F.; Zappala, V. (1984). "Lightcurves and phase relations of the asteroids 82 Alkmene and 444 Gyptis." *Icarus* **57**, 251-258.

JPL (2023). Small-Body Database Lookup. *https://ssd.jpl.nasa.gov/tools/sbdb_lookup.html*

Kostov, A.; Bonev, T. (2017). "Transformation of Pan-STARRS1 gri to Stetson BVRI magnitudes. Photometry of small bodies observations." *Bulgarian Astron. J.* **28**, 3 (ArXiv:1706.06147v2).

Tonry, J.L.; Denneau, L.; Flewelling, H.; Heinze, A.N.; Onken, C.A.; Smartt, S.J.; Stadler, B.; Weiland, H.J.; Wolf, C. (2018). "The ATLAS All-Sky Stellar Reference Catalog." *Ap. J.* **867**, A105.

Warner, B.D.; Harris, A.W.; Pravec, P. (2009). "The Asteroid Lightcurve Database." *Icarus* **202**, 134-146. Updated 2023 Oct 1. *https://minplanobs.org/mpinfo/php/lcdb.php*

LIGHTCURVE AND ROTATION PERIOD ANALYSIS OF 4382 STRAVINSKY

Wayne Hawley
Old Orchard Observatory (Z09)
Fiddington, UK
hawley.wayne@gmail.com

Patrick Wiggins
University of Utah (718)
Utah, USA

Jean-Francois Gout
Tree Gate Farm Observatory (W05)
Mississippi, USA

Brian Scott
Calne Observatory (247)
Wiltshire, UK

Scott Hopkins
Medina Dome Observatory (V58)
Texas, USA

Kent DeGroff
Whiskey Creek Observatory (V19)
New Mexico, USA

(Received: 2026 January 12)

Photometric observations of asteroid 4382 Stravinsky were obtained during 2025 Sep - Dec. For 4382 Stravinsky, we found P = 12.20 ± 0.01 h, A = 0.1339 ± 0.0309 magnitudes. Ďurech et al. (2019) reports a period of 12.19702 h.

Minor planet 4382 Stravinsky is an inner main-belt asteroid that was discovered on 1989 November 29 by F. Borngen at Tautenburg. Our photometric observations of 4382 Stravinsky were made from 2025 September 23 to 2025 December 31. Photometry and period determination were carried out with *TychoTracker Pro* Version 12.6.1. (*TT*). The photometric analysis was performed using standard differential techniques on images with the comparison stars employed selected by *TT* to be within the colour range of +0.50 < (B-V) < +0.90.

The Asteroid Terrestrial-impact Last Alert System (ATLAS) catalog (Tonry et al., 2015; Kostov and Bonev, 2017) was used as the source of reference stars. *TT*'s period determination operates by finding model lightcurves based on a user-defined number of Fourier components which best fit the asteroid photometric data. The program lists the candidate periods found within a user-defined period range and sampling frequency, based on minimizing Root Mean Square Errors (RMSE), between the modelled and photometric magnitudes. The candidate periods are listed in increasing RMSE value and the entire suite of RMSE values is plotted as a "periodogram" for quality control. In these periodograms the object yielded a clear 'best-fit' period solution having well defined minima as shown in the following figures. Periodograms often exhibit several possible candidate periods, in which case an examination of the rotational phase plot for each of these is then conducted looking for a credible lightcurve. Where the object shape is the dominant factor in producing the observed magnitude changes, (typically having lightcurve amplitudes of >0.2 mag), the rotational phase plot often has two peaks and two troughs (bimodal) and this is usually chosen as the most likely for such asteroids.

In this paper no attempt is made to find an absolute magnitude and a value of G = 0.15 has been used throughout the calculations. Time-series magnitude estimates from different nights and observing locations using a variety of imaging equipment were offset in magnitude to bring them into alignment when producing the raw and rotational-phase plots. The same offset was used for each instance of an individual imaging setup. When this paper is accepted for publication all the observations will be loaded into the Asteroid Lightcurve Data Exchange Format (ALCDEF) database.

The lightcurve period and amplitude results reported here are based on a total of 795 exposures obtained during 2025 September to December. Our analysis found a synodic rotation period of 12.20 ± 0.01 h and peak-to-peak amplitude of 0.1339 ± 0.0309 mag. These results are summarized in Table 1 below. Column 3 gives the span of dates over which the observations were made. Column 4 is the range of phase angles for each date range, if this is preceded by an asterisk this means the asteroid passed through minimum phase angle during the observing period. Columns 5 and 6 give the range of values for the Phase Angle Bisector (PAB) longitude and latitude respectively, for the mid date of the observation set. Column 7 gives the period and Column 8 the minimum possible formal error in hours given by TT. Columns 9 and 10 give the amplitude and its associated uncertainty in magnitude. Dips in the results from the period analysis have been checked to see if they are monomodal or bimodal and a bimodal period has been chosen for the best-fit result. Information given for the object is taken from the NASA Jet Propulsion Laboratory (JPL) Small-Body Database Lookup webpage (2023).

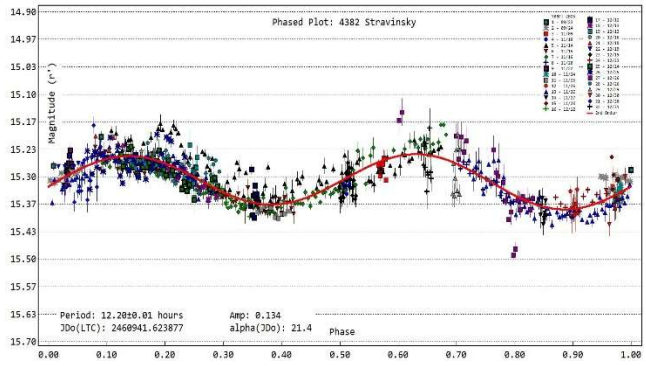

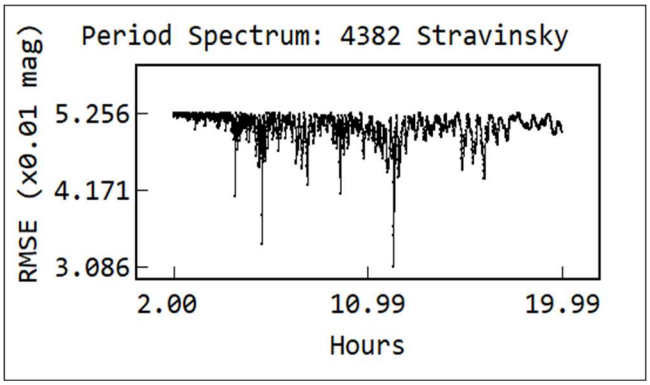

Number	Name	yyyy mm/dd	Phase	L_{PAB}	B_{PAB}	Period (h)	P.E.	Amp	A.E.	Grp
4382	Stravinsky	2025 09/23-12/31	*6.1,23.6	44	-7	12.20	0.01	0.134	0.03	9104

Table I. Observing circumstances and results. The phase angle is given for the first and last date. If preceded by an asterisk, the phase angle reached a minimum during the period. L_{PAB} and B_{PAB} are the approximate phase angle bisector longitude/latitude at mid-date range (see Harris et al., 1984). Grp is the asteroid family/group (Warner et al., 2009).

Observatory	Telescope (m)	Camera	Filter	Object (sessions)
Old Orchard Observatory (Z09), Hawley	0.35 f/6.7	SX 694 Trius Pro (2x2)	SR	4382 (9)
University of Utah (718), Wiggins	0.35 *f*/5.5	SBIG ST-10XME (3x3)	C	4382 (11)
Tree Gate Farm Observatory (W05), Gout	0.28 f/1.9	ASI 2600 MM (2x2)	C	4382 (1)
Calne Observatory (247), Scott	0.35 *f*/5.5	SX 684 (2x2)	C	4382 (1)
Whiskey Creek Observatory (V19), DeGroff	0.35 f/4.2	QHY 268 M (2x2)	C	4382 (6)
Medina Dome Observatory (V58), Hopkins	0.3 *f*/8	ASI 6200 MM	C	4382 (4)

Table II. List of observers and equipment. The number in parentheses in the last column is the number of sessions for the given object.

Acknowledgements

Our thanks are extended to Daniel Parrott, author of *Tycho Tracker Pro*. This work has made use of data from the Asteroid Terrestrial-impact Last Alert System (ATLAS) project. ATLAS is primarily funded to search for near earth asteroids through NASA grants NN12AR55G, 80NSSC18K0284, and 80NSSC18K1575; byproducts of the NEO search include images and catalogs from the survey area. The ATLAS science products have been made possible through the contributions of the University of Hawaii Institute for Astronomy, the Queen's University Belfast, the Space Telescope Science Institute, and the South African Astronomical Observatory. The ATLAS Catalog makes use of the formulae to convert Pan-STARRS gri to BVRI (Kostov and Bonev, 2017).

References

Ďurech, J.; Hanuš, J.; Vančo, R. (2019). "Inversion of asteroid photometry from Gaia DR2 and the Lowell Observatory photometric database." *A&A* **631**, A2.

Harris, A.W.; Young, J.W.; Scaltriti, F.; Zappala, V. (1984). "Lightcurves and phase relations of the asteroids 82 Alkmene and 444 Gyptis." *Icarus* **57**, 251-258.

JPL (2023). Small-Body Database Lookup. *https://ssd.jpl.nasa.gov/tools/sbdb_lookup.html*

Kostov, A.; Bonev, T. (2017). "Transformation of Pan-STARRS1 gri to Stetson BVRI magnitudes. Photometry of small bodies observations." *Bulgarian Astron. J.* **28**, 3 (ArXiv:1706.06147v2).

Tonry, J.L.; Denneau, L.; Flewelling, H.; Heinze, A.N.; Onken, C.A.; Smartt, S.J.; Stadler, B.; Weiland, H.J.; Wolf, C. (2018). "The ATLAS All-Sky Stellar Reference Catalog." *Ap. J.* **867**, A105.

Warner, B.D.; Harris, A.W.; Pravec, P. (2009). "The Asteroid Lightcurve Database." *Icarus* **202**, 134-146. Updated 2023 Oct 1. *https://minplanobs.org/mpinfo/php/lcdb.php*

LIGHTCURVE AND ROTATION PERIOD ANALYSIS OF ASTEROIDS 1354 BOTHA AND 6514 TORAHIKO

Wayne Hawley
Old Orchard Observatory (Z09)
Somerset, UK
hawley.wayne@gmail.com

Joan Genebriera
Astropriorat Observatory (M02)
Catalonia, SPAIN

Mohammad Odeh
Al Khatim Observatory (M44)
Abu Dhabi, UAE

Nidhal Guessoum, Rawan Mohamed Shah
Department of Physics
American University of Sharjah PO Box 26666, Sharjah, UAE.

Emmanuel Kardasis
Pelagia-Eleni Observatory (247)
Attica, GREECE

Brian Scott
Calne Observatory (247)
Wiltshire, UK

Kent DeGroff
Whiskey Creek Observatory (V19)
New Mexico, USA

Jean-Francois Gout
Tree Gate Farm Observatory (W05)
Mississippi, USA

(Received: 2025 December 24)

Photometric observations of asteroid 1354 Botha were obtained during 2025 Sep-Nov. Photometric observations of asteroid 6514 Torahiko were obtained during 2025 Nov-Dec.

Photometry and period determination were carried out with *TychoTracker Pro* Version 12.6.1. (TT). The photometric analysis was performed using standard differential techniques on images with the comparison stars employed selected by TT to be within the colour range of +0.50 < (B-V) < +0.90.

The Asteroid Terrestrial-impact Last Alert System (ATLAS) catalog (Tonry et al., 2018; Kostov and Bonev, 2017) was used as the source of reference stars. *TT*'s period determination operates by finding model lightcurves based on a user-defined number of Fourier components which best fit the asteroid photometric data. The program lists the candidate periods found within a user-defined period range and sampling frequency, based on minimizing Root Mean Square Errors (RMSE), between the modelled and photometric magnitudes. The candidate periods are listed in increasing RMSE value and the entire series of RMSE values is plotted as a "periodogram" for quality control. In these periodograms the object yielded a clear 'best-fit' period solution with well-defined minima as shown in the following figures. Periodograms often exhibit several possible candidate periods, in which case an examination of the rotational phase plot for each of these is conducted to look for a credible lightcurve. Where the object shape is the dominant factor in producing the observed magnitude changes, (typically having lightcurve amplitudes of >0.2 mag), the rotational phase plot often has two peaks and two troughs (bimodal), and this is usually chosen as the most likely for such asteroids.

In this paper, no attempt is made to find an absolute magnitude, and a value of G = 0.15 has been used throughout the calculations. Time-series magnitude estimates from different nights and observing locations, using a variety of imaging equipment, were offset in magnitude to bring them into alignment when producing the raw and rotational-phase plots. The same offset was used for each instance of an individual imaging setup. When this paper is accepted for publication all the observations will be loaded into the Asteroid Lightcurve Data Exchange Format (ALCDEF) database.

The results are summarized in Table 1 below. Column 3 gives the span of dates over which the observations were made. Column 4 is the range of phase angles for each date range; if this is preceded by an asterisk, it means the asteroid passed through minimum phase angle during the observing period. Columns 5 and 6 give the range of values for the Phase Angle Bisector (PAB) longitude and latitude respectively, for the mid date of the observation set. Column 7 gives the period, and Column 8 the minimum possible formal error in hours, as given by TT. Columns 9 and 10 give the amplitude and its associated uncertainty. Dips in the results from the period analysis have been checked to see if they are monomodal or bimodal, and a bimodal period has been chosen for the best-fit result. Information given for the object is taken from the NASA Jet Propulsion Laboratory (JPL) Small-Body Database Lookup webpage (2023).

1354 Botha is an outer main-belt asteroid that was discovered on 1935 April 03 by C. Jackson at Johannesburg (UO). The lightcurve period and amplitude results reported here are based on a total of 638 exposures obtained during 2025 Sep-Nov. Our analysis found a synodic rotation period of 8.375 ± 0.005 h and peak-to-peak amplitude of 0.249 ± 0.0387 mag. This period agrees with earlier results reported in the Lightcurve Database (LCDB) from Wiles (2023) and Fornas et al. (2024). There is also an earlier result in the LCDB, Behrend (2003web) of 4h.

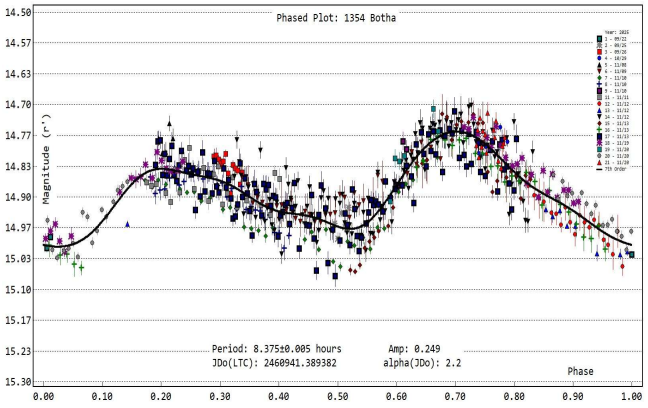

Number	Name	yyyy mm/dd	Phase	L_{PAB}	B_{PAB}	Period (h)	P.E.	Amp	A.E.	Grp
1354	Botha	2025 09/22-11/20	*1.3,16.4	5	-1	8.375	0.005	0.249	0.04	9106
6514	Torahiko	2025 11/25-12/11	4.4,12.3	58	-3	8.729	0.004	0.176	0.02	9105

Table I. Observing circumstances and results. The phase angle is given for the first and last date. If preceded by an asterisk, the phase angle reached a minimum during the period. L_{PAB} and B_{PAB} are the approximate phase angle bisector longitude/latitude at mid-date range (see Harris et al., 1984). Grp is the asteroid family/group (Warner et al., 2009).

Observatory	Telescope (m)	Camera	Filter	Object (sessions)
Old Orchard Observatory (Z09), Hawley	0.35 f/6.7	SX694 Trius Pro (2×2)	SR	1354 (8) 6514 (4)
Pelagia-Eleni Observatory (247), Kardasis	0.35 *f*/8	ASI 183 MM Pro (1×1)	L	1354 (1)
Tree Gate Farm Observatory (Q59), Armstrong	0.28 f/1.9	ASI 2600 MM Pro (1×1)	C	1354 (4) 6514 (1)
Whiskey Creek Observatory (V19), DeGroff	0.457m Newt f/4.2	QHY 268M (2x2)	C	1354 (3)
Calne Observatory (247), Scott	0.28 f/8 SCT	SX-H674 (2x2)	L	1354 (1)
Al Khatim Observatory (M44), Odeh, Guessoum, Shah	0.36 *f*/7.7	ASI 2600 MM Pro (2x2)	SR	1354 (2)
Astropriorat Observatory (M02), Genebriera	0.41 f/3	QHY 600 CMOS (1×1)	SR	1354 (2) 6514 (1)

Table II. List of observers and equipment. The number in parentheses in the last column is the number of sessions for the given object.

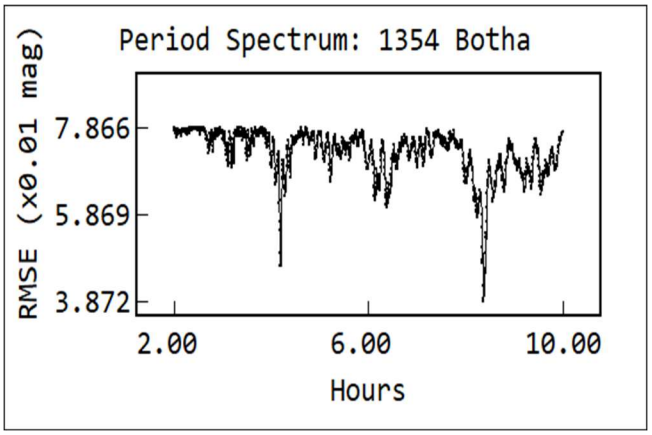

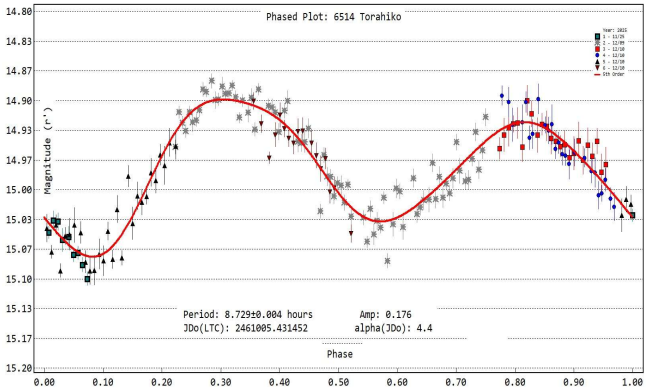

6514 Torahiko is a an middle main-belt asteroid that was discovered 1987 Nov. 25 by Seki at Geisei. The lightcurve period and amplitude results reported here are based on a total of 184 exposures obtained during 2025 Nov-Dec. Our analysis found a synodic rotation period of 8.729 ± 0.004 h and peak-to-peak amplitude of 0.1764 ± 0.017 mag. Earlier periods are reported in the LCDB from Pravec (2016web), 8.7207h; and Pál et al. (2020), 8.71697 h.

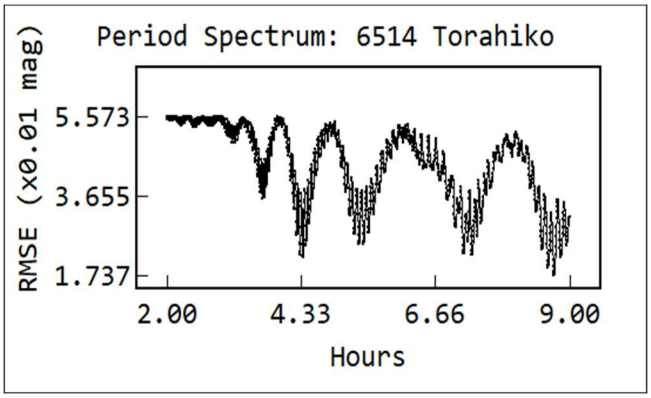

Acknowledgements

Our thanks are extended to Daniel Parrott, author of *Tycho Tracker Pro*. This work has made use of data from the Asteroid Terrestrial-impact Last Alert System (ATLAS) project. ATLAS is primarily funded to search for near earth objects (NEOs) through NASA grants NN12AR55G, 80NSSC18K0284, and 80NSSC18K1575; byproducts of the NEO search include images and catalogs from the survey area. The ATLAS science products have been made possible through the contributions of the University of Hawaii Institute for Astronomy, the Queen's University Belfast, the Space Telescope Science Institute, and the South African Astronomical Observatory. The ATLAS Catalog makes use of the formulae to convert Pan-STARRS gri to BVRI (Kostov and Bonev, 2017).

References

Behrend, R. (2003web). Observatoire de Geneve website. *http://obswww.unige.ch/~behrend/page_cou.html*

Fornas, G.; Huet, F.; Barberá, R.; Fornas, Á.; Mas, V. (2024). "Lightcurve Analysis for Twelve Main-Belt and One PHA Asteroids." *Minor Planet Bulletin* **51**, 33-38.

Pál, A.; Szakáts, R.; Kiss, C.; Bódi, A.; Bognár, Z.; Kalup, C.; Szabó, R. (2020). "Solar system objects observed with TESS-first data release: bright main-belt and Trojan asteroids from the southern survey." *The Astrophysical Journal Supplement Series* **247**, 26.

Wiles, M. (2023). "Rotation Period and Lightcurve Determination for Fourteen Minor Planets." *Minor Planet Bulletin* **50**, 290-294.

Pravec, P. (2016web). *https://space.asu.cas.cz/~ppravec/newres.txt*

Harris, A.W.; Young, J.W.; Scaltriti, F.; Zappala, V. (1984). "Lightcurves and phase relations of the asteroids 82 Alkmene and 444 Gyptis." *Icarus* **57**, 251-258.

JPL (2023). Small-Body Database Lookup. *https://ssd.jpl.nasa.gov/tools/sbdb_lookup.html*

Kostov, A.; Bonev, T. (2017). "Transformation of Pan-STARRS1 gri to Stetson BVRI magnitudes. Photometry of small bodies observations." *Bulgarian Astron. J.* **28**, 3 (ArXiv:1706.06147v2).

Tonry, J.L.; Denneau, L.; Flewelling, H.; Heinze, A.N.; Onken, C.A.; Smartt, S.J.; Stadler, B.; Weiland, H.J.; Wolf, C. (2018). "The ATLAS All-Sky Stellar Reference Catalog." *Ap. J.* **867**, A105.

Warner, B.D.; Harris, A.W.; Pravec, P. (2009). "The Asteroid Lightcurve Database." *Icarus* **202**, 134-146. Updated 2023 Oct 1. *https://minplanobs.org/mpinfo/php/lcdb.php*

Warner, B.D., ed. (2021). Asteroid Lightcurve Data Exchange Format (ALCDEF) Database Bundle V1.0. urn:nasa:pds:gbo.ast.alcdef-database::1.0. NASA Planetary Data System. *https://doi.org/10.26033/b8cw-s522*

LIGHTCURVES AND ROTATION PERIODS OF FOUR MAIN-BELT ASTEROIDS

Federico Palaia
Civico Osservatorio Astronomico di Rozzano (D66)
Viale Palmiro Togliatti 105
20089 Rozzano MI, ITALY
info@astrofilirozzano.it

Mauro Santarossa, Mirko Gusmaroli, Nicola Montecchiari
Gruppo Astrofili Rozzano, ITALY

(Received: 2026 January 9)

During 2025 June through October, photometric observations of several main-belt asteroids were obtained primarily with the 0.40m *f*/10 Meade ACF telescope, SBIG ST10-XME and Moravian G4-9000 CCD camera (clear filter) at Civico Osservatorio Astronomico di Rozzano (D66). Typical exposures were 90-120-180s, guided, and calibrated with dark and flat frames. Tycho Tracker was used for image alignment and calibration; *MPO Canopus* performed differential photometry and Fourier period analysis.

2684 Douglas. The only previously published lightcurve analysis is that of Benitez et al. (2021), who derived a synodic rotation period of 4.007 ± 0.001 h and a peak-to-peak amplitude of 0.62 mag. Their phased lightcurve exhibited considerable scatter in one of the minima, with some points lying more than 0.10 mag below the mean Fourier curve, prompting the authors to suggest possible binarity.

Our observations, obtained over an interval of more than three months, yield a well-constrained synodic period of 4.084 ± 0.001 h and an amplitude of 0.51 ± 0.07 mag (sixth-order Fourier model). The ~2 % difference in period is typical of the small systematic shifts expected when the asteroid is observed at significantly different sub-Earth latitudes between apparitions. The lower amplitude is fully consistent with the smaller range of phase angles covered in the present work compared to Benitez et al. (2021).

The lightcurve confirms the pronounced asymmetry reported earlier: one minimum remains systematically deeper and shows deviations reaching ~0.10 mag from the best-fit Fourier curve, while the opposite minimum is smooth and well behaved. To test the binary hypothesis, the data were searched for a secondary period using *MPO Canopus*. No statistically significant secondary periodicity was found in the 1-30 h range. Attempts to subtract tentative secondary periods in the 10-20 h interval slightly reduced the scatter in the primary minimum, but the resulting secondary lightcurve was essentially featureless and the corresponding peak in the period spectrum did not meet the usual significance criteria. We therefore conclude that the observed asymmetry is most likely produced by concave surface features, albedo variegation, or shape irregularities rather than the presence of a satellite.

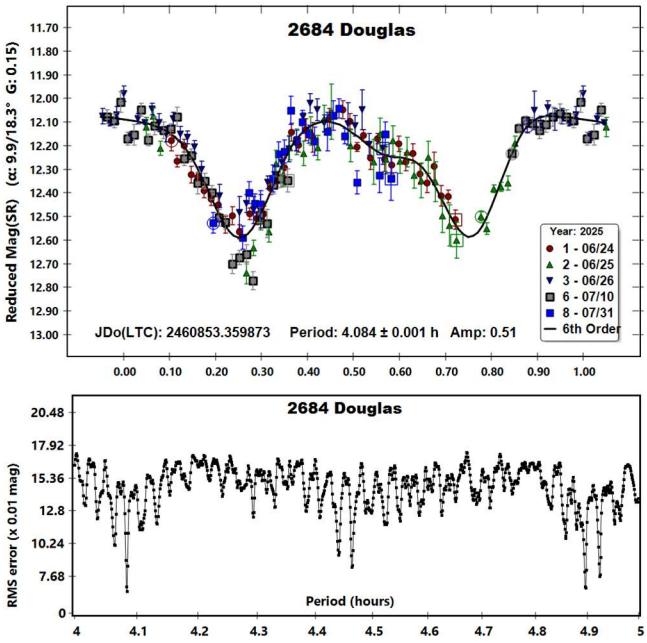

3159 Prokof'ev. Previous lightcurve results for this asteroid are limited and inconsistent. Moravec et al. (2013) obtained a period of 3.89 ± 0.05 h with an amplitude of 0.42 mag from relatively dense photometry. Waszczak et al. (2015), using sparse data from the Palomar Transient Factory survey, derived a period of 3.886 ± 0.001 h and amplitude of 0.08 mag.

Our data set includes three sessions (2025 Oct 10, 11, and 13) contributed by N. Montecchiari from a private remote observatory in Tuscany (MPC code M27, 0.25-m RC telescope, QSI583wsg CCD camera, dark-sky site). These data, reduced with the author's *Variabilia* software, were combined with the observations from Rozzano and analyzed jointly in *MPO Canopus*.

The resulting best-fit synodic period is 4.201 ± 0.001 h (fourth-order Fourier model, RMS = 0.029 mag). When the period is constrained to values near 3.887 h, the RMS rises to 0.031 mag and the minimum in the period spectrum becomes noticeably shallower. The fitted peak-to-peak amplitude is 0.05 ± 0.03 mag. Given that the RMS scatter of the individual sessions is 0.022-0.032 mag and the overall fit RMS is 0.029 mag, an amplitude of this magnitude is only marginally above the noise level and must be considered uncertain. The low value is nevertheless consistent with the observations and indicates either a near pole-on aspect during the apparition or an intrinsically small equatorial ellipticity (or both).

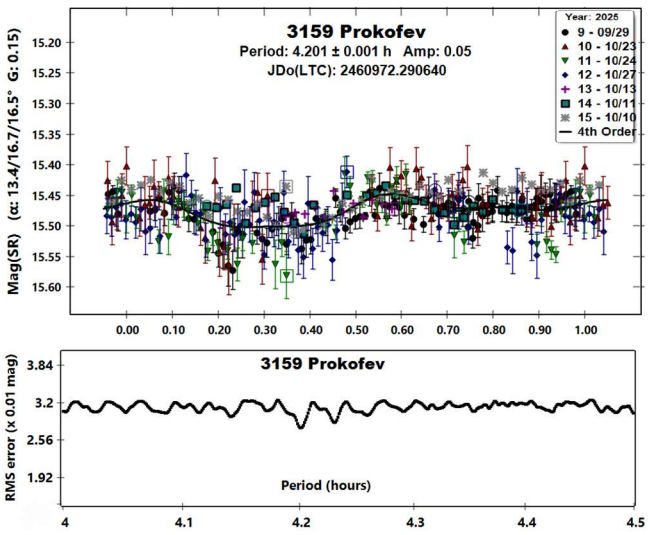

1586 Thiele. Previously reported lightcurve results for this asteroid are available through the literature and the ALCDEF archive, but they show some dispersion in both the derived rotation period and amplitude. Behrend (2003web) reported a period of 3.12 ± 0.5 h with a peak-to-peak amplitude of 0.30 ± 0.06 mag, later refined by Behrend (2004web) to 3.12 ± 0.10 h and an amplitude of 0.38 ± 0.02 mag. Childers and Church (2007), using high-speed photometry, derived a period of 3.086 ± 0.038 h and a significantly smaller amplitude of 0.14 ± 0.01 mag; however, their published lightcurve exhibits substantial scatter.

Our observations consist of a single session obtained under excellent and stable meteorological conditions, with very steady seeing throughout the run. Images were acquired using a Moravian G4-9000 CCD camera with 90-s exposures and a clear filter. To check for possible systematic effects, the data set was divided into two subsets corresponding to observations obtained before and after the meridian flip; these subsets were reduced and analyzed independently and were found to be fully consistent. The combined data were then used for the final period analysis in *MPO Canopus*.

The resulting best-fit synodic rotation period is 3.304 ± 0.005 h, derived using a tenth-order Fourier model, which provides the minimum RMS residual of 0.014 mag. The corresponding peak-to-peak amplitude is 0.38 mag. The scatter of the data is very small, and individual points closely follow the Fourier curve, with no systematic deviations evident in either half of the observing session.

Number	Name	yyyy mm/dd	Phase	L_{PAB}	B_{PAB}	Period(h)	P.E.	Amp	A.E.	Grp
2684	Douglas	2025 06/24-07/31	9.9,18.3	252	12	4.084	0.001	0.51	0.07	MBA
3159	Prokof'ev	2025 09/29-10/27	13.4,20.2	343	14	4.201	0.001	0.05	0.03	MBA
1586	Thiele	2025 12/29-12/30	8.0	112	-2	3.304	0.005	0.38	0.01	MBA
1912	Anubis	2026 01/04-01/07	11.5,12.5	76	0.4	4.630	0.002	0.35	0.04	MBA

Table I. Observing circumstances and results. The phase angle is given for the first and last date. If preceded by an asterisk, the phase angle reached an extrema during the period. L_{PAB} and B_{PAB} are the approximate phase angle bisector longitude/latitude at mid-date range (see Harris et al., 1984). Grp is the asteroid family/group (Warner et al., 2009).

The data were also phased to the periods reported by Behrend (2004web) and by Childers and Church (2007), but these solutions produced noticeably inferior fits. The amplitude derived in the present work is consistent with the maximum values reported by Behrend (2004web), while the longer period differs significantly from the ~3.1 h solutions previously published. The much lower amplitude reported by Childers and Church (2007) is not supported by our observations and is likely influenced by the larger scatter present in their data. Despite being based on a single night, the low RMS and internal consistency of the data indicate that the derived period and amplitude provide a reliable characterization of the lightcurve of 1586 Thiele during the present apparition.

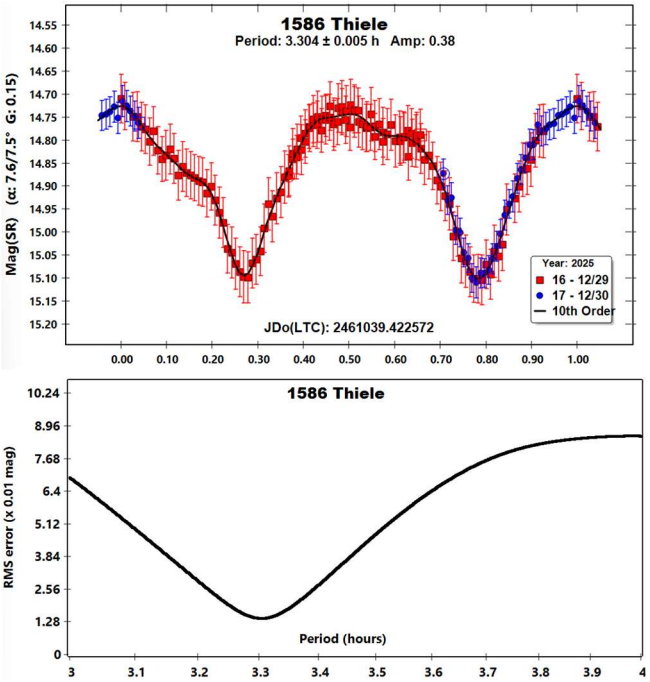

1912 Anubis. Previously published lightcurve information for this asteroid is limited to sparse-photometry results from the Palomar Transient Factory survey, reported by Waszczak et al. (2015). Two data sets are available from that study. The first, obtained on 2010 Oct 27, yielded a rotation period of 4.626 ± 0.001 h with a reported maximum amplitude of 0.47 mag. A second solution, based on data from 2012 Jan 26, gave a period of 4.628 ± 0.001 h and a significantly smaller amplitude of 0.18 mag. The difference in amplitude between the two determinations likely reflects the sparse nature of the data and/or different observing geometries.

Our observations were obtained over three observing nights during the same apparition and provided sufficient coverage to derive a well-defined lightcurve. Images were acquired using a CCD camera with 90-s exposures and a clear filter. The data were calibrated and aligned with *Tycho Tracker* and analyzed using *MPO Canopus*.

The resulting best-fit synodic rotation period is 4.630 ± 0.002 h, with a peak-to-peak amplitude of 0.35 ± 0.04 mag. The phased lightcurve is well behaved, with low scatter and a stable solution across the three nights, indicating that the derived period is robust. Our period is in agreement with the values reported by Waszczak et al. (2015), while the intermediate amplitude is consistent with expectations for different viewing aspects and phase-angle coverage. The present results therefore provide a refined lightcurve solution for 1912 Anubis based on dense photometric observations.

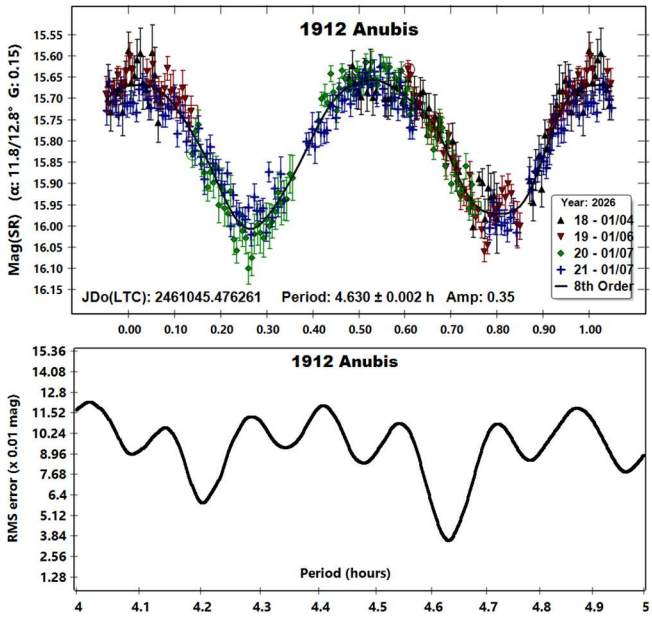

Acknowledgements

We express our gratitude to the Gruppo Astrofili Rozzano for their unwavering support and for providing access to the instrumentation whenever needed. Special thanks are extended to the president, Michele Bini, for his belief in this project and his encouragement throughout the study.

References

Behrend, R. (2003web, 2004web). Observatoire de Genève web site. *http://obswww.unige.ch/~behrend/page_cou.html*

Benitez, E.; Campanella, A.; Cowger, D.; Kirk, R.; Weller, J.; Wilkerson, L.; Wroblewski, A. (2021). "Analysis of Lightcurves to Find the Rotation Periods of Three Asteroids." *Minor Planet Bulletin* **48**, 8-10.

Childers, D.; Church, A. (2007). "High-speed Photometric Analysis for Minor Planets 1586 Thiele, 4246 Telemann, (10662) 32-1 T-2, and (49880) 1999 XP135." *Minor Planet Bulletin* **34**, 124-125.

Harris, A.W.; Young, J.W.; Scaltriti, F.; Zappala, V. (1984). "Lightcurves and phase relations of the asteroids 82 Alkmene and 444 Gyptis." *Icarus* **57**, 251-258.

Moravec, P.; Letfullina, A.; Ditteon, R. (2013). "Asteroid Lightcurve Analysis at the Oakley Observatories: 2012 May - June." *Minor Planet Bulletin* **40**, 17-20.

Warner, B.D.; Harris, A.W.; Pravec, P. (2009). "The Asteroid Lightcurve Database." *Icarus* **202**, 134-146. Updated 2023 Oct. *http://www.minorplanet.info/lightcurvedatabase.html*

Waszczak, A.; Chang, C.-K.; Ofek, E.O.; Laher, R.; Masci, F.; Levitan, D.; Surace, J.; Cheng, Y.-C.; Ip, W.-H.; Kinoshita, D.; Helou, G.; Prince, T.A.; Kulkarni, S. (2015). "Asteroid Light Curves from the Palomar Transient Factory Survey: Rotation Periods and Phase Functions from Sparse Photometry." *Astron. J.* **150**, A75.

LIGHTCURVE AND ROTATION PERIODS FOR 6422 AKAGI AND 7723 LUGGER

Michael Fauerbach
Florida Gulf Coast University
and SARA Observatories
10501 FGCU Blvd.
Ft. Myers, FL 33965-6565 USA
mfauerba@fgcu.edu

Michael P. Lucas
Florida Space Institute
12354 Research Parkway
University of Central Florida
Orlando, FL 32826 USA

(Received: 2025 December 16)

Photometric observations of Eunomia family member 6422 Akagi and Mars-crossing asteroid 7723 Lugger were obtained to verify their synodic rotation periods. We found: 6422 Akagi P = 7.795±0.001 h with A = 0.92±0.05 mag; 7723 Lugger P = 4.835±0.001 h with A = 0.36 ±0.02 mag.

Photometric observations of asteroids 6422 Akagi and 7723 Lugger were obtained with the 0.6-m telescope of the Southeastern Association for Research in Astronomy (SARA) consortium at Cerro Tololo Inter-American Observatory. The telescope is coupled with an Andor iKon-L series CCD, and a SDSS R filter was used for all images. A detailed description of the instrumentation and setup can be found in Keel et al. (2017). Images were calibrated with dark and flat frames and converted to standard magnitudes using solar colored field stars from the ATLAS All-Sky Stellar Reference Catalogue, distributed with *MPO Canopus* (Warner, 2025). All new data for these asteroids can be found in the Asteroid Lightcurve Data Exchange Format (ALCDEF) database.

6422 Akagi is a member of the Eunomia family (Nesvorný et al., 2015). The asteroid was observed on three nights over a period of four weeks with 258 total observations. The lightcurve database (LCDB, Warner et al., 2009) lists a period of 7.74 h based on (Chang et al., 2016). Two later papers by Ďurech et al. (2016, 7.74756 h) and Pál et al. (2020, 7.75104 h), refine this value. This current work derived a rotational period of 7.795 ± 0.001 h with an amplitude of 0.92 mag (Figure 1a) in fair agreement with the previously published results. Despite the relatively dense lightcurve the result is somewhat ambiguous. We also display our data fit to the period derived by Ďurech et al. (2016), which at first glance provides a better fit to the data (Figure 1b). However, it should be pointed out that the two datasets from 2025 July 25 and 2025 July 26 are at a phase angle close to zero, whereas the data from 2025 June 26 was taken at a larger phase angle of 13.5 degrees (Table I). It is therefore understandable that the latter data show a larger brightness variation, however it is difficult to explain why the partially illuminated dataset is overall significantly brighter than the almost fully illuminated one. We therefore prefer the derived period of 7.795 ± 0.001 h and are looking forward to the next apparition to further investigate the discrepancy in reported periods.

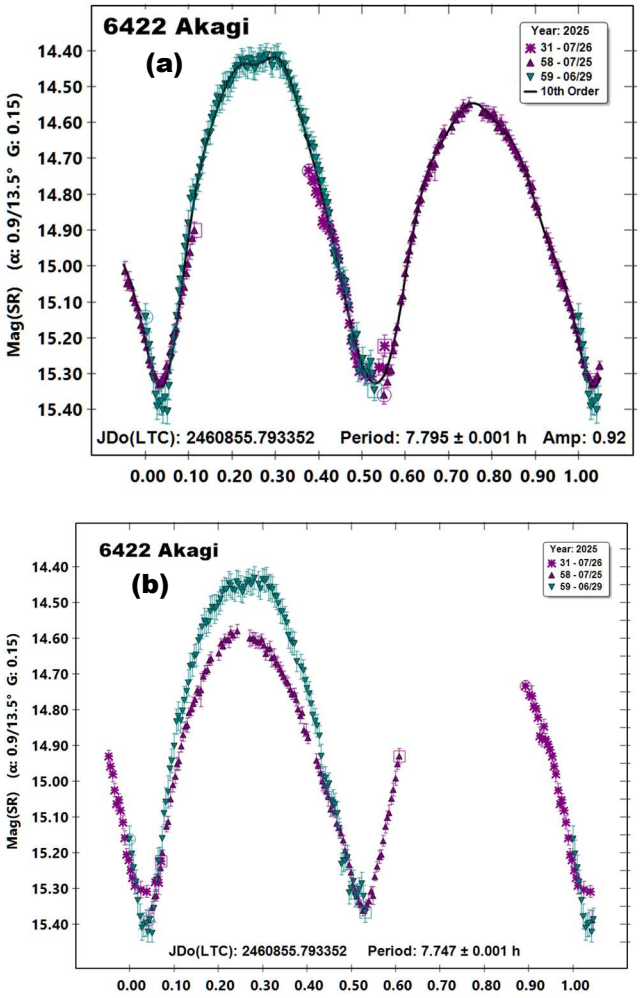

Figure 1. Rotational lightcurve of 6422 Akagi. (a) Derived 7.795 h period from this work. (b) Our photometric data fit to the 7.747 h period derived by by Ďurech et al. (2016).

7723 Lugger. This Mars-crossing asteroid was observed on four nights over a roughly four-week time span with 152 total observations. The derived rotational period of 4.835 ± 0.001 h with an amplitude of 0.36 mag in excellent agreement with the prior measured rotation period by McNeill et al. (2019, 4.831 h) and Pál et al. (2020, 4.83445 h); both based on Transiting Exoplanet Survey Satellite (TESS) data.

Number	Name	yyyy mm/dd	Phase	L_{PAB}	B_{PAB}	Period(h)	P.E.	Amp	A.E.	Grp
6422	Akagi	2025 06/29-07/26	13.5, 0.9	302.0	2.9	7.795	0.001	0.92	0.05	EUN
7723	Lugger	2025 09/16-10/09	14.3,26.1	340.7	-8.7	4.835	0.001	0.36	0.02	MC

Table I. Observing circumstances and results. The phase angle is given for the first and last date. If preceded by an asterisk, the phase angle reached an extrema during the period. L_{PAB} and B_{PAB} are the approximate phase angle bisector longitude/latitude at mid-date range (see Harris et al., 1984). Grp is the asteroid family/group (Warner et al., 2009): MC: Mars-Crosser, EUN = Eunomia.

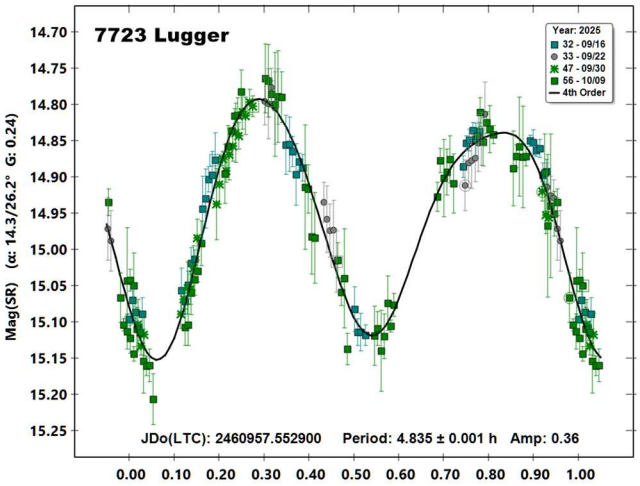

Acknowledgement

The authors would like to acknowledge partial support for this work from the University of Central Florida, Space Research Initiative Grant #110835.

References

Chang, C.-K.; Lin, H.-W.; Ip, W.-H.; Prince, T.A.; Kulkarni, S.R.; Levitan, D.; Laher, R.; Surace, J. (2016). "Large Super-fast Rotator Hunting Using the Intermediate Palomar Transient Factory." *The Astrophysical Journal Supplement Series* **227**, 13 pp.

Ďurech, J.; Hanuš, J.; Oszkiewicz, D.; Vančo, R. (2016). "Asteroid models from the Lowell photometric database." *Astronomy & Astrophysics* **587**, A48.

Harris, A.W.; Young, J.W.; Scaltriti, F.; Zappala, V. (1984). "Lightcurves and phase relations of the asteroids 82 Alkmene and 444 Gyptis." *Icarus* **57**, 251-258.

Keel, W.C.; Oswalt, T.; Mack, P.; Henson, G.; Hillwig, T.; Batcheldor, D.; Berrington, R.; De Pree, C.; Hartmann, D.; Leake, M.; Licandro, J.; Murphy, B.; Webb, J.; Wood, M. A. (2017). "The Remote Observatories of the Southeastern Association for Research in Astronomy (SARA)." *Publications of the Astronomical Society of the Pacific* **129**:015002 (12pp). *http://iopscience.iop.org/article/10.1088/1538-3873/129/971/015002/pdf*

McNeill, A.; Mommert, M.; Trilling, D.E.; Llama, J.; Skiff, B. (2019). "Asteroid Photometry from the Transiting Exoplanet Survey Satellite: A Pilot Study." *The Astrophysical Journal Supplement Series* **245**, 8 pp.

Nesvorný, D.; Brož, M.; Carruba, V. (2015). "Identification and dynamical properties of asteroid families." in Michel, P. et al., Ed. Asteroids IV, University of Arizona Press, Tucson, 297-321.

Pál, A.; Szakáts, R.; Kiss, C.; Bódi, A.; Bognár, Z.; Kalup, C.; Kiss, L.L.; Marton, G.; Molnár, L.; Plachy, E.; Sárneczky, K.; Szabó, G.M.; Szabó, E. (2020). "Solar System Objects Observed with TESS - First Data Release: Bright Main-belt and Trojan Asteroids from the Southern Survey." *The Astrophysical Journal Supplement Series* **247**, 9 pp.

Warner, B.D.; Harris, A.W.; Pravec, P. (2009). "The Asteroid Lightcurve Database." *Icarus* **202**, 134-146. Updated 2023 Oct 01. *http://www.minorplanet.info/lightcurvedatabase.html*

Warner, B.D. (2025). MPO Software, *MPO Canopus* version 12. *https://minplanobs.org/bdwpub/php/mpocanopus.php*

DISCOVERY AND PHOTOMETRIC-SPECTROSCOPIC STUDIES OF APOLLO ASTEROID 2024 QS

Filipp Dmitrievich Romanov
American Association of Variable Star Observers (AAVSO)
185 Alewife Brook Parkway, Suite 410
Cambridge, MA 02138 USA
filipp.romanov.27.04.1997@gmail.com
ORCID iD: 0000-0002-5268-7735

Andrea Farina
University of Padova
Department of Physics and Astronomy
Vicolo dell'Osservatorio, 3
Padova 35122 ITALY
ORCID iD: 0009-0005-5257-8319

Nicolas Erasmus
South African Astronomical Observatory
1 Observatory Road, Observatory
Cape Town 7925 SOUTH AFRICA
ORCID iD: 0000-0002-9986-3898

Ahmed Magdy Abdelaziz (ORCID iD: 0000-0003-1169-4071)
Yasser Hassan Hendy (ORCID iD: 0000-0002-2356-8315)
Tarek Mahmoud Kamel (ORCID iD: 0009-0004-4325-5588)
National Research Institute of Astronomy and Geophysics
EL Marsad Street 1
Helwan, Cairo 11421 EGYPT

(Received: 2025 December 19 Revised: 2026 February 16)

This paper describes the discovery and presents the results of photometric and spectroscopic studies of the Apollo Near-Earth asteroid 2024 QS from 2024 September 3 to 8 using the telescopes of three observatories. 2024 QS appears most likely to be classified within the C-complex or X-complex, and the rotation period was determined to be 5.58 hours with an amplitude of 0.5 mag.

On 2024 August 26, while conducting a search for asteroids near the ecliptic and close to the opposition region of the sky, the first author found (by viewing the images) a Near-Earth asteroid (NEA) candidate in the eight images with 300 seconds exposures using a Luminance filter; the images were acquired remotely between 13:42:01 and 14:29:44 UT with the telescope T59 (0.51-m f/6.8 reflector + CCD with field of view of 36.8 × 36.8 arcmin) of iTelescope.Net located at the Siding Spring Observatory (MPC code Q62), Australia.

After the candidate object was posted on the Near-Earth Object Confirmation Page (NEOCP) of the Minor Planet Center under the temporary designation RFD0073, it was observed on 2024-08-27.143727 UT using the remote telescope T73 (0.356-m f/7.2 reflector + CMOS) of iTelescope.Net in Rio Hurtado, Chile (MPC code X07). After receiving follow-up observations from other observatories, this asteroid received the provisional designation 2024 QS, as announced on 2024 August 28 in the Minor Planet Electronic Circular (MPEC) 2024-Q53 (Romanov et al., 2024).

This NEA belongs to the Apollo group. It has an absolute magnitude of 24.6 and an orbital period of ≈ 1.79 years. The object passed at a minimum distance of approximately 12 lunar distances from Earth on 2024 September 9, at 00:39 UT. The last observation was on 2025-02-21.5 UT at the Canada-France-Hawaii Telescope (3.6-m f/4.1 reflector + CCD; MPC code T14).

Spectroscopy

A spectrum of 2024 QS was obtained with the Copernico telescope (1.82-m f/9 reflector) at the Asiago Observatory, Cima Ekar Observing Station (MPC code 098), Italy. The exposure time was 1200 seconds, and the observation was carried out on 2024 September 3 at 23:45:57.2 UT. At the time of the observation, the predicted magnitude was 19.1 and the phase angle was 29.7°. The Asiago Faint Object Spectrograph and Camera (AFOSC) was used with a 1.69-arcsec slit and the Volume Phase Holographic Grism VPH #6 (dispersion ≈ 3.5 Å/px, spectral resolution R ≈ 500 over the 450–1000 nm wavelength range).

The spectrum was reduced using standard procedures in the *Image Reduction and Analysis Facility (IRAF)* package (Tody, 1986), including bias subtraction, flat-field correction, background removal, and wavelength calibration with an HgCd lamp. The asteroid spectrum was then divided by the solar analogue Landolt 112-1333, observed under the same instrumental conditions. The spectrum was normalized at 5500 Å using a linear-regression method.

The resulting spectrum was compared with the taxonomic templates of DeMeo et al. (2009). Due to the low signal-to-noise ratio, it is difficult to assign a taxonomic complex with confidence. Flat spectral-types, such as C- or X-complex are preferred, although an S-complex cannot be ruled out. Figure 1 shows the spectrum (in blue) together with four taxonomic curves: S, X, C and B.

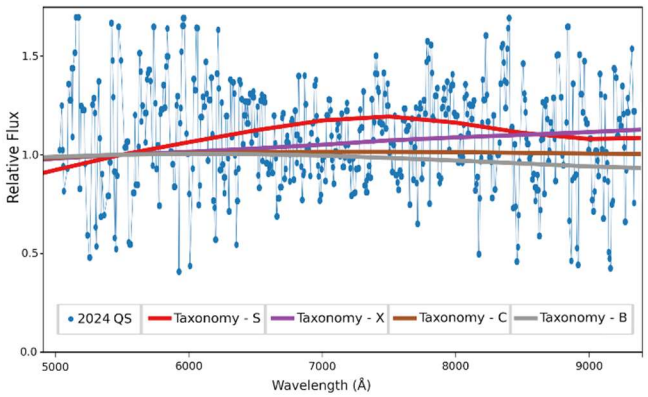

Figure 1: Spectrum of 2024 QS.

Photometry

Images of the asteroid were taken over three consecutive nights using two telescopes located in Africa in the northern and southern hemispheres, which was possible due to the location of 2024 QS near the celestial equator.

Images from the South African Astronomical Observatory were taken using Lesedi telescope (MPC code M28): 1.0-m f/8 reflector + CCD, with unfiltered exposures of 15 seconds, on 2024 Sep 5/6 from 23:01:27 to 00:03:22 UT and on 2024 Sep 7/8 from 23:10:03 to 01:13:45 UT.

Images from the Kottamia Astronomical Observatory (MPC code 088) in Egypt were taken using the 1.88-m f/4.9 reflector + CCD, with unfiltered exposures of 15 seconds. There were some issues with the guiding (software problem), therefore the asteroid was not present in all images, part of the images obtained on 2024 Sep 6/7 from 22:49 to 00:29 UT were used for the analysis.

The first author extracted photometry from the images using *Tycho Tracker Pro v12.6* software (Parrott, 2020) and analyzed the data. Photometry was done in comparison with the Sloan r' magnitudes of nearby stars (with color indices B-V from 0.4 to 0.9) from the ATLAS star catalog (Tonry et al., 2018) and an offset of 0.15 mag was applied for Kottamia data. Light-time and H-G corrections were applied, received period spectrum plot (4th order analysis) shows several periods including around 4.5 h., 5.6 h. and 7.4 h., the periodogram is shown in the Figure 2. Similar periods with a difference ± 0.1 hours were found by analyzing the photometry made by comparison with magnitudes of stars from other bands and when applied different fit orders, and a period of 5.581 ± 0.004 hours with an amplitude of 0.522 ± 0.125 mag was chosen as the best solution, the phased lightcurve is shown in the Figure 3.

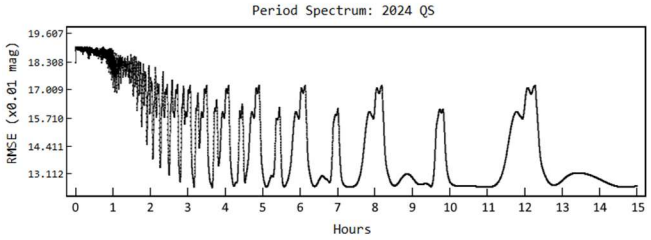

Figure 2: Periodogram search between 0 hours and 15 hours.

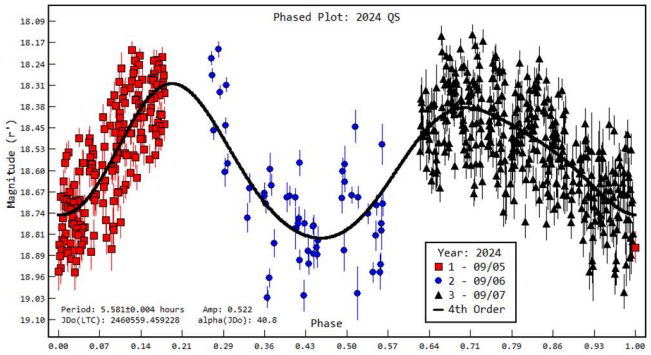

Figure 3: Phased lightcurve for 2024 QS.

According to the rotation period vs. size distribution in the Asteroid Lightcurve Database (LCDB) (Warner et al., 2009), the determined rotation period P = 5.58 hours is longer than most other asteroids of similar size.

Acknowledgements

Based on observations collected at Copernico (or/and Schmidt) telescope(s) (Asiago, Italy) of the INAF - Osservatorio Astronomico di Padova. Filipp Romanov is grateful to: iTelescope.Net for giving him some complimentary points for observing time to use their remote telescopes since 2019; the AAVSO for granting him a complimentary membership (with annual renewal) since the beginning of 2021 to the end of 2026; Daniel Parrott for providing the software *Tycho Tracker* for free; John Maikner (Comet Hunter Observatory2, New Ringgold; MPC code W62) for responding to the request and promptly making the first follow-up observations of 2024 QS on 2024 Aug 27; Dr. Andrea Pastorello (INAF - Padova Astronomical Observatory) who transmitted the request for observations to Andrea Farina; Dr. Tomasz Kwiatkowski (Adam Mickiewicz University) who transmitted the request for observations to Dr. Ahmed Magdy Abdelaziz Moursi; Dr. Amanda A. Sickafoose (Planetary Science Institute) who transmitted the request for observations to Dr. Nicolas Erasmus; everyone who made astrometric observations of 2024 QS and sent them to the Minor Planet Center.

References

DeMeo, F.E.; Binzel, R.P.; Slivan, S.M.; Bus, S.J. (2009). "An extension of the Bus asteroid taxonomy into the near-infrared." *Icarus* **202**, 160-180.

iTelescope - Leaders in Internet Astronomy since 2006. (n.d.). *https://itelescope.net/*

Parrott, D. (2020). "Tycho Tracker: A New Tool to Facilitate the Discovery and Recovery of Asteroids Using Synthetic Tracking and Modern GPU Hardware." *Journal of the American Association of Variable Star Observers* **48**, 262. *https://www.tycho-tracker.com*

Romanov, F.D.; Maikner, J.; Hug, G.; Holmes, R.; Linder, T.; Wang, Z.; Liu, B.; Skachedub, A.V.; Heogner, C.; Ludwig, F.; Hartmann, M.; Stecklum, B.; Losse, F.; Ivanov, A.; Barcov, A. and 12 colleagues (2024). "2024 QS." *Minor Planet Electronic Circulars*, MPEC 2024-Q53. *https://minorplanetcenter.net/mpec/K24/K24Q53.html*

Tody, D. (1986). "The IRAF Data Reduction and Analysis System." *Proceedings of the Society of Photo-Optical Instrumentation Engineers (SPIE) Conference Series* **627**, 733.

Tonry, J.L.; Denneau, L.; Flewelling, H.; Heinze, A.N.; Onken, C.A.; Smartt, S.J.; Stalder, B.; Weiland, H.J.; Wolf, C. (2018). "The ATLAS All-Sky Stellar Reference Catalog." *The Astrophysical Journal* **867**, 105.

Warner, B.D.; Harris, A.W.; Pravec, P. (2009). "The asteroid lightcurve database." *Icarus* **202**, 134-146. Updated 2023 Oct. *https://minplanobs.org/MPInfo/php/lcdb.php*

Name	yyyy mm/dd	Phase	L_{PAB}	B_{PAB}	Period(h)	P.E.	Amp	A.E.
2024 QS	2024 09/05-09/08	40.8,57.1	10	-10	5.581	0.004	0.52	0.13

Table I. Observing circumstances and results. The phase angle is given for the first and last dates. L_{PAB} and B_{PAB} are the approximate phase angle bisector longitude/latitude at mid-date range).

LIGHTCURVE AND ROTATION PERIOD OF 2025 FA22

Arushi Nath
MonitorMyPlanet Observatory (R60), Nerpio, SPAIN
Arushi@MonitorMyPlanet.com

(Received: 2026 January 12)

Photometric observations of the potentially hazardous asteroid 2025 FA22 were obtained on six nights during its close approach in September 2025. Analysis of R-band lightcurves yields a synodic rotation period of 13.075 ± 0.002 h with a peak-to-peak amplitude of 0.62 mag, implying a significantly elongated shape with a minimum equatorial axis ratio of a/b ≳ 1.77. Rotation-corrected BVRI photometry indicates moderately red colors consistent with an S-complex taxonomic classification.

CCD photometry measurements of asteroid 2025 FA22 were obtained remotely at the MonitorMyPlanet Observatory (MPC code R60) in Nerpio, Spain. Observations were conducted using a 0.305-m (12-inch) Ritchey-Chrétien telescope operated at an effective focal ratio of f/6 using a 0.75× focal reducer, mounted on a Sky-Watcher EQ8-R equatorial mount and equipped with an ASI2600 monochrome camera and a filter wheel containing Johnson-Cousins U, B, V, R, I filters. Images were binned 2×2, providing a pixel scale of 0.848 arcsec pixel^{-1}. Observations were obtained on six nights between 2025 September 19 and 26 (UT), spanning solar phase angles from approximately 60° to 25°.

Standard bias, dark, and flat-field corrections were applied to all images prior to photometric extraction. Differential photometry was performed using ensemble comparison stars within each field. Image reduction and photometric calibration were carried out using *Tycho Tracker* software, with reference magnitudes drawn from the ATLAS star catalog in the red band.

Time-series observations were obtained primarily in the R band, with exposure times adjusted to accommodate the rapidly changing apparent motion during the close approach. Period analysis of the combined R-band dataset was performed using a fourth-order Fourier series fit. The resulting periodogram (Figure 1) exhibits a well-defined minimum corresponding to a synodic rotation period of 13.075 ± 0.002 h.

The composite phased lightcurve, combining all six nights of data (Figure 2), displays a stable, double-peaked morphology with a peak-to-peak amplitude of 0.62 mag, consistent with principal-axis rotation. Amplitude Error (A.E.) was estimated as 0.06 mag from √2 times the RMS residual scatter of the lightcurve. Assuming a triaxial ellipsoid viewed near the equatorial plane and negligible albedo variegation, the observed amplitude implies a minimum equatorial axis ratio of a/b ≳ 1.77.

Multi-filter BVRI observations were obtained on 2025 September 22 (UT). Rotational effects were corrected by interpolating R-band magnitudes to the rotational phases corresponding to the B, V, and I measurements. Weighted mean color indices were derived, with uncertainties propagated in quadrature.

The resulting rotation-corrected colors are B-R = 1.22 ± 0.02, V-R = 0.45 ± 0.02, and R-I = 0.36 ± 0.04, leading to derived colors of B-V = 0.77 ± 0.03 and V-I = 0.81 ± 0.05. Compared with solar colors, the asteroid is consistently redder across all indices. When interpreted within the broadband photometric taxonomy framework of Lin et al. (2018), these colors place 2025 FA22 within the S-complex, overlapping the S-Q region.

Acknowledgements

The author thanks the Masason Foundation for providing funding for the telescope and AstroCamp for hosting my observatory in Nerpio, Spain.

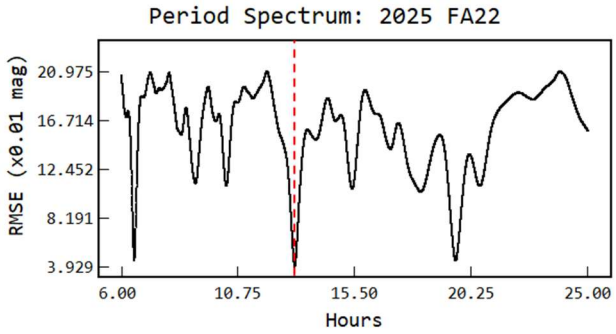

Figure 1. Periodogram (6-25 h) computed with a 4th-order Fourier fit showing the preferred solution at 13.075 h.

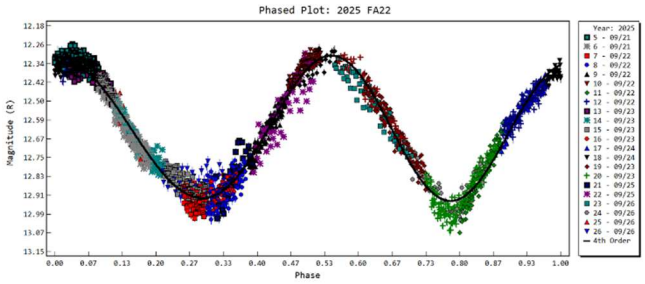

Figure 2. Lightcurve of 2025 FA22 combining all six nights (2025 Sept 19-26) phased to a period of 13.075 hours.

References

Harris, A.W.; Young, J.W.; Scaltriti, F.; Zappala, V. (1984). "Lightcurves and phase relations of the asteroids 82 Alkmene and 444 Gyptis." *Icarus* **57**, 251-258.

Lin, C.-H.; Ip, W.-H.; Lin, Z.-Y.; Cheng, Y.-C.; Lin, H.-W.; Chang, C.-K. (2018). "Photometric survey and taxonomic identifications of 92 near-Earth asteroids." *Planetary and Space Science* **152**, 116-135. *https://doi.org/10.1016/j.pss.2017.12.019*

Parrott, D. (2025). *Tycho Tracker*: Photometry and astrometry software. *https://www.tycho-tracker.com*

Warner, B.D.; Harris, A.W.; Pravec, P. (2009). "The Asteroid Lightcurve Database." *Icarus* **202**, 134-146. Updated 2023 Oct 1. *https://minplanobs.org/mpinfo/php/lcdb.php*

Number	Name	yyyy mm/dd	Phase	L_{PAB}	B_{PAB}	Period(h)	P.E.	Amp	A.E.	Grp
	2025 FA22	2025 09/19-09/26	60.2, 25.0	12.1	10.3	13.075	0.002	0.62	0.06	PHA

Table I. Observing circumstances and results. The phase angle is given for the first and last date. L_{PAB} and B_{PAB} are the approximate phase angle bisector longitude/latitude at mid-date range (see Harris et al., 1984). Grp is the asteroid family/group (Warner et al., 2009).

COLLABORATIVE ASTEROID PHOTOMETRY FROM UAI: 2025 OCTOBER-DECEMBER

Riccardo Papini, Marco Iozzi, Lorenzo Franco
UAI - Unione Astrofili Italiani, Rome, ITALY
mioxzy@gmail.com

Paolo Bacci, Martina Maestripieri
GAMP - San Marcello Pistoiese (104), Pistoia, ITALY

Nello Ruocco
Osservatorio Astronomico Nastro Verde (C82)
Sorrento, ITALY

Giovanni Battista Casalnuovo
Filzi School Observatory (D12), Laives, ITALY

Paolo Fini, Guido Betti, Andrea Boattini
Beato Ermanno Astronomical Observatory (L73)
Impruneta, ITALY

Gianni Galli
GiaGa Observatory (203), Pogliano Milanese, ITALY

Vincenzo della Vecchia
45th Parallel Observatory (D43), Pino Torinese, ITALY

Adriano Valvasori
ALMO Observatory (G18), Padulle (BO), ITALY

Alessandro Marchini, Riccardo Papini
Astronomical Observatory, DSFTA - University of Siena (K54)
Via Roma 56, 53100 - Siena, ITALY

Giulio Scarfi
Iota Scorpii Observatory (K78), La Spezia, ITALY

Marco Iozzi, Gianfranco Ferrini
GRAM - Osservatorio Astronomico Beppe Forti (K83)
Montelupo Fiorentino, ITALY

Marco Iozzi
HOB Astronomical Observatory (L63)
Capraia Fiorentina, ITALY

(Received: 2026 January 14)

Photometric observations of three asteroids were made in order to acquire lightcurves for shape/spin axis modeling. Lightcurves were acquired for 1346 Gotha, 1551 Argelander, and 4807 Noboru.

Collaborative asteroid photometry was done inside the Italian Amateur Astronomers Union (UAI, 2025) group. The targets were selected mainly in order to acquire lightcurves for shape/spin axis modeling. Table I shows the observing circumstances and results.

The CCD/CMOS photometric observations were made in 2025 October-December using the instrumentation described in Table II. Lightcurve analysis was done by Papini and Iozzi (UAI group, 2025) with *MPO Canopus* (Warner, 2023). All the images were calibrated with dark and flat frames and converted to standard magnitudes using solar-colored field stars from CMC15 and ATLAS catalogues, distributed with *MPO Canopus*. For brevity, "LCDB" is a reference to the asteroid lightcurve database (Warner et al., 2009).

1346 Gotha is a middle main-belt asteroid historically classified as a S-type. Collaborative observations were made over three nights. We found a bimodal solution with a synodic period of P = 2.640 ± 0.001 h and an amplitude A = 0.14 ± 0.02 mag. The period is close to the previously published results in the LCDB.

The reflectance spectrum for 1346 Gotha, extracted from Gaia ESA Archive (2025), is close to a S-type when compared with the Bus-DeMeo taxonomy (DeMeo et al., 2009) and also agrees with the taxonomic attribution by Franco (2025). The B-V = 0.84 value listed in the JPL Small-Body Database is also consistent with the reference index for S-types (Shevchenko and Lupishko, 1998; B-V = 0.86 ± 0.04).

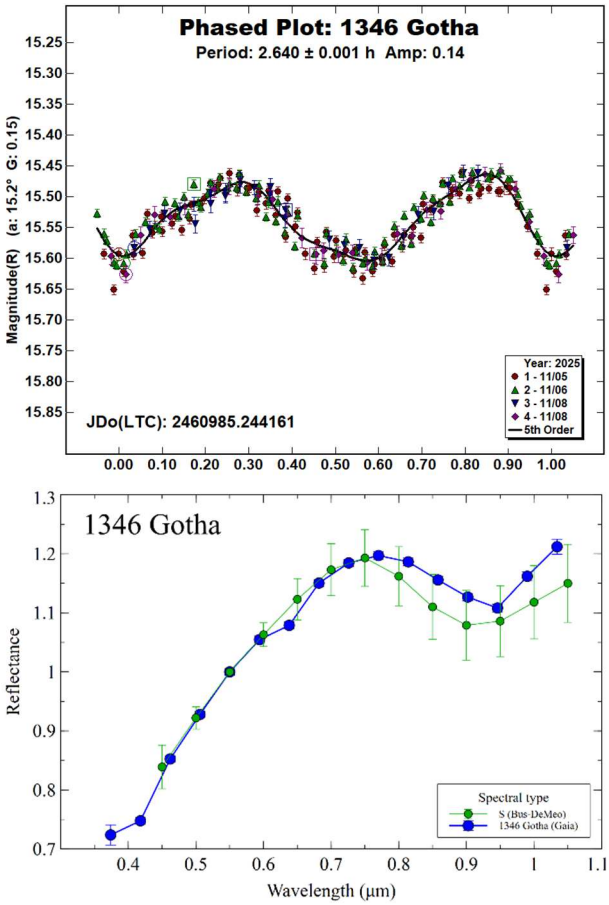

1551 Argelander is an inner main-belt asteroid historically classified as a S-type. Collaborative observations were made over nine nights. We found a bimodal solution with a synodic period of P = 4.059 ± 0.001 h and an amplitude A = 0.42 ± 0.08 mag. The period is close to the previously published results in the LCDB.

The reflectance spectrum for 1551 Argelander, extracted from Gaia ESA Archive (2025), is close to a S-type when compared with the Bus-DeMeo taxonomy (DeMeo et al., 2009) and also agrees with the taxonomic attribution by Franco (2025). Multiband photometry was acquired by G. Casalnuovo (D12) on 2025 November 12, A. Valvasori (G18) on 2025 November 28, by G. Ferrini and M. Iozzi (K83) on 2025 December 5 and by M. Iozzi (L63) on 2025 December 27. From these observations, we found a mean color index V-R = 0.47 ± 0.04 mag, which is consistent with a S-Type asteroid (Shevchenko and Lupishko, 1998; 0.49 ± 0.05).

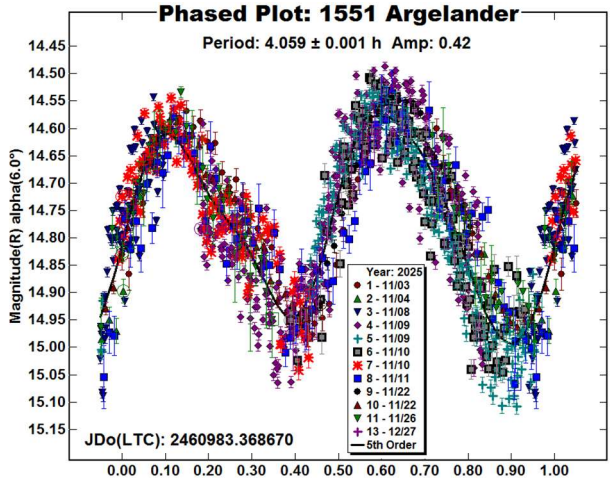

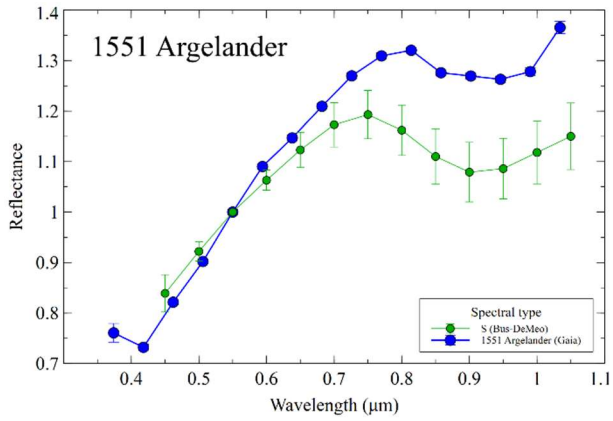

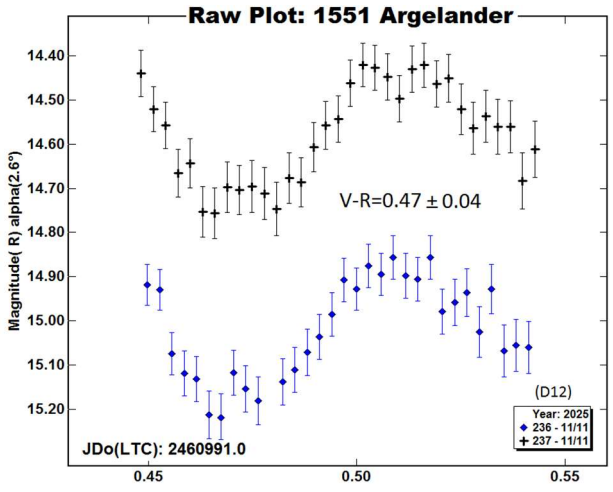

4807 Noboru is an inner main-belt asteroid historically classified as a S-type. Collaborative observations were made over five nights. We found a bimodal solution with a synodic period of P = 4.042 ± 0.001 h and an amplitude A = 0.17 ± 0.02 mag. The period is close to the previously published results in the LCDB.

The reflectance spectrum for 4807 Noboru, extracted from Gaia ESA Archive (2025), is close to a S-type when compared with the Bus-DeMeo taxonomy (DeMeo et al., 2009) and also agrees with the taxonomic attribution by Franco (2025). Multiband photometry was acquired by G. Casalnuovo (D12) on 2025 November 26 and P. Bacci and M. Maestripieri (104) on 2025 November 29, from which we found a color index V-R = 0.45 ± 0.03 mag, which is close to a S-Type asteroid (Shevchenko and Lupishko, 1998; 0.49 ± 0.05).

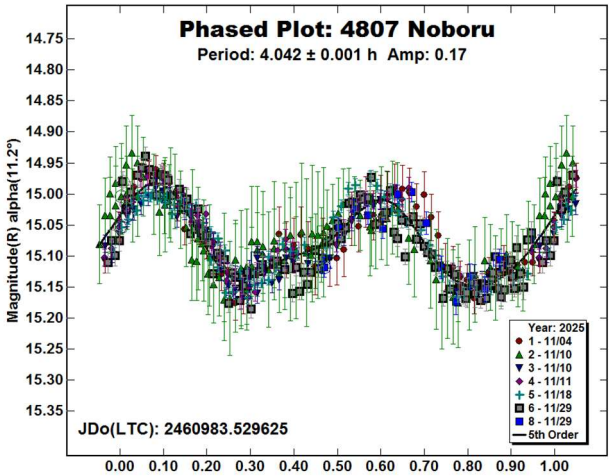

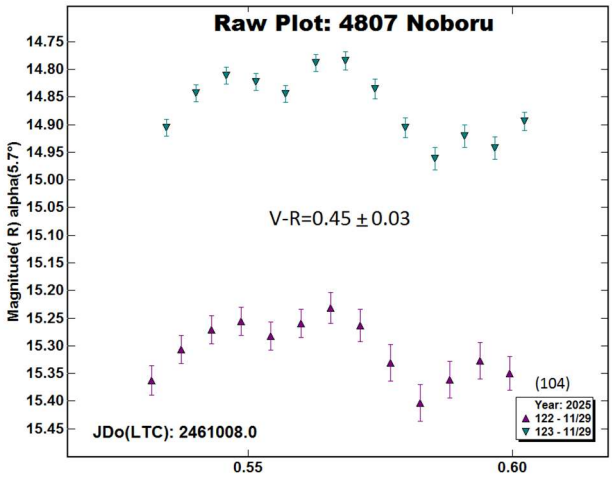

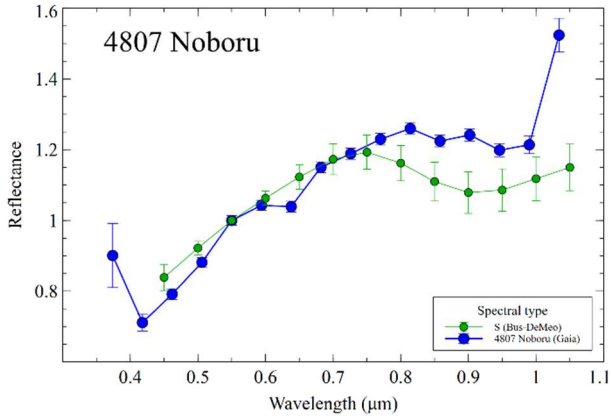

References

DeMeo, F.E.; Binzel, R.P.; Slivan, S.M.; Bus, S.J. (2009). "An extension of the Bus asteroid taxonomy into the near infrared." *Icarus* **202**, 160-180.

Franco, L. (2025). "On The Gaia Reflectance Spectra." *Minor Planet Bulletin* **52**, 351-354.

Gaia ESA Archive (2025), version 3.7. *https://gea.esac.esa.int/archive/*

Harris, A.W.; Young, J.W.; Scaltriti, F.; Zappala, V. (1984). "Lightcurves and phase relations of the asteroids 82 Alkmene and 444 Gyptis." *Icarus* **57**, 251-258.

JPL (2025). Small Body Database Search Engine https://ssd.jpl.nasa.gov

Shevchenko, V.G.; Lupishko, D.F. (1998). "Optical properties of Asteroids from Photometric Data." *Solar System Research* **32**, 220-232.

Number	Name	2025 mm/dd	Phase	L_{PAB}	B_{PAB}	Period(h)	P.E.	Amp	A.E.	Grp
1346	Gotha	11/05-11/08	15.2-16.3	17	-12	2.640	0.001	0.14	0.02	MB-M
1551	Argelander	11/03-12/27	*6.0-18.8	52	-4	4.059	0.001	0.42	0.08	MB-I
4807	Noboru	11/04-11/29	*10.6-5.6	59	1	4.042	0.001	0.17	0.02	MB-I

Table I. Observing circumstances and results. The first line gives the results for the primary of a binary system. The second line gives the orbital period of the satellite and the maximum attenuation. The phase angle is given for the first and last date. If preceded by an asterisk, the phase angle reached an extrema during the period. L_{PAB} and B_{PAB} are the approximate phase angle bisector longitude/latitude at mid-date range (see Harris et al., 1984). Grp is the asteroid family/group (Warner et al., 2009).

Observatory (MPC code)	Telescope	CCD/CMOS	Filters	Observed Asteroids (#Sessions)
GAMP (104)	0.60-m NRT f/4.0	Apogee Alta	C, V, Rc	4807(5)
Osservatorio Astronomico Nastro Verde (C82)	0.35-m SCT f/6.3	SBIG ST10XME (bin 2×2)	C	1346(2), 4807 (1)
Filzi School Observatory (D12)	0.35-m NRT f/8.0	QHY9 (bin 4×4)	C, V, Rc	4807(2), 1551 (1)
Beato Ermanno Astronomical Observatory (L73)	0.31-m SCT F/6.0	QHY174M (bin 2×2)	Rc	1551(3)
GiaGa Observatory (203)	0.36-m SCT f/5.8	Moravian G2-3200	C, Rc	1551(2)
45th Parallel Observatory (D43)	0.25-m RCT f/5.6	IMX533	C	1551(2)
ALMO Observatory (G18)	0.30-m NRT f/4.0	ZWO ASI533MM PRO	V, Rc	1551(1)
Astronomical Observatory, University of Siena (K54)	0.30-m MCT f/5.6	SBIG STL-6303e (bin 2×2)	C	1346(1)
Iota Scorpii(K78)	0.40-m RCT f/6.1	Player One 455M Pro (bin 4×4)	Rc	4807(1)
GRAM - Osservatorio Astronomico Beppe Forti (K83)	0.25-m SCT f/6.3	ATIK 383L+ (bin 2×2)	V, Rc	1551(1)
HOB Astronomical Observatory (L63)	0.20-m SCT f/6.0	ATIK 383L+ (bin 2×2)	V,Rc	1551(1)

Table II. Observing Instrumentations. NRT: Newtonian Reflector, MCT: Maksutov-Cassegrain, RCT: Ritchey-Chretien, SCT: Schmidt-Cassegrain.

PHOTOMETRY OF 21 ASTEROIDS AT SOPOT ASTRONOMICAL OBSERVATORY: 2025 JUNE - DECEMBER

Vladimir Benishek
Belgrade Astronomical Observatory
Volgina 7, 11060 Belgrade 38, SERBIA
vlaben@yahoo.com

(Received: 2026 January 14)

Lightcurves and synodic rotation periods for 21 asteroids obtained from photometric data collected at the Sopot Astronomical Observatory in the time span 2025 June-December. For a large portion of the asteroids included, synodic rotation periods were derived for the first time.

Photometric observations of 21 asteroids were conducted at Sopot Astronomical Observatory (SAO) from 2025 June through December in order to determine the asteroids' synodic rotation periods. For this purpose, two 0.35-m *f*/6.3 Meade LX200GPS Schmidt-Cassegrain telescopes were employed. The telescopes are equipped with a SBIG ST-8 XME and a SBIG ST-10 XME CCD cameras. The exposures were unfiltered and unguided for all targets. Both cameras were operated in 2×2 binning mode, which produces image scales of 1.66 arcsec/pixel and 1.25 arcsec/pixel for ST-8 XME and ST-10 XME cameras, respectively. Prior to measurements, all images were corrected using dark and flat field frames.

Photometric reduction was conducted using *MPO Canopus* (Warner, 2018). Differential photometry with up to five comparison stars of near solar color ($0.5 \leq$ B-V ≤ 0.9) was performed using the Comparison Star Selector (CSS) utility. This helped ensure a satisfactory quality level of night-to-night zero-point calibrations and correlation of the measurements within the standard magnitude framework. Field comparison stars were calibrated using standard Cousins R magnitudes derived from the Carlsberg Meridian Catalog 15 (VizieR, 2025) Sloan r' magnitudes using the formula (R = r' - 0.22) as well as G-band data from the Gaia DR3 catalog converted to Johnson-Cousins V magnitudes using a third-degree transformation polynomial from the Gaia DR3 catalog documentation available online. The polynomial includes stellar color indices G_{bp}-G_{rp}, *i.e.*, the difference in magnitudes in the blue and red Gaia passbands:

$$G - V = -0.02704 + 0.01424(G_{bp} - G_{rp}) - 0.2156(G_{bp} - G_{rp})^2 + 0.01426(G_{bp} - G_{rp})^3$$

The asteroid Johnsons-Cousins V magnitudes measured using the converted comparison star magnitudes were subjected to magnitude corrections to compensate for the change in viewing geometry and solar phase angle, as described in detail in section 15.1.3 of the reference Warner (2016).

In some instances, small zero-point adjustments were necessary in order to achieve the best match between individual data sets in terms of achieving the most favorable statistical indicators of Fourier fit goodness.

Lightcurve construction and period analysis was performed using *Perfindia* custom-made software developed in the R statistical programming language (R Core Team, 2025) by the author. The essence of its algorithm is reflected in finding the most favorable solution for rotational period by minimizing the *residual standard error* of the lightcurve Fourier fit. A description of the method implemented in the *Perfindia* algorithm is given in the reference Benishek (2025).

The lightcurve plots presented in this paper show so-called 2% error for rotational periods, i.e. an error that would cause the last data point in a combined data set by date order to be shifted by 2% (Warner, 2012a) and represented by the following formula:

$$\Delta P = \frac{0.02 \cdot \mathrm{T}}{P^2}$$

where P and T are the rotational period and the total time span of observations, respectively. Both of these quantities must be expressed in the same units. Table I gives the observing circumstances and results.

2411 Zellner. Photometric data obtained on two consecutive nights in 2025 September at SAO indicate a bimodal solution for a rotation period of $P = 2.975 \pm 0.007$ h, which is in good agreement with previously determined period results listed in the Asteroid Lightcurve Database records (LCDB; Warner et al., 2009): 2.975 h (Marchini et al., 2017), 3.00 h (Pravec, 2017web), 3.040 h (Benishek, 2018), and a sidereal one of 2.976477 h found by Ďurech et al. (2020).

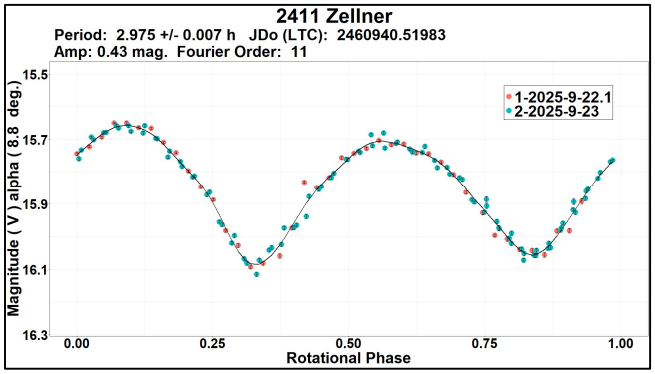

3149 Okudzhava. Period analysis conducted over the extensive combined dataset obtained on eight nights in 2025 September-October led to a bimodal solution for period of $P = 2.6619 \pm 0.0002$ h as the statistically most favorable one.

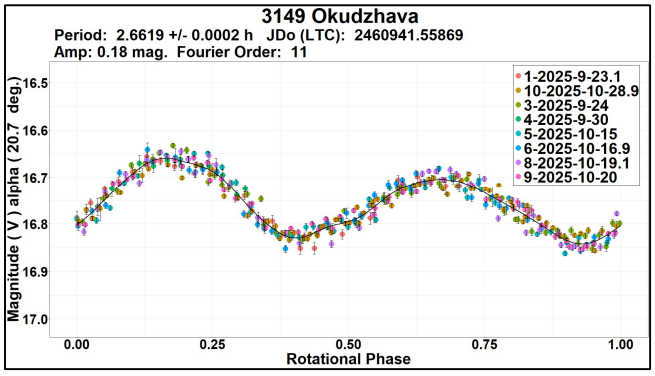

3918 Brel. This long-term program target of the *Photometric Survey for Asynchronous Binary Asteroids* was observed at SAO 2025 in

July-August over two nights, from which a rotation period of P_1 = 3.0972 ± 0.0004 h was derived. This result is in excellent agreement with all previously found values listed in the LCDB, ranging from 3.0966 to 3.0980 hours. As was the case with observations by other authors within this *Survey* during some previous apparitions in 2005 and 2007, no deviations in the rotational light curve were seen in the newly obtained data from these two nights. However, data obtained by Marc Deldem of Les Barres Observatory in France in late 2025 August indicated the existence of deviations in the rotational light curve, which were later confirmed by Dr. Petr Pravec to originate from the existence of a satellite (Deldem et al., 2025). As part of the Survey campaign, the SAO also contributed to the confirmation of this discovery with observations in 2025 October. From these more recent observations, conducted in a different viewing geometry compared to the initially obtained data set from July-August, a period of P_2 = 3.0970 ± 0.0004 h was found.

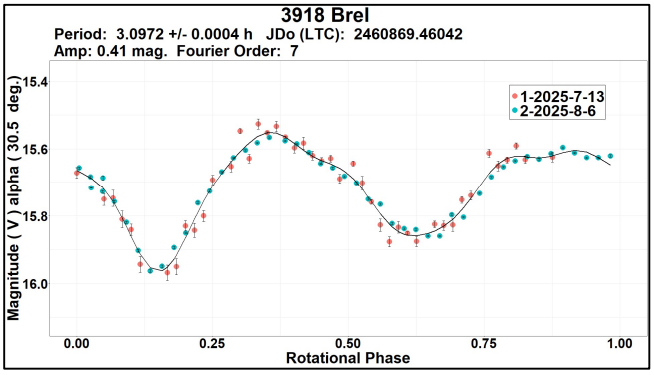

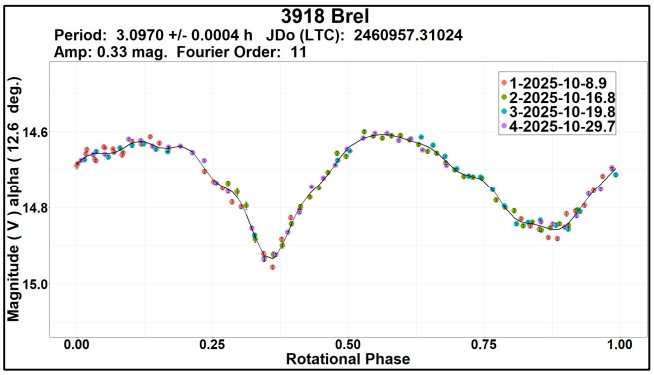

4217 Engelhardt. Period found from observations carried out in early 2025 November over three nights is highly consistent with previously reported results by Warner (2005a, 3.066 h; 2012b, 3.0661 h) and by Behrend (2018web, 3.06592 h).

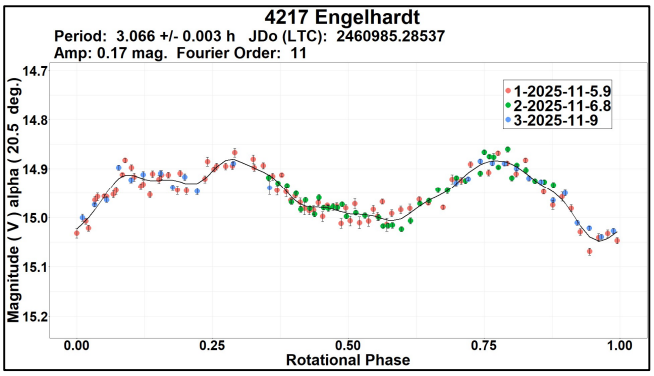

4391 Baldois. A trimodal period solution of P = 3.7199 ± 0.0006 h, derived as the statistically most favorable one from data acquired over three nights in 2025 August - September somewhat deviates from the only previous result by Carbognani (2011, 3.448 h).

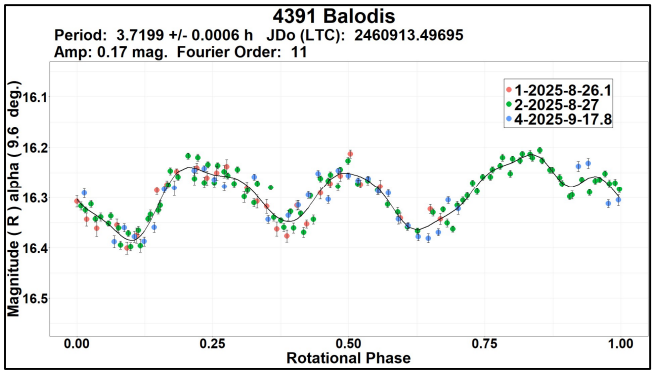

4875 Ingalls. Dense combined data obtained in 2025 June-July resulted in a bimodal lightcurve phased to a period of P = 3.777 ± 0.002 h, which is highly consistent with two previously reported results: 3.78 h (Garceran et al., 2016) and 3.7783 h (Benishek, 2020).

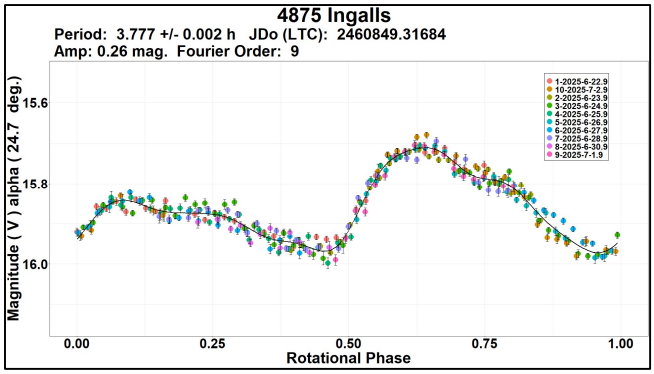

5498 Gustafsson. Prior to this determination, there were no known results for the rotational period of this asteroid. Data from two consecutive nights in 2025 September unambiguously yielded a bimodal period of P = 5.12 ± 0.02 h, densely covering the entire rotational cycle.

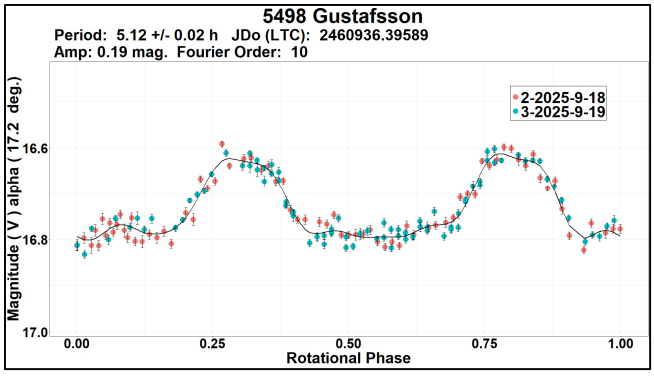

5705 Ericsterken. No previous rotation period determination information was found in the LCDB for this asteroid either. Dense photometric dataset from three consecutive nights in early 2025 November indicates a bimodal period of P = 3.713 ± 0.007 h.

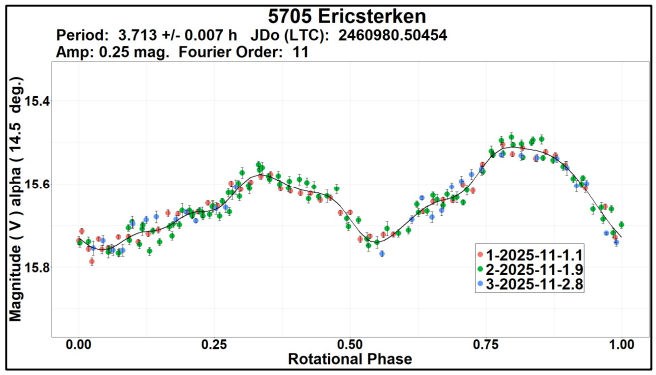

6015 Paularego. Another asteroid with no previously known rotation period. The 2025 July observations strongly suggest a period of $P = 2.833 \pm 0.002$ h as the statistically most plausible one. The data densely cover the entire rotational cycle over multiple nights. Given the rather low amplitude of the obtained lightcurve (<0.1 mag.), further observations in subsequent favorable apparitions for the sake of verifying the obtained result would be highly recommended.

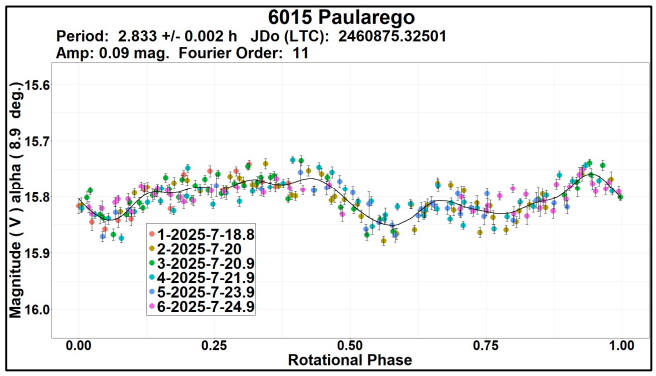

6198 Shirakawa. A serach of LCDB for previous rotation period reports has not found any results in this case as well. A dense combined dataset from four nights in 2025 December shows a bimodal period of $P = 2.7571 \pm 0.0006$ h as the statistically most plausible solution.

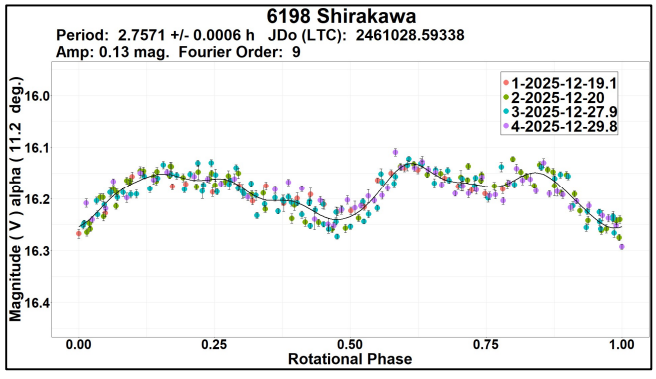

6441 Milenajesenska. Previous rotational period determinations were not found in this case either. Observations made over three nights in late 2025 June indicate an unambiguous solution for a period of $P = 2.817 \pm 0.004$ h, associated with a fairly large amplitude bimodal lightcurve of over 0.4 mag at low solar phase angles.

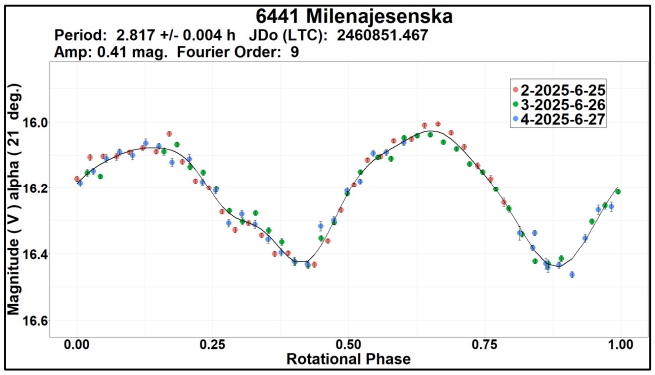

7223 Dolgorukij. There are no previous rotation period determination results in the LCDB. Dense photometric data acquired throughout 2025 August yielded a synodic rotation period of $P = 4.0123 \pm 0.0005$ h as the statistically most favorable solution. Due to the rather small amplitude of the obtained lightcurve of only 0.1 magnitude, further evaluation of this result by observations in subsequent apparitions is strongly recommended.

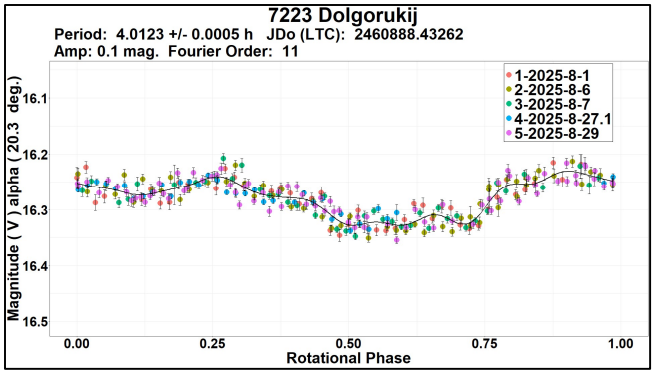

(7653) 1991 UV. Previously reported results for the rotational period were not found in the LCDB. A bimodal period of $P = 2.8649 \pm 0.0002$ h was determined from observations made in 2025 July-August.

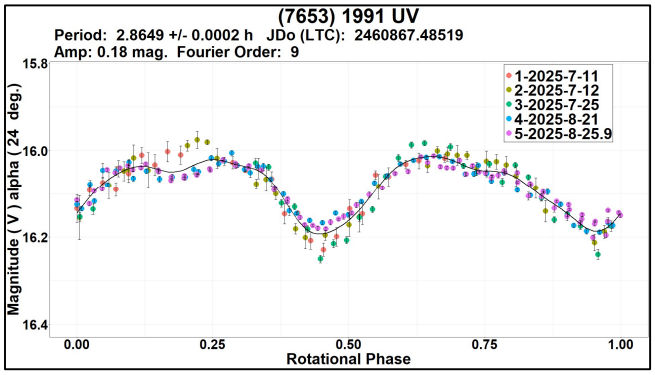

8345 Ulmerspatz. The bimodal period result of $P = 17.12 \pm 0.04$ h obtained from photometric data collected over eight nights in 2025 August fits very well into the entire series of previously reported results for the period from the LCDB ranging from 17.03 h to 17.416 h, despite the somewhat sparse data coverage of one of the lightcurve maxima.

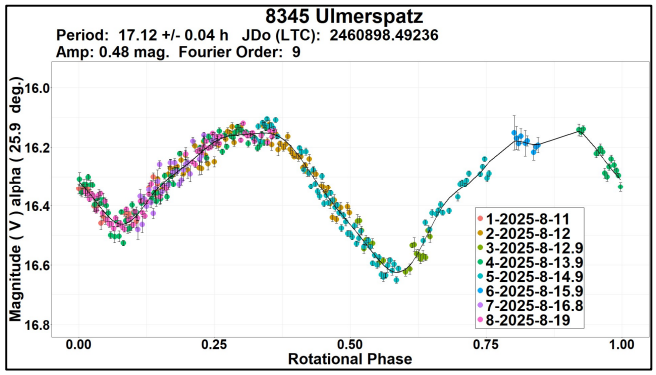

(11865) 1989 SC. There are no previous rotation period determinations for this asteroid. Dense photometric observations from 2025 late August-September resulted in a bimodal lightcurve phased to a period of $P = 2.4483 \pm 0.0003$ h as the most favorable solution.

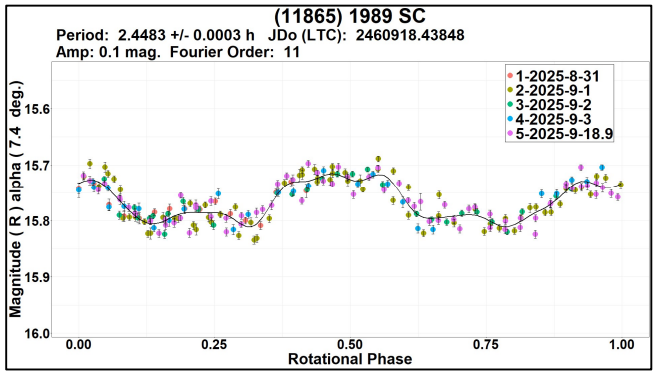

(18108) 2000 NT5. The bimodal solution for a rotational period of $P = 2.9151 \pm 0.0004$ h, derived from data obtained over five nights in 2025 August-September agrees well with the two values found by Warner (2005b, 2.920 h; 2011, 2.910 h).

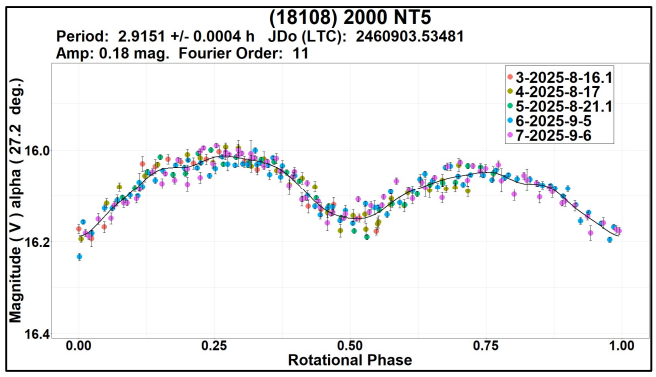

19379 Labrecque. Dense observations at SAO over 3 nights in 2025 November-December resulted in a bimodal lightcurve with a period of $P = 2.5928 \pm 0.0002$ h, strongly corroborating the period result of 2.60 h found from single night data by Skiff et al. (2023) in contrast to the result shown by Behrend (2007web, 8.30 h) associated with a noisy lightcurve containing some data gaps.

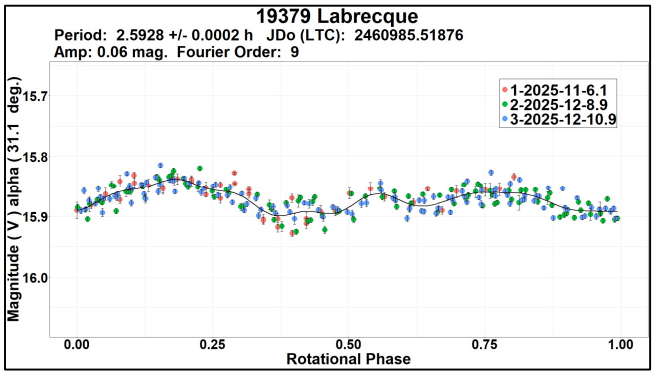

(21122) 1992 YK. Slightly different from the only previously known value from Erasmus et al. (2019, 2.95 h), the newly obtained bimodal period of $P = 3.0135 \pm 0.0008$ h from the SAO data could be considered very reliable given its best statistical plausibility across a wide range of periods examined, quite dense coverage of the corresponding bimodal rotation cycle and small data scatter.

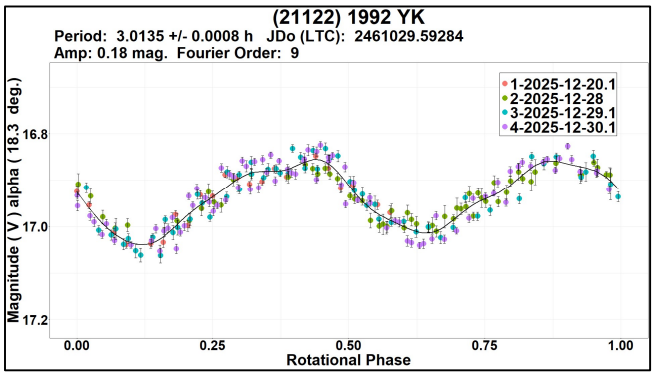

(22445) 1996 TT14. No previous reports on rotation period determinations were found in the LCDB. Observations conducted on four nights in the second half of 2025 September resulted in a bimodal lightcurve with a period of $P = 2.991 \pm 0.003$ h.

Number	Name	2025/mm/dd	Phase	L_{PAB}	B_{PAB}	Period (h)	P.E.	Amp	A.E.	Grp
2411	Zellner	09/22-09/23	8.8, 8.2	15	-2	2.975	0.007	0.43	0.02	MB-I
3149	Okudzhava	09/23-10/29	20.7, 3.8	36	-4	2.6619	0.0002	0.18	0.02	MB-I
3918	Brel	07/12-08/06	30.5,24.7	346	2	3.0972	0.0004	0.41	0.04	MB-I
3918	Brel	10/08-10/29	12.6,22.9	2	-6	3.0970	0.0004	0.33	0.02	MB-I
4217	Engelhardt	11/05-11/09	20.5,21.6	16	17	3.066	0.003	0.17	0.02	MB-I
4391	Balodis	08/25-09/17	*9.6, 5.0	347	3	3.7199	0.0006	0.17	0.02	MB-I
4875	Ingalls	06/22-07/02	24.7,27.8	234	6	3.777	0.002	0.26	0.02	FLOR
5498	Gustafsson	09/17-09/19	16.3,15.7	20	1	5.12	0.02	0.19	0.03	MB-I
5705	Ericsterken	11/01-11/02	14.5,13.5	61	5	3.713	0.007	0.25	0.02	MB-I
6015	Paularego	07/18-07/24	8.9, 6.8	307	10	2.833	0.002	0.09	0.03	MB-I
6198	Shirakawa	12/19-12/29	11.2, 5.8	104	6	2.7571	0.0006	0.13	0.02	FLOR
6441	Milenajesenska	06/24-06/27	13.7,12.6	293	3	2.817	0.004	0.41	0.03	HER
7223	Dolgorukij	07/31-08/29	20.3, 6.2	343	2	4.0123	0.0005	0.10	0.02	MB-I
7653	1991 UV	07/10-08/26	*24.0, 1.9	330	3	2.8649	0.0002	0.18	0.03	MB-I
8345	Ulmerspatz	08/10-08/19	25.9,25.1	5	29	17.12	0.04	0.48	0.03	PHO
11865	1989 SC	08/30-09/19	*7.4, 5.5	348	-1	2.4483	0.0003	0.10	0.01	MB-I
18108	2000 NT5	08/16-09/06	26.6,22.0	22	11	2.9151	0.0004	0.18	0.03	MB-I
19379	Labrecque	11/06-12/11	31.1,24.0	83	34	2.5928	0.0002	0.06	0.02	PHO
21122	1992 YK	12/20-12/30	18.3,14.5	124	9	3.0135	0.0008	0.18	0.03	V
22445	1996 TT14	09/19-09/23	4.1, 5.5	355	-5	2.991	0.003	0.21	0.03	MB-I
34459	2000 SC91	11/15-12/11	*9.8, 8.3	68	12	2.7790	0.0003	0.11	0.02	EUN
35663	1998 QT50	08/25-08/27	7.2, 8.2	320	-1	3.214	0.004	0.28	0.03	MB-O

Table I. Observing circumstances and results. Phase is the solar phase angle given at the start and end of the date range. If preceded by an asterisk, the phase angle reached an extrema during the period. L_{PAB} and B_{PAB} are the average phase angle bisector longitude and latitude. Grp is the asteroid family/group (Warner et al., 2009): MB-I = main-belt inner, MB-O = main-belt outer, PHO = Phocaea, HER = Hertha, FLOR = Flora, EUN = Eunomia, V = Vesta.

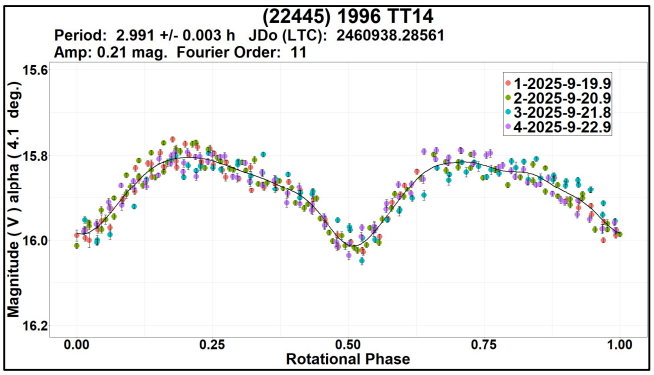

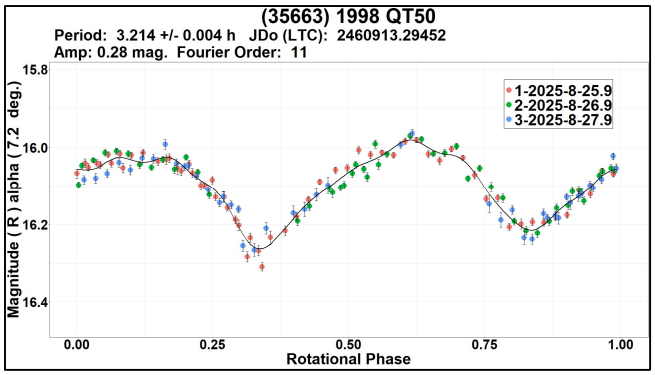

(34459) 2000 SC91. The derived period of P = 2.7790 ± 0.0003 h is fully consistent with two earlier values by Albers et al. (2010, 2.7791 h) and from Fauerbach and Nelson (2019, 2.781 h).

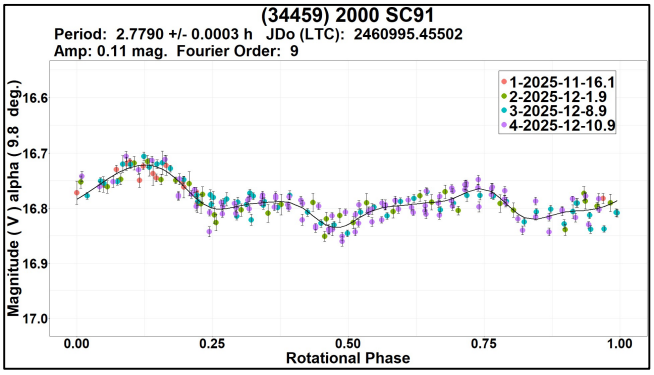

(35663) 1998 QT50. No records on previous rotation period determinations were found. Data from three consecutive nights in the second half of 2025 August show an unambiguous bimodal period of P = 3.214 ± 0.004 h.

Acknowledgements

Observational work at Sopot Astronomical Observatory is generously supported by Gene Shoemaker NEO Grants awarded by the Planetary Society in 2018 and 2022.

References

Albers, K.; Kragh, K.; Monnier, A.; Pligge, Z.; Stolze, K.; West, J.; Yim, A.; Ditteon, R. (2010). "Asteroid Lightcurve Analysis at the Oakley Southern Sky Observatory: 2009 October thru 2010 April." *Minor Planet Bull.* **37**, 152-158.

Behrend, R. (2007web, 2018web). Observatoire de Geneve web site. *http://obswww.unige.ch/~behrend/page_cou.html*

Benishek, V. (2018). "Lightcurve and Rotation Period Determinations for 29 Asteroids." *Minor Planet Bull.* **45**, 82-91.

Benishek, V. (2020). "Photometry of 39 Asteroids at Sopot Astronomical Observatory: 2019 September - 2020 March." *Minor Planet Bull.* **47**, 231-241.

Benishek, V. (2025). "Synodic Rotation Periods and Lightcurves for 26 Asteroids from Sopot Astronomical Observatory: 2024 October - 2025 March." *Minor Planet Bull.* **52**, 239-245.

Carbognani, A. (2011). "Lightcurves and Periods of Eighteen NEAs and MBAs." *Minor Planet Bull.* **38**, 57-63.

Deldem, M.; Behrend, R.; Pravec, P.; Fatka, P.; Durkee, R.; Ruocco, N.; Labrevoir, O.; Benishek, V.; Augustin, D.; Ergashev, K.; Burkhonov, O. (2025). "3918 Brel" CBET IAU **5642**.

Ďurech, J.; Tonry, J.; Erasmus, N.; Denneau, L.; Heinze, A.N.; Flewelling, H.; Vanco, R. (2020). "Asteroid Models Reconstructed from ATLAS Photometry." *Astronomy & Astrophysics* **643**, id.A59, 5 pp.

Erasmus, N.; McNeill, A.; Mommert, A.; Trilling, D.E.; Sickafoose, A.A.; Paterson, K. (2019). "A Taxonomic Study of Asteroid Families from KMTNET-SAAO Multiband Photometry." *Astrophys. J. Suppl. Series* **242**, id. 15.

Fauerbach, M.; Nelson, K.M. (2019). "Photometric Observations of 1007 Pawlowia, 1774 Kulikov, 2764 Moeller, 5110 Belgirate, (8505) 1990 YK, and (34459) 2000 SC91." *Minor Planet Bull.* **46**, 21-23.

Gaia Data Processing and Analysis Consortium (DPAC). "Gaia DR3 documentation." European Space Agency. Available at *https://gea.esac.esa.int/archive/documentation/GDR3/index.html*.

Garceran, A.C.; Aznar, A.; Mansego, E.A.; Rodriguez, P.B.; de Haro, J.L.; Silva, A.F.; Silva, G.F.; Martinez, V.M.; Chiner, O.R. (2016). "Nineteen Asteroid Lightcurves at Asteroids Observers (OBAS) - MPPD: 2015 April - September." *Minor Planet Bull.* **43**, 92-97.

Marchini, A.; Ballini, E.; Chianese, E.; Maggioni, E.; Scali, S.; Trefoloni, B.; Papini, R.; Salvaggio, F. (2017). "Rotation Period Determination for 2411 Zellner, 5293 Bentengahama and 9148 Boriszaitsev." *Minor Planet Bull.* **44**, 274-276.

Pravec, P. (2017web). Photometric Survey for Asynchronous Binary Asteroids web site. *http://www.asu.cas.cz/~ppravec/newres.txt*

R Core Team (2025). "R: A language and environment for statistical computing." R Foundation for Statistical Computing. Vienna, Austria. *https://www.R-project.org/*

Skiff, B.A.; McLelland, K.P.; Sanborn, J.J.; Koehn, B.W. (2023). "Lowell Observatory Near-Earth Asteroid Photometric Survey (NEAPS): Paper 5." *Minor Planet Bull.* **50**, 74-101.

VizieR (2025). *http://vizier.u-strasbg.fr/viz-bin/VizieR*

Warner, B.D. (2005a). "Asteroid lightcurve analysis at the Palmer Divide Observatory - fall 2004." *Minor Planet Bull.* **32**, 29-32.

Warner, B.D. (2005b). "Lightcurve analysis for asteroids 242, 893, 921, 1373, 1853, 2120, 2448 3022, 6490, 6517, 7187, 7757, and 18108." *Minor Planet Bull.* **32**, 4-7.

Warner, B.D.; Harris, A.W.; Pravec, P. (2009). "The asteroid lightcurve database." *Icarus* **202**, 134-146. Updated 2024 Oct. *https://minplanobs.org/MPInfo/php/lcdbsummaryquery.php*

Warner, B.D. (2011). "Upon Further Review: VI. An Examination of Previous Lightcurve Analysis from the Palmer Divide Observatory." *Minor Planet Bull.* **38**, 96-101.

Warner, B.D. (2012a). *The MPO Users Guide: A Companion Guide to the MPO Canopus/PhotoRed Reference Manuals*. BDW Publishing, Eaton, CO.

Warner, B.D. (2012b). "Asteroid Lightcurve Analysis at the Palmer Divide Observatory: 2011 September - December." *Minor Planet Bull.* **39**, 69-80.

Warner, B.D. (2016). *A Practical Guide to Lightcurve Photometry and Analysis* (2nd ed.). Springer International Publishing Switzerland.

Warner, B.D. (2018). *MPO Canopus* software, version 10.7.11.3. *http://www.bdwpublishing.com*

REVIEW AND STUDY OF THE LIGHTCURVES AND ROTATION PERIODS OF 10 ASTEROIDS

Rafael González Farfán (Z55)
Observatorio Uraniborg
Écija, Sevilla, SPAIN
uraniborg16@gmail.com

Faustino García de la Cuesta (J38)
La Vara, Valdés
Asturias, SPAIN

Esteban Reina Lorenz (232)
Masquefa, Can Parellada
Barcelona, SPAIN

Carlos Botana Albá (Y85)
Observatorio en Magalofes
Fene, A Coruña, SPAIN

Javier De Elías Cantalapiedra (L46)
Observatorio en Majadahonda
Madrid, SPAIN

Javier Ruiz Fernández (J96)
Observatorio de Cantabria
Cantabria, SPAIN

Fernando Limón Martínez (Z50)
Observatorio Mazariegos
Mazariegos, Palencia, SPAIN

José María Fernández Andújar (Z77)
Observatorio Inmaculada del Molino
Sevilla, SPAIN

Javier Polancos Ruiz
Observatorio La Portilla
Llanes, Asturias. SPAIN

(Received: 2025 November 2 Revised: 2026 January 30)

In this paper, we present the results of the study and monitoring of the lightcurves and rotation periods of 10 asteroids. In some cases, these studies confirmed data previously obtained in earlier observations, while in others, we present new results, which we hope will be confirmed (or not) by subsequent observations.

As on other occasions, the images obtained were calibrated in the conventional mode, without photometric filter, and with the application of darks, bias and flats. Data analysis and processing were performed using *FotoDif* (2021), *Tycho Tracker* (2023) and *Periodos* (2020) software. In addition, all data were light-time corrected. The results are summarized below. Individual lightcurve plots along additional comments as required are also presented.

The 10 asteroids studied were: 85 Io (6.875 h), 922 Schlutia (7.860 h), 940 Kordula (15.558 h), 994 Otthild (5.950 h), 995 Sternberga (11.182 h), 1453 Fennia (4.412 h), 4382 Stravinsky (12.196 h), 4583 Lugo (19.913 h) 5505 Rundetaarn (3.809 h), and 7842 Ishitsuka (7.270 h).

85 Io. Although this asteroid has been extensively studied, our team decided to monitor it during 2025 September just in case it revealed any surprises. One of the most recent studies was conducted in 2020 by Martikainen et al. (2021). The results obtained there are identical to ours, *i.e.*, $P = 6.875 \pm 0.013$ h and $A = 0.24 \pm 0.02$ mag. The most recent 3-D model registered in DAMIT is from 2017.

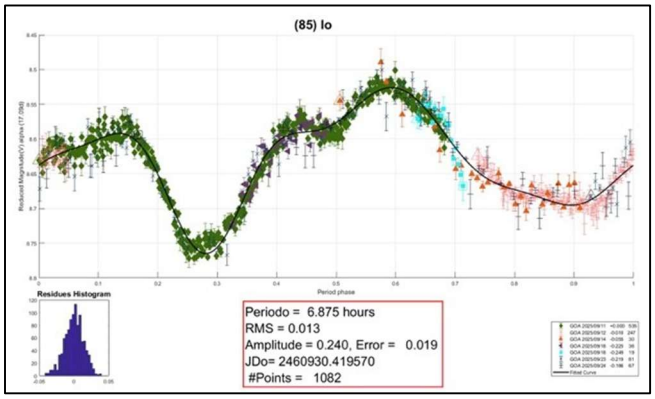

922 Schlutia. Discovered in 1919, this asteroid was the subject of our study from late 2025 September to early October. Among the latest results found in the literature (Durech et. al., 2020) is a rotation period that basically coincides with that obtained by our team: $P = 7.860 \pm 0.016$ h and $A = 0.14 \pm 0.02$ mag.

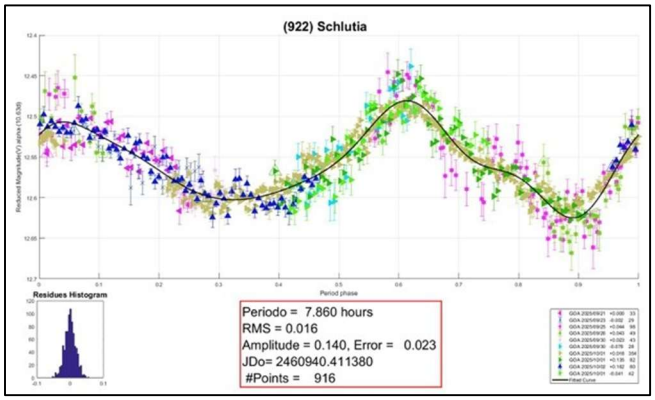

940 Kordula. During 2025 August and September, our team tracked this asteroid until we were able to plot its complete rotation curve. Based on this, the calculated period does not differ significantly from those previously published (Durech et al., 2020). $P = 15.558 \pm 0.009$ h and $A = 0.27 \pm 0.01$ mag.

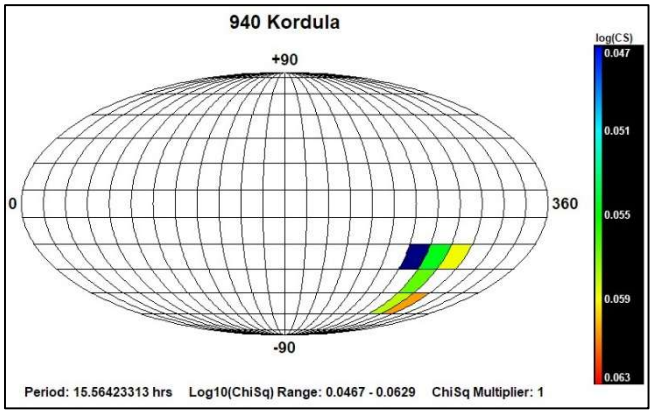

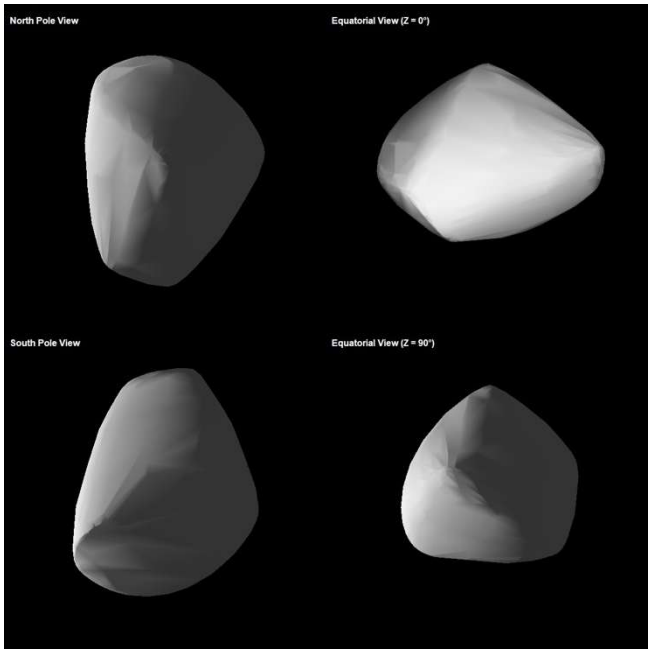

In addition, we combined our lightcurves (Grupo de Observación de Asteroides; GOAS, 2026) with dense lightcurves from DAMIT, applying the lightcurve inversion method (Kaasalainen and Torppa, 2001) implemented in the *MPO* package *LCInvert* (BDW Publishing, 2016). So, we obtained a spin axis of (J2000: $\lambda = 268°$, $\beta = -44°$, $P = 15.56423313$ h).

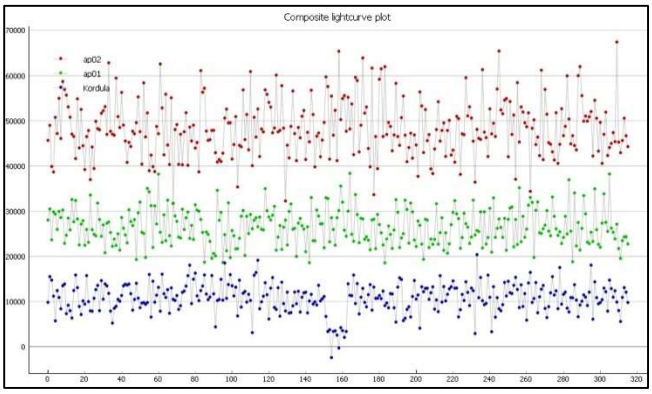

We were able to compare that model with the one resulting from positive occultations in 2023, observing a good match.

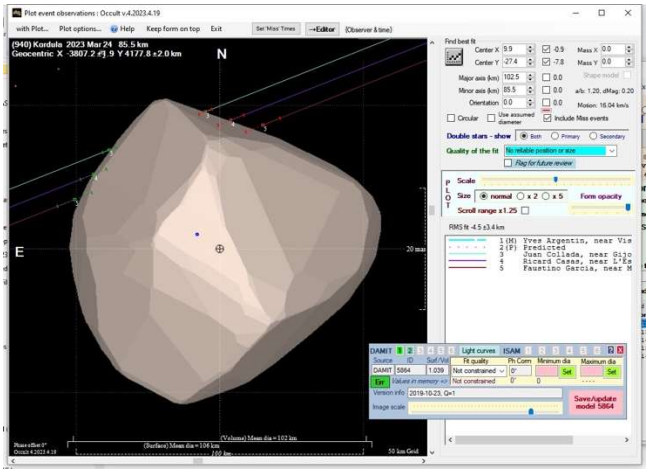

994 Otthild. The lightcurve for this asteroid was plotted by our team in late 2025 September and early October, following a note on the JPL website announcing that the existing data was based on limited observations. Therefore, it could be an object of special interest. However, recent results (Colazo et al., 2021) coincide with ours, which seems to clear up any doubts. We obtained $P = 5.950 \pm 0.014$ h, $A = 0.11 \pm 0.02$ mag.

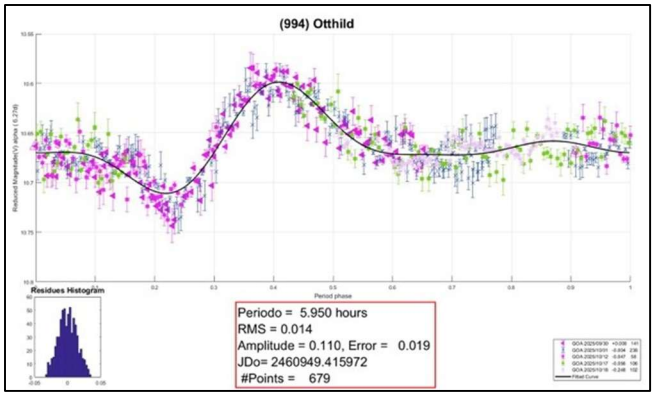

Although we did not have sufficient quality data to obtain a 3-D model, we were able to record a positive occultation of the star HIP 115074 by this asteroid on the night of 2025 October 28.

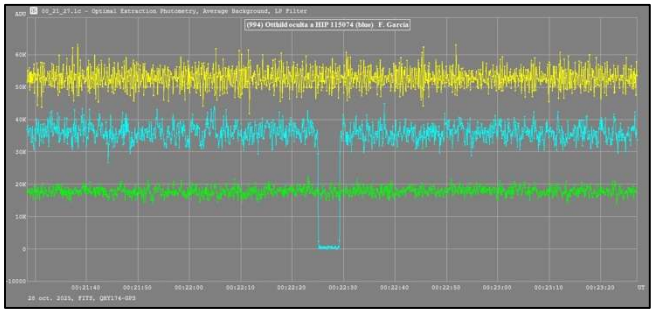

995 Sternberga. Most of our observations of this asteroid took place in 2025 September. We noticed discrepancies between the results published by JPL (2025) and ALCDEF (2026) regarding rotation periods, which was one reason for choosing it as a target. The lightcurve we obtained seems to support the ALCDEF (2026) result. Thus, we obtained a $P = 11.182 \pm 0.008$ h, $A = 0.11 \pm 0.01$ mag.

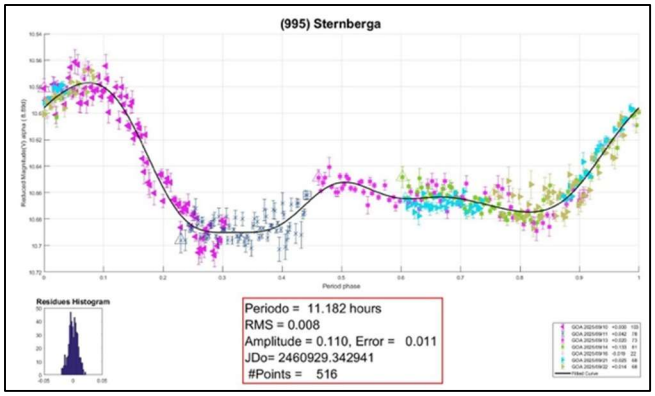

1453 Fennia. This was an asteroid proposed by our group for 2025 October. It appears to be a synchronous binary system, located in the innermost regions of the asteroid belt, with a diameter of only 7 km. Our studies allowed us to deduce a rotation period that practically coincides with those previously published, $P = 4.412 \pm 0.030$ h, $A = 0.18 \pm 0.04$ mag.

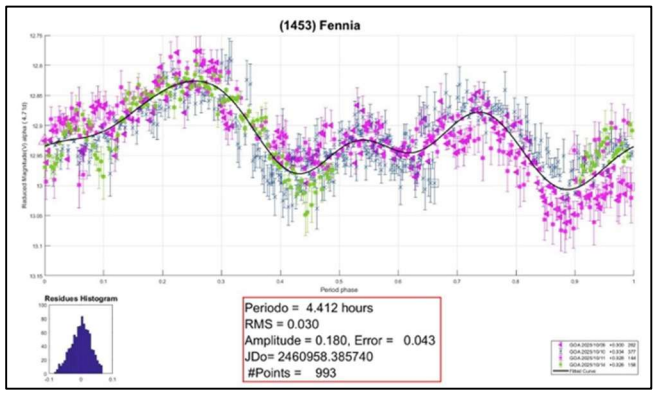

We were able to derive a 3-D model by combining our dense lightcurves with those from ALCDEF as well as AstDys sparse data (from ATLAS, CATALINA, PALOMAR and USNO), applying the lightcurve inversion method (Kaasalainen and Torppa, 2001) implemented in the MPO package *LCInvert* (BDW Publishing, 2016). We obtained a spin axis of (J2000: $\lambda = 313°$, $\beta = -8°$, $P = 4.41210381$ h).

It is important to say that 1453 is a known binary asteroid. To generate a spin axis model properly, the effects of the secondary should be removed from the combined light, leaving any variations due only the primary. Sparse data rarely, if ever, allow the proper corrections prior to modeling, corrections that were also omitted from our dense lightcurves.

The lightcurve inversion process usually does not allow a unique solution, especially if the latitude of the pole is near the equatorial plane. In such cases, up to four mirrored solutions are possible, each in longitude and latitude (Kaasalainen and Torppa, 2001). Warner et al. (2014) found a weak pole solution for this asteroid after subtracting the effects of the secondary. His solution (J2000: $\lambda = 187°$, $\beta = -11°$) is a solution mirrored in longitude only.

4382 Stravinsky. There is no data published in JPL (2025) or ALCDEF (2026) on the rotation period of this asteroid, which made it the focus of our attention in late 2025 September and early October. Our observations allowed us to deduce a period of $P = 12.196 \pm 0.014$ h, $A = 0.12 \pm 0.02$ mag.

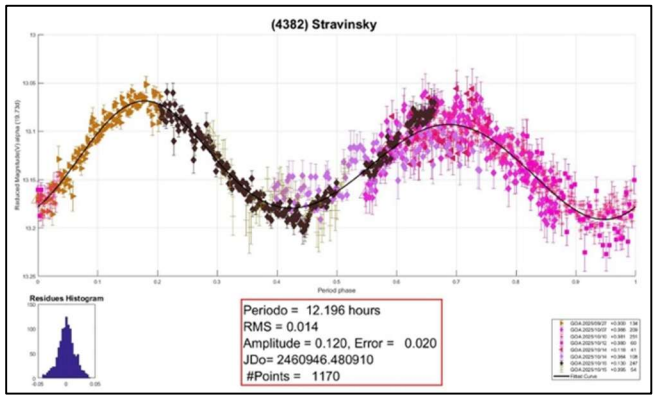

4583 Lugo. The few lightcurves we found in the literature for this asteroid give a result of about 12 hours for the rotation period, which is inconclusive, as is noted on the JPL (2025) website. Our team observed it during the month of 2025 October, allowing us to derive a very different result: $P = 19.913 \pm 0.036$ h, $A = 0.48 \pm 0.05$ mag.

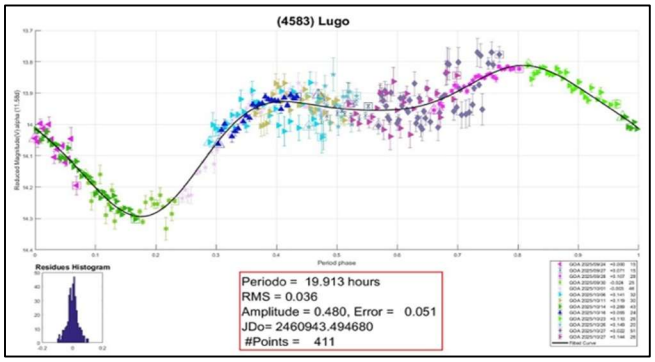

We should note that our period is almost 1.5x that of previous results. The 3:2 alias raises the possibility of a miscount of rotations over the span of our observations, or by the previous authors, which is sometimes called a *rotational alias*. Additional observations by a collaboration of observers over a wide range of longitudes may be required to reach a more conclusive result.

5505 Rundetaarn. We did not find any results in the literature for the rotation period of this asteroid, so it was studied during the month of 2025 October. Our data allowed us to determine $P = 3.809 \pm 0.010$ h, $A = 0.13 \pm 0.02$ mag.

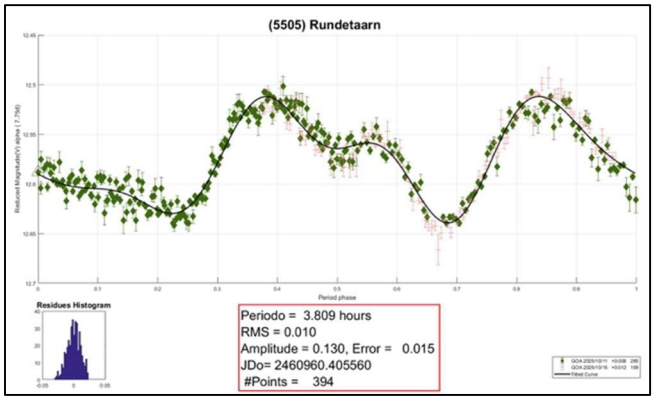

7842 Ishitsuka. There is no published data in JPL (2025) or ALCDEF (2026) on the rotation period of this main belt asteroid, discovered in 1994. During 2025 September, it was the subject of our team's research. The measurements taken allowed us to deduce a period $P = 7.270 \pm 0.031$ h, $A = 0.51 \pm 0.04$ mag.

Number	Asteroid	2025 mm/dd	Phase	Period(h)	P.E.	Amp	A.E.
85	Io	09/11-09/25	17.1-10.9	6.875	0.013	0.24	0.02
922	Schlutia	09/21-10/02	10.6-05.0	7.860	0.068	0.14	0.02
940	Kordula	08/22-09/18	3.4-11.0	15.558	0.009	0.27	0.01
994	Otthild	09/30-10/18	6.3-14.7	5.950	0.014	0.11	0.02
995	Sternberga	09/10-09/22	16.5-20.1	11.182	0.008	0.11	0.01
1453	Fennia	10/09-10/14	4.8-8.0	4.412	0.030	0.18	0.04
4382	Stravinsky	09/27-10/16	19.7-11.6	12.196	0.014	0.12	0.02
4583	Lugo	09/25-10/29	12.1-24.3	19.913	0.036	0.48	0.05
5505	Rundetaarn	10/11-10/15	7.7-7.1	3.809	0.010	0.13	0.02
7842	Ishitsuka	09/13-09/26	5.8-3.1	7.270	0.031	0.51	0.04

Table I. Observing circumstances and results. Phase is the solar phase angle given at the start and end of the date range. If preceded by an asterisk, the phase angle reached an extrema during the period.

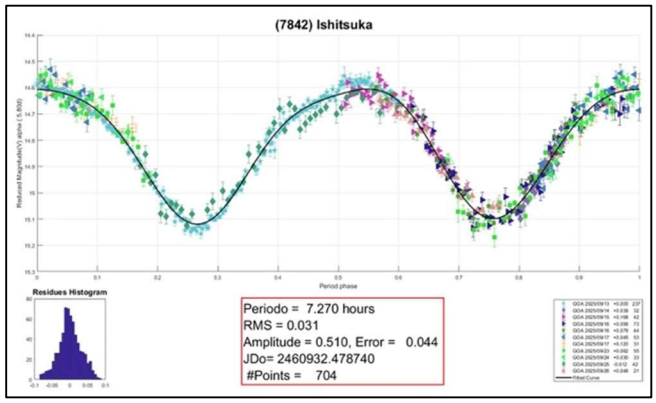

Observer	Telescope	Camera
Botana Alba, Carlos(Y85)	Newton 8"	ZWO ASI183M Pro
De Elias Cantalapiedra, Javer (L46)	CDK 12.5"	QHY268m
Fernández Andújar, Jose M.(Z77)	SC 8"	Atik 460ex m
García de la Cuesta, Faustino (J38)	RCX 10"	SBIG ST8XE
González Farfán, Rafael(Z55)	SC 11"	Atik414ex m
Limón Martínez, Fernando (Z50)	SC 8"	ZWO ASI533MM Pro
Polancos Ruiz, Javier	Vixen ED103S	Atik 314L m
Reina Lorent, Esteban (232)	SC 10"	ZWO 294MM
Ruiz Fernández, Javier (J96)	RC 16"	ST8XME

References

ALCDEF (2026). Asteroid Lightcurve Data Exchange Format web site. *https://alcdef.org*

Bdw Publishing (2016). *MPO LCInvert* software. *https:/bdwpubplishing.com*

Colazo, M.; Stechina, A.; Fornari, C.; Santucho, M.; and 21 colleagues (2021) "Rotation periods and lightcurve analysis of 18 asteroids from Córdoba Observatory." *Minor Planet Bull*. **48**, 50-55.

DAMIT. *https://damit.cuni.cz/*

Durech, J.; Tonry, J.; Erasmus, N.; Denneau, L.; Heinze, A.N.; Flewelling, H.; Vančo, R. (2020). "Asteroid models reconstructed from ATLAS photometry." *Astron. Astrophys*. **643**, A59.

FotoDif (2021) software. *http://astrosurf.com/orodeno/fotodif/index.htm*

GOAS (2026). Grupo de Observación de Asteroides. *https://sites.google.com/view/goas2*

JPL (2025). Small-Body Database Lookup. *https://ssd.jpl.nasa.gov/tools/sbdb_lookup.html#/?sstr=52768*

Kaasalainen, M.; Torppa, J. (2001). "Optimization Methods for Asteroid Lightcurve Inversion. I. Shape Determination." *Icarus* **153**, 24-36.

Martikainen, J.; Muinonen, K.; Penttila, A.; Cellino, A.; Wang, X.-B. (2021). "Asteroid absolute magnitudes and phase curve parameters from Gaia photometry." *Astron. Astrophys*. **649**, A98.

Períodos (2020) software. *http://www.astrosurf.com/salvador/Programas.html*

Tycho Tracker (2023) software. *https://www.tycho-tracker.com*

Warner, B.D.; Harris, A.W.; Stephens, R.D. (2014). American Astronomical Society, DPS meeting #46, id.509.12.

LIGHTCURVE ANALYSIS FOR FOUR MAIN-BELT, ONE NEAR-EARTH, AND ONE POTENTIALLY HAZARDOUS ASTEROID

Gonzalo Fornas (J57)
Asociación Valenciana de Astronomía
(Centro Astronómico Alto Turia)
C/ Profesor Blanco 16. 46014 Valencia, SPAIN
gon@iicv.es

Alvaro Fornas (J57)
Asociación Valenciana de Astronomía (CAAT)

Alfonso Carreño (Y76)
Nova Canet Observatory

Enrique Rathmann (Y78)
Asociación Valenciana de Astronomía (CAAT)
Tros Alt Observatory

Vicente Mas (J57)
Asociación Valenciana de Astronomía (CAAT)

(Received: 2025 December 16)

Photometric observations for four main-belt, one near-Earth, and one potentially hazardous asteroid. We derived the following synodic rotation periods: 1717 Arlon, 5.2269 ± 0.0001 h; 19122 Amandabosh, 7.8132 ± 0.0024 h; 24641 Enver, 9.0498 ± 0.0019 h; (23576) 1995 DZ3, 4.2947 ± 0.0005 h; (612356) 2002 JX8, 3.33720 ± 0.00044 h; 2025 FA22, 13.017 ± 0.002 h.

We report on the photometric analysis of six asteroids by Asociación Valenciana de Astronomía (AVA). The data were obtained during the last quarter of 2025. We present graphic results of the data analysis, mainly lightcurves, with the plot phased to a given period. We managed to obtain several accurate and complete lightcurves and calculated their rotation periods as accurately as possible.

Observatory	Telescope	CCD
C.A.A.T. J57	17”-DK	QHY- 600
C.A.A.T. J57	10”-NW	ZWO ASI 1600
Z93	SC-8”	SBIG ST8300
Y78	SC-8”	ZWO ASI 294 MM PRO
Y76	SC-9.25”	ATIK 314L+

Table I. List of instruments used for the observations.

We focused on asteroids with no reported period and those where the reported period was poorly established and needed confirmation. The targets were selected from the Collaborative Asteroid Lightcurve (CALL) website (*http://www.minorplanet.info/call.html*), the Minor Planet Center (*http://www.minorplanet.net*). The Asteroid Lightcurve Database (LCDB; Warner et al., 2009) was consulted to locate previously published results.

Images were measured using *MPO Canopus V12* (Bdw. Publishing) with a differential photometry technique. The comparison stars were restricted to near solar-color to minimize color dependencies, especially at larger air masses. The lightcurves show the synodic rotation period. The amplitude (peak-to-peak) that is shown is that for the Fourier model curve and not necessarily the true amplitude.

1717 Arlon. This inner main-belt asteroid was discovered on 1954 Jan at Uccle by S.J. Arend. We made observations on 2024 Oct 1 to Dec 30. From our data we derive a synodic rotation period of 5.2269 ± 0.0001 h and an amplitude of 0.13 mag. Behrend (2006web, 2008web, 2018web) got periods of 5.873 h, 5.1082 h and 5.261 h. Pravec (2011web) got periods of 5.1477 h, 5.1496 h and 3.51482 h. Cooney et al. (2006a) and Cooney et al. (2006b) found periods of 5.1884 h and 5.148 h, respectively. Oey (2014) found a period of 5.148 h and Franco et al. (2019) found 5.1448 h.

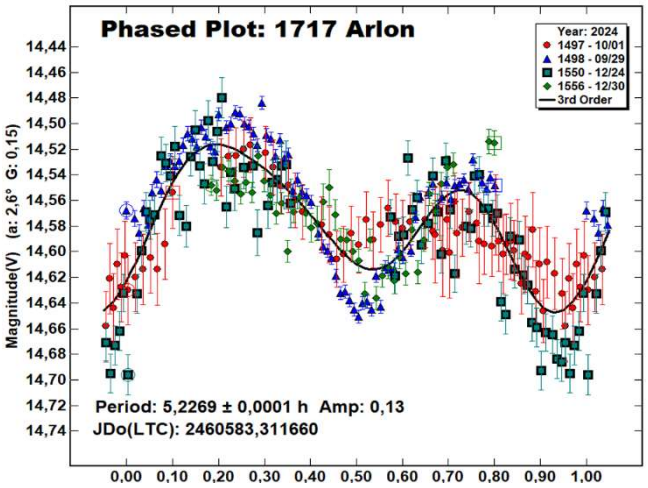

19122 Amandabosh. This inner main-belt asteroid was discovered on 1985 Nov at Anderson Mesa by E. Bowell. We made observations on 2025 Nov 21 to 28. From our data we derive a synodic rotation period of 7.8132 ± 0.0024 h and an amplitude of 0.63 mag. We have no previous information about its rotation period.

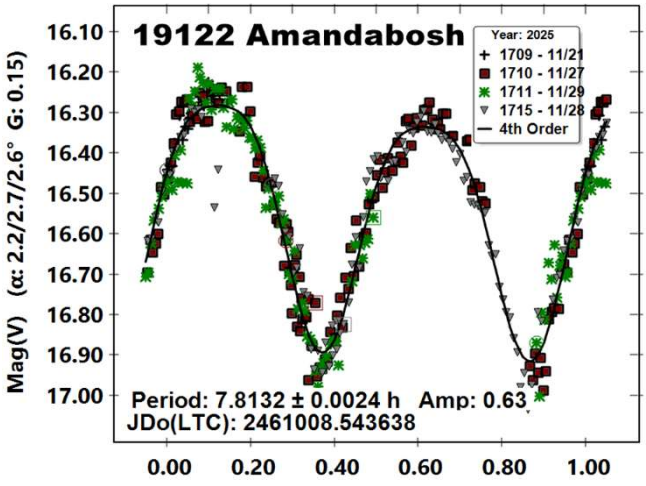

24641 Enver. This inner main-belt asteroid was discovered on 1983 Sep at Nauchny by L.G. Karachkina. We made observations on 2025 Aug 26 to Sep 1. From our data we derive a synodic rotation period of 9.0498 ± 0.0019 h and an amplitude of 0.37 mag. We have no previous information about its rotation period.

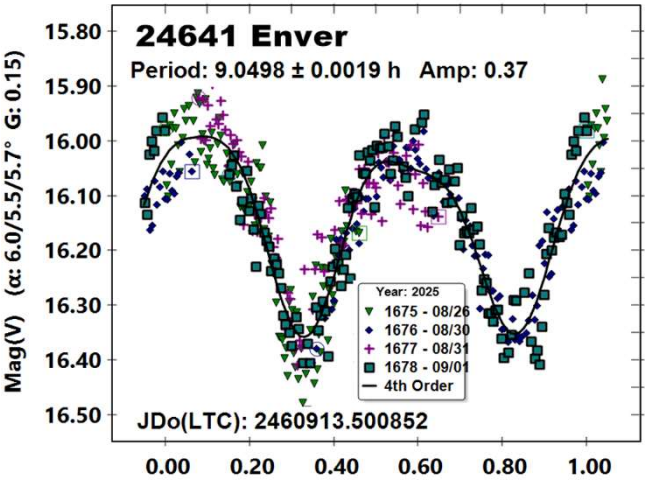

There is a second possible period of 7.5996 h, and more data should be necessary to be sure of which is the real one. We will try next time it's possible.

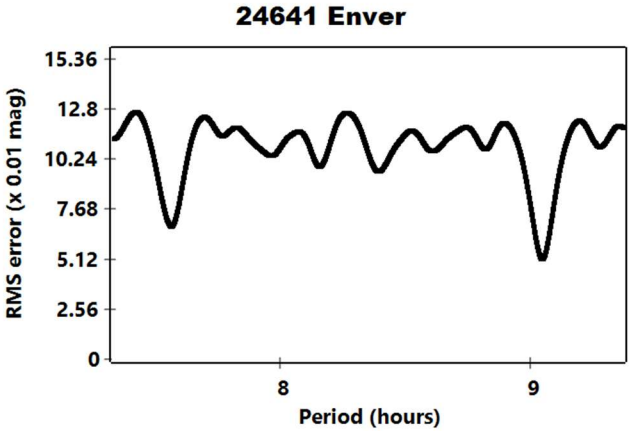

(23576) 1995 DZ3. This outer main belt-asteroid was discovered on 1995 Feb at Kitt Peak by Spacewatch. We made observations on 2025 Sep 17 to 20. From our data we derive a synodic rotation period of 4.2947 ± 0.0005 h and an amplitude of 0.26 mag. We have no previous information about its rotation period.

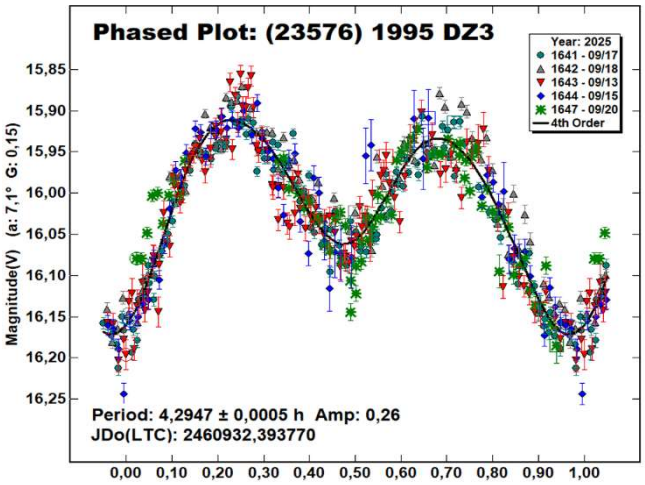

(612356) 2002 JX8. This Near-Earth asteroid was discovered on May 2002 at Socorro by LINEAR. We made observations on 2025 April 28 to May 16. From our data we derive a synodic rotation period of 3.33720 ± 0.00044 h and an amplitude of 0.17 mag. We have no previous information about its rotation period.

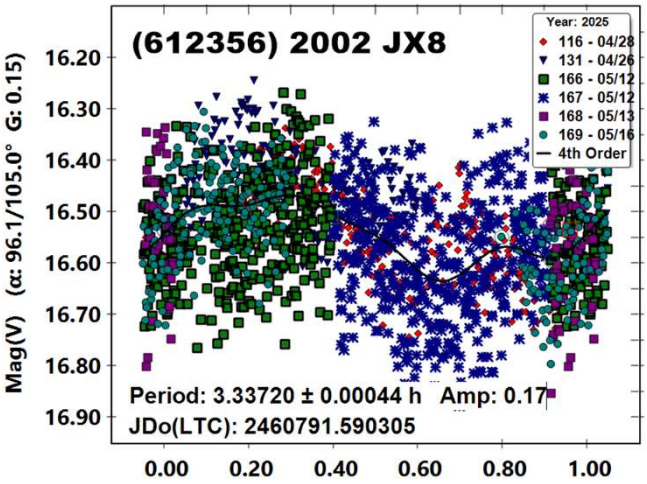

2025 FA22. This is a PHA with an Apollo orbit. The initial reported observation was by Pan-STARRS 2, Haleakala on 2025-3-29. We made observations on 2025 Sep 19 to 24. From our data we derive a synodic rotation period of 13.017 ± 0.002 h and an amplitude of 1.33 mag. We have no previous information about its rotation period.

Number	Name	yyyy mm/dd	Phase	L_{PAB}	B_{PAB}	Period(h)	P.E.	Amp	A.E.	Grp
1717	Arlon	2024/10/01-12/30	14.3,27.0	169,9	-0.05	5.2269	0.0001	0.13	0.03	MB-I
19122	Amandabosh	2025/11/21-28	2.7,2.1	62.5	.95	7.8132	0.0024	0.63	0.03	MB-I
24641	Enver	2025/08/26-09/01	6.0,5.6	337.5	8.5	9.0498	0.0019	0.37	0.03	MB-I
23576	1995 DZ3	2025/09/17-20	7.1,7.3	355	13.3	4.2947	0.0005	0.26	0.05	MB-O
612356	2002 JX8	2025/04/28-05/16	96.1,104.2	218.1	35.1	3.33720	0.00044	0.17	0.05	NEA
	2025 FA22	2025/09/19-24	65.2,28.5	20.1	4.4	13.017	0.002	1.33	0.03	PHA

Table I. Observing circumstances and results. The phase angle is given for the first and last date. If preceded by an asterisk, the phase angle reached an extrema during the period. L_{PAB} and B_{PAB} are the approximate phase angle bisector longitude/latitude at mid-date range (see Harris et al., 1984). Grp is the asteroid family/group (Warner et al., 2009).

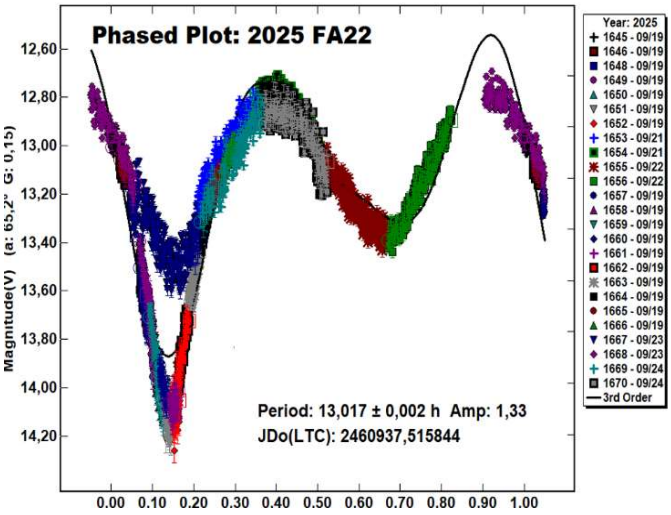

References

Behrend, R. (2006web, 2008web, 2018web). Observatoire de Geneve web site. *http://obswww.unige.ch/~behrend/page_cou.html*

Cooney, W.; Gross, J.; Terrell, D.; Stephens, R.; Pravec, P.; Kusnirak, P.; Durkee, R.; Galad, A. (2006a). "(1717) Arlon"; CBET 369.

Cooney, W.; Gross, J.; Terrell, D.; Pravec, P.; Kusnirak, P. and 13 collaborators (2006b). "(1717) Arlon." CBET 504.

Franco, L.; Marchini, A.; Battista Casalnuovo, G.; Chinaglia, B.; Baj, G.; Scarfi, G.; Galli, G.; Bacci, P.; Maestripieri, M.; Valvasori, A.; Caselli, C.; Punzo, P.; Montigiani, N.; Mannucci, M.; Bachini, M.; Succi, G.; Bacci, R. (2019). "Lightcurves for 224 Oceana, 359 Georgia, 1453 Fennia and 1717 Arlon." *Minor Planet Bull.* **46**, 350-352.

Harris, A.W.; Young, J.W.; Saltriti, F.; Zappala, V. (1984). "Lightcurves and phase relations of the asteroids 82 Alkmene and 444 Gyptis." *Icarus* **57**, 251-258.

Oey, J. (2014). "Lightcurve Analysis of Asteroids from Blue Mountains Observatory in 2013." *Minor Planet Bull.* **41**, 276-281.

Pravec, P. (2011web) Ondrejov Asteroid Photometry Project. *https://space.asu.cas.cz/~ppravec/*

Warner, B.D.; Harris, A.W.; Pravec, P. (2009). "The Asteroid Lightcurve Database." *Icarus* **202**, 134-146. Updated 2016 Sep. *http://www.minorplanet.info/lightcurvedatabase.html*

PHOTOMETRIC OBSERVATIONS AND LIGHTCURVE ANALYSIS OF 5 MAIN-BELT ASTEROIDS FROM ASPIRE COLLABORATION

Charles Galdies
Institute of Earth Systems, University of Malta
Msida, MALTA
charles.galdies@um.edu.mt

Stephen M. Brincat
Flarestar Observatory (MPC 171)
Fl. 5 George Tayar Street, San Gwann SGN 3160, MALTA

Marek Bucek
Luckystar Observatory (MPC M55)
Dr. Lučanského 547, Važec 032 61, SLOVAKIA

Vincent Zammit
Stellar Horizon Observatory
No.8, Maranatha, Triq Tal-Fieres, Kirkop KKP 1502, MALTA

(Received: 2025 November 4 Revised: 2026 February 15)

We present CCD photometric observations of five main-belt asteroids obtained from three observatories in Malta and one in Slovakia during twenty-one nights between December 2023 and January 2024. The targets were (1146) Biarmia, (4460) Bihoro, (4602) Heudier, (7572) Znokai and (57518) 2001 SB286. Derived synodic rotation periods are 5.4708 ± 0.0005 h, 6.2599 ± 0.0046 h, 2.7196 ± 0.0036 h, 5.9253 ± 0.0076 h, and 2.8064 ± 0.0033 h, with amplitudes between 0.09 and 0.15 mag.

The periods and amplitudes of asteroid lightcurves presented in this paper are the product of collaborative work by the ASPIRE (Asteroid and Stellar Photometric Research) group. Observations were conducted with 0.2-m to 0.25-m Schmidt-Cassegrain telescopes equipped with CCD cameras at the Znith, Flarestar, Luckystar and Stellar Horizon Observatories. Image calibration used dark-frame subtraction and flat-field correction. Differential aperture photometry was obtained with *MPO Canopus* (Warner, 2017) using Sloan-R zero-point magnitudes. Near-solar-color comparison stars were selected through the Comparison Star Selector function of *MPO Canopus* based on the Asteroid Terrestrial-impact Last Alert System (ATLAS) catalog (Tonry et al., 2018). Table 1 displays the details of the instrumentation and number of observation nights for each target. Fourier analysis was applied to derive synodic rotation periods for each asteroid.

Observatory/ Country	Scope and Type	Camera	Observed Asteroids (#Nights)
Flarestar Obs. (MPC: 171)/ MALTA	0.25-m SCT	Moravian G2-1600	# 1146 (3)
Luckystar Obs. (MPC: M55)/ SLOVAKIA	0.25-m SCT	Atik 460EX	# 4460 (5) #57518 (8) # 4602 (5) # 7572 (4)
Stellar Horizon Obs. / MALTA	0.30-m SCT	ASI6200 MM	# 1146 (1)
Znith Astronomy Obs./ MALTA	0.2-m SCT	Moravian G2-1600	# 4460 (1)

Table I. Instrumentation and Observation Runs. SCT: Schmidt-Cassegrain Telescope.

(1146) Biarmia was discovered on 1929 May 7 by Grigory Neujmin at Simeiz Observatory, Crimea (JPL, 2025) and named for Bjarmaland, a region mentioned in Norse sagas (JPL, 2024). This asteroid orbits the Sun in the outer main-belt, with an average distance of about 3.04 AU. Its orbit is moderately eccentric (e ≈ 0.255) with an orbital plane of about 17°, completing a full revolution every 5.31 years. It was observed over four nights between 2025 April 6 and May 26 with three nights from Flarestar Observatory and another from Stellar Horizon. Our analysis gives a period of 5.4708 ± 0.0005 h and an amplitude of 0.14 ± 0.02 mag. The LCDB lists values of 5.468 - 5.470 h with amplitudes around 0.20 mag (U = 3) based on measurements compiled by Durkee (2009) and Behrend (2020web) with a U=3 value. Our result is fully consistent with these published values.

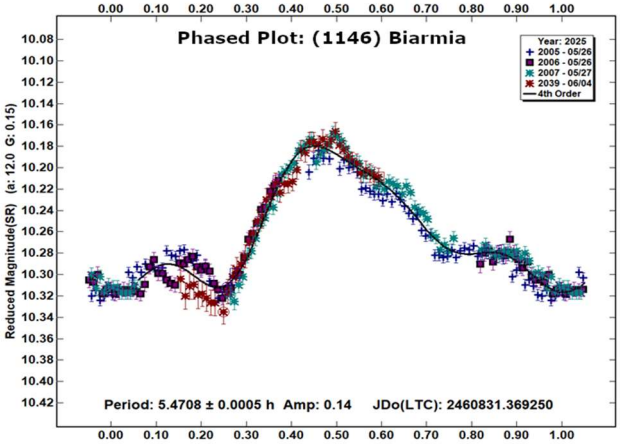

(4460) Bihoro was discovered on 1990 February 28 by Kin Endate and Kazuro Watanabe at Kitami Observatory, Japan (JPL, 2025) and named for the town of Bihoro in Hokkaidō (JPL, 2024). According to the JPL Small-Body Database, Bihoro follows an elliptical path around the Sun with a semi-major axis of about 2.92 astronomical units (AU). Its orbit is moderately elongated, having an eccentricity of 0.18. The asteroid's orbital plane is inclined by approximately 27.05°, making it one of the more inclined objects in the main belt. Its orbital period is around 4.99 years. Znith Observatory observed it for one night on 2024 January 19 and Luckystar Observatory for six nights between 2023 December 12-20 and 2024 January 10-11. The derived synodic period is 9.922 ± 0.0092 h with an amplitude of 0.14 ± 0.04 mag. The complete period spectrum of this target is shown below. The LCDB lists a previous period of 9.923 ± 0.11 h with a U of 2+ (Wiles, 2024).

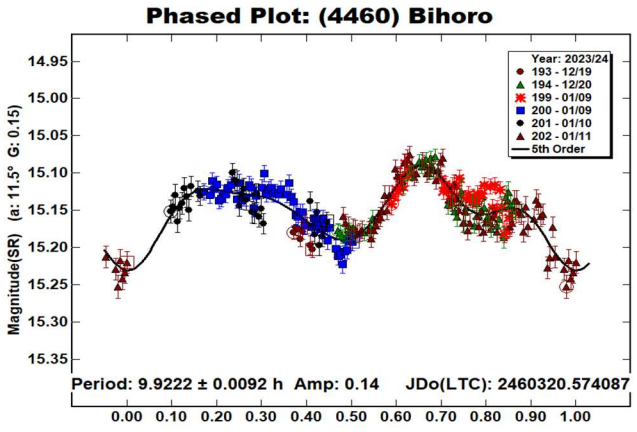

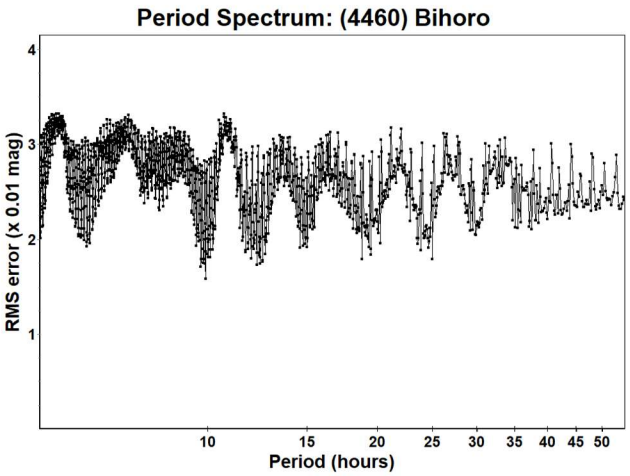

(4602) Heudier. This asteroid was discovered on 1986 October 28 at Caussols (CERGA, OCA, France) and named for astronomer Jean-Louis Heudier of Calern Observatory (JPL, 2025). Heudier travels around the Sun at an average distance defined by a semi-major axis of about 2.619 AU, an orbital eccentricity of 0.16, and with an orbital plane that is tilted by approximately 12.39°. Its orbital period is roughly 4.24 years, placing it firmly within the central region of the asteroid belt. Heudier was observed from Luckystar Observatory for five nights between 2024 August 10 and 15. The derived period is 2.7196 ± 0.0036 h and amplitude 0.09 ± 0.06 mag. No rotation period for Heudier is listed in the LCDB (Warner et al., 2009), making this the first reported lightcurve for this asteroid.

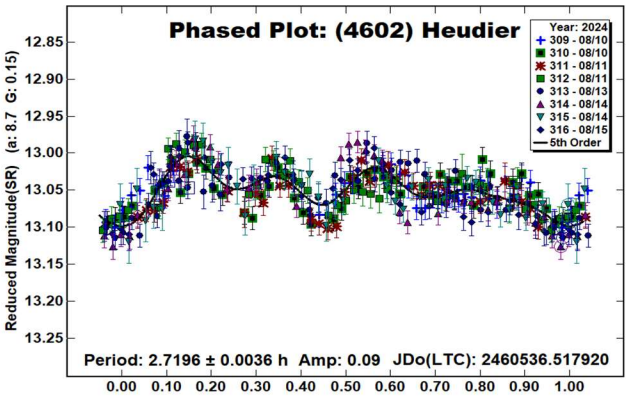

(7572) Znokai was discovered on 1989 September 23 by Kin Endate and Kazuro Watanabe at Kitami Observatory (JPL, 2025) and named for "Z-no-kai," a Japanese educational society promoting astronomy (JPL, 2025). According to the JPL Small-Body Database, Znokai travels around the Sun at an average distance defined by a semi-major axis of about 2.92 AU. Its orbit is moderately elongated, with an eccentricity of 0.18 and an orbital plane that is inclined by around 27.05°. Its orbital period is about 4.99 years.

This asteroid was observed from Luckystar Observatory for four nights between 2024 November 9 and 20. We derived a period of 5.9253 ± 0.0076 h and an amplitude of 0.10 ± 0.04 mag. No LCDB entry with a numerical period was found, and the Minor Planet Bulletin index lists the object without results. Our measurement therefore represents the first secure rotation period determination for Znokai.

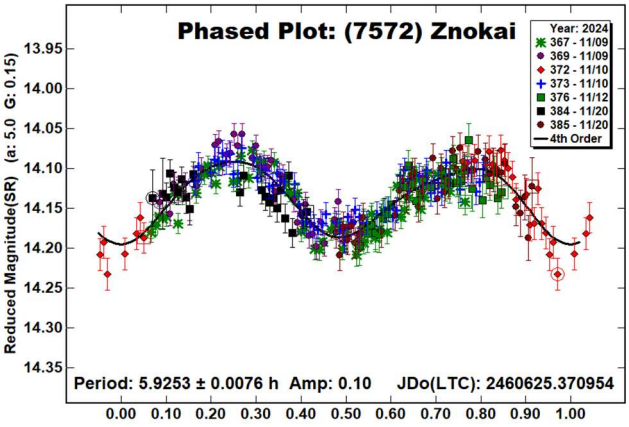

(57518) 2001 SB286 was discovered on 2001 September 28 by C.W. Juels at Fountain Hills, Arizona (JPL, 2025). This asteroid's orbit has a semi-major axis of 2.86 AU, eccentricity 0.22, inclination 15.3° and an orbital period of 4.86 years (JPL, 2025). We observed it from Luckystar Observatory for ten nights between 2025 May 8 and 14. A period of 2.8064 ± 0.0033 h and amplitude of 0.15 ± 0.06 mag were derived. A search of the LCDB (Warner et al., 2009) revealed no previous entry listing a rotation period, indicating that this result is likely a first determination for this object.

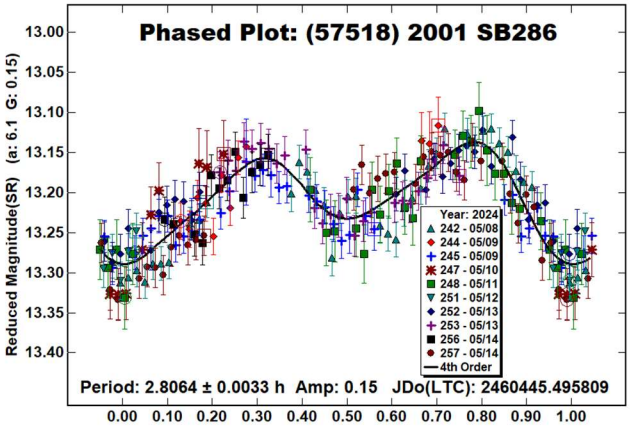

Acknowledgements

We would like to thank Brian Warner for his work in the development of *MPO Canopus* and for his efforts in maintaining the CALL website (Warner, 2016; 2021). This research has made use of the JPL's Small-Body Database (JPL, 2025).

References

Behrend, R. (2020web). Observatoire de Geneve web site. *http://obswww.unige.ch/~behrend/page_cou.html*

Durkee, R.I. (2009). "The Lightcurves of 1146 Biarmia and 5598 Carlmurray." *Minor Planet Bulletin* **36**, 170.

Harris, A.W.; Young, J.W.; Scaltriti, F.; Zappala, V. (1984). "Lightcurves and phase relations of the asteroids 82 Alkmene and 444 Gyptis." *Icarus* **57**, 251-258.

JPL (2025). Small-Body Database Lookup. *https://ssd.jpl.nasa.gov/tools/sbdb_lookup.html#/?sstr=4460&view=OPD*

Tonry, J.L.; Denneau, L.; Flewelling, H.; Heinze, A.N.; Onken, C.A.; Smartt, S.J.; Stalder, B.; Weiland, H.J.; Wolf, C. (2018). "The ATLAS All-Sky Stellar Reference Catalog." *The Astrophysical Journal* **867**, 105.

Warner, B.D. (2017). MPO Software, *MPO Canopus* version 10.7.10.0. Bdw Publishing. *https://minplanobs.org/BdwPub/php/displayhome.php*

Warner, B.D.; Harris, A.W.; Pravec, P. (2009). "The asteroid lightcurve database." *Icarus* **202**, 134-146. Updated 2023 Oct. *https://minplanobs.org/MPInfo/php/lcdb.php*

Wiles, M. (2024). "Rotational Period and Lightcurve Determination for Seven Minor Planets." *Minor Planet Bulletin* **51**, 330-332.

Number	Name	yyyy mm/dd	Phase	L_{PAB}	B_{PAB}	Period(h)	P.E.	Amp	A.E.	Grp
1146	Biarmia	2025 05/26-06/04	12.0,10.2	260.6	16.3	5.4708	0.0005	0.14	0.02	MB
4460	Bihoro	2023 12/19-2024 01/19	11.5,13.6	89.9	27.7	6.2599	0.0046	0.12	0.05	MB
4602	Heudier	2024 08/10-08/15	8.8, 8.4	323.7	16.5	2.7196	0.0036	0.09	0.06	Eun
7572	Znokai	2024 11/09-11/20	5.0,10.7	42.0	5.5	5.9253	0.0076	0.10	0.04	MB
57518	2001 SB286	2024 05/08-05/14	6.2, 6.4	228.6	12.5	2.8064	0.0033	0.15	0.06	MB

Table I. Observing circumstances and results. The phase angle is given for the first and last date. If preceded by an asterisk, the phase angle reached an extrema during the period. L_{PAB} and B_{PAB} are the approximate phase angle bisector longitude/latitude at mid-date range (see Harris et al., 1984). Grp is the asteroid family/group (Warner et al., 2009).

PHOTOMETRIC OBSERVATIONS AND LIGHTCURVE ANALYSIS OF (2600) LUMME, (3667) ANNE-MARIE, (11861) TERUHIME, (26328) LITOMYSL, AND (5480) 1989 YK8

Charles Galdies
Institute of Earth Systems, University of Malta
Msida, MALTA
charles.galdies@um.edu.mt

Stephen M. Brincat
Flarestar Observatory (MPC 171), Fl. 5 George Tayar Street,
San Gwann SGN 3160, MALTA

Marek Bucek
Luckystar Observatory (MPC M55), Dr. Lučanského 547,
Važec 032 61, SLOVAKIA

Vincent Zammit
Stellar Horizon Observatory
No.8, Maranatha, Triq Tal-Fieres
Kirkop KKP 1502, MALTA

(Received: 2025 November 4)

We present CCD photometric observations of five main-belt asteroids: (2600) Lumme, (3667) Anne-Marie, (11861) Teruhime, (26328) Litomysl, and (5480) 1989 YK8. Our results were obtained from four observatories in Malta and Slovakia during the period January 2024 to May 2025. Observations were performed over 27 nights using small Schmidt-Cassegrain telescopes equipped with CCD cameras. The resulting lightcurves yielded synodic rotation periods ranging from 4.6802 h to 15.5437 h with amplitudes between 0.09 and 0.95 mag. These data contribute new or refined period determinations for several objects, expanding the photometric record of main-belt asteroids.

Observations were obtained using 0.2-m to 0.25-m Schmidt-Cassegrain telescopes equipped with CCD detectors at Znith, Flarestar, Luckystar and Stellar Horizon Observatories. Standard image calibrations (bias, dark, and flat-field corrections) were applied. Differential aperture photometry was carried out with *MPO Canopus* (Warner, 2017) using Sloan R band reference magnitudes. Comparison stars were selected via the Comparison Star Selector tool in *MPO Canopus*, referencing the ATLAS all-sky catalog (Tonry et al., 2018). Period analysis employed Fourier and phase-dispersion techniques to derive synodic rotation periods and amplitudes.

Observatory/ Country	Scope and Type	Camera	Observed Asteroids (#Nights)
Flarestar Obs. (MPC: 171)/ MALTA	0.25-m SCT	Moravian G2-1600	#11861 (2)
Luckystar Obs. (MPC: M55)/ SLOVAKIA	0.25-m SCT	Atik 460EX	#11861 (1) #26328 (4) #5480 (6)
Stellar Horizon Obs./ MALTA	0.30-m SCT	ASI 6200 MM	#26328 (7)
Znith Astronomy Obs./ MALTA	0.2-m SCT	Moravian G2-1600	#2600 (7)

(2600) Lumme. This stony asteroid was discovered on 1940 January 17 by Y. Vaisala at Turku Observatory, Finland and named after astronomer Kalevi Lumme (JPL, 2025). It has an estimated diameter of 15.1 km and an absolute magnitude (H) of 11.6. It was observed from Znith Observatory for seven nights between 2025 May 2 and 17 using a 0.2-m SCT and Moravian G2-1600 camera. The derived rotation period is 9.688 ± 0.004 h with an amplitude of 0.16 ± 0.15 mag. No rotation period for this object is currently listed in the LCDB.

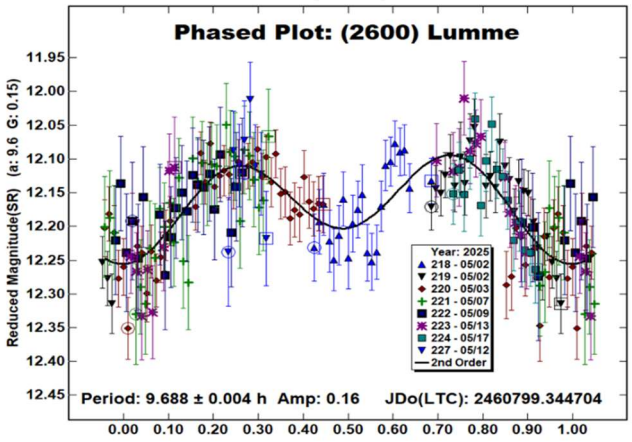

(3667) Anne-Marie was discovered on 1979 October 25 by H. Debehogne at La Silla Observatory (JPL, 2025) and named in honor of the discoverer's daughter Anne-Marie (JPL, 2024). It has an estimated diameter of 22.3 km and an absolute magntidue (H) of 12.28. This C-type asteroid was observed from Luckystar Observatory for four nights between 2024 January 28 and February 16. The synodic rotation period was determined as 12.2813 ± 0.0202 h with an amplitude of 0.09 ± 0.05 mag. No published period could be found in the LCDB for this asteroid.

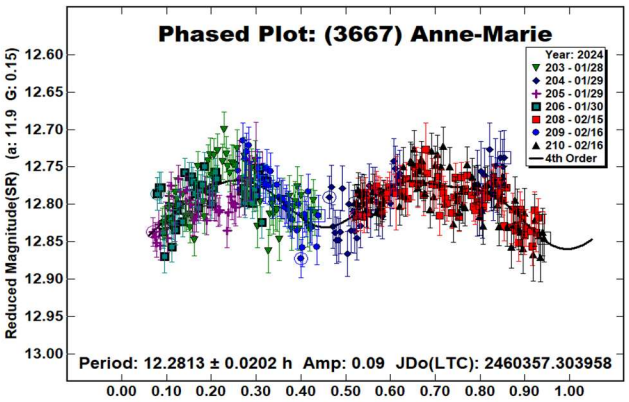

(11861) Teruhime. Discovered on 1988 December 7 by M. Yanai and K. Watanabe at Kitami Observatory (JPL, 2025), it was named for Teruhime, a noblewoman of the Sengoku period in Japan (JPL, 2025). This C-type asteroid has an approximate diameter of 11.7 km and absolute magnitude (H) of 12.4. It was observed from Flarestar Observatory for two nights (April 30 - May 7, 2025) and from Luckystar Observatory for one additional night (April 30). The derived period is 4.897 ± 0.001 h with a large amplitude of 0.95 ± 0.02 mag, indicative of a highly elongated shape. No rotation period for this object is currently listed in the LCDB (Warner et al., 2009) therefore this measurement represents a new determination.

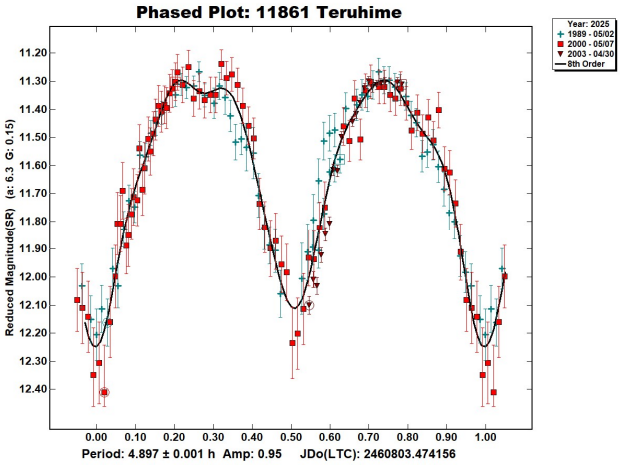

(26328) Litomysl. Discovered on 1998 October 23 by M. Tichy and Z. Moravec at Klet Observatory and named after the Czech town Litomyšl (JPL, 2025). This approximately 5 km asteroid has an absolute magnitude (H) of 14.2. Observed from Luckystar Observatory for 4 nights and from Stellar Horizon Observatory for 7 nights between 2024 November 9 and 20. The derived period is 4.6802 ± 0.0038 h with an amplitude of 0.22 ± 0.10 mag. No rotation period for this object is currently listed in the LCDB (Warner et al., 2009) therefore this measurement represents a new determination.

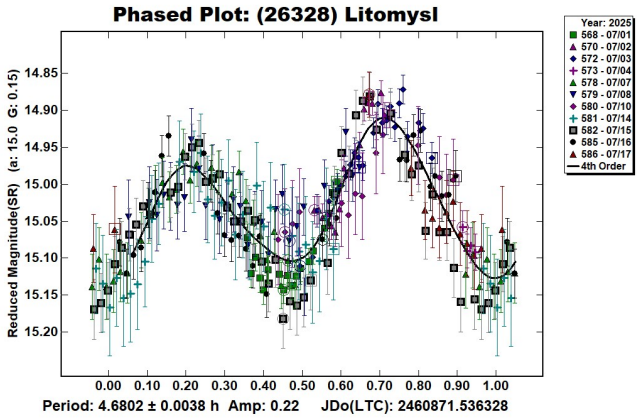

(5480) 1989 YK8 was discovered on 1989 December 21 by Y. Mizuno and T. Furuta at Kani Observatory (JPL, 2025). Its diameter is 15.1 km and an absolute magntidue (H) of 11.46. This asteroid was observed from Luckystar Observatory for six nights between 2025 April 19 and 28. The derived rotation period is 15.5437 ± 0.0684 h with an amplitude of 0.13 ± 0.04 mag. No rotation period was found in the LCDB (Warner et al., 2009) making this a new lightcurve result.

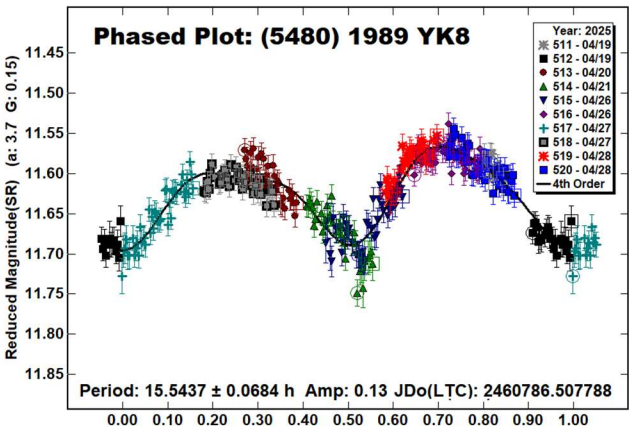

Acknowledgements

We thank Brian Warner for developing the *MPO Canopus* software and for maintaining the CALL website (Warner, 2016; 2021). This study used data from the JPL Small-Body Database (JPL, 2025), Minor Planet Center discovery records (MPC, 2025), and the LCDB (Warner et al., 2009; updated 2023) for comparison of rotation periods.

References

Harris, A.W.; Young, J.W.; Scaltriti, F.; Zappala, V. (1984). "Lightcurves and phase relations of the asteroids 82 Alkmene and 444 Gyptis." *Icarus* **57**, 251-258.

JPL (2025). Small-Body Database Browser. *https://ssd.jpl.nasa.gov/sbdb.cgi*

MPC (2025). Minor Planet Center Discovery Circumstances. *https://minorplanetcenter.net*

Tonry, J.L.; Denneau, L.; Flewelling, H.; Heinze, A.N.; Onken, C.A.; Smartt, S.J.; Stalder, B.; Weiland, H.J.; Wolf, C. (2018). "The ATLAS all-sky stellar reference catalog." *Astrophys. J.* **867**, 105.

Warner, B.D.; Harris, A.W.; Pravec, P. (2009). "The Asteroid Lightcurve Database." *Icarus* **202**, 134-146. Updated 2023. *http://www.minorplanet.info/lightcurvedatabase.html*

Warner, B.D. (2016). Collaborative Asteroid Lightcurve Link website. *http://www.minorplanet.info/call.html*

Warner, B.D. (2017). MPO Software, *MPO Canopus* v10.7.10.0. Bdw Publishing. *http://www.minorplanetobserver.com/*

Warner, B.D. (2021). Asteroid Lightcurve Photometry Database (ALCDEF). *https://minplanobs.org/alcdef/index.php*

Number	Name	yyyy mm/dd	Phase	L_{PAB}	B_{PAB}	Period(h)	P.E.	Amp	A.E.	Grp
2600	Lumme	2025 05/02-05/17	9.4, 13.3	200.6	13.3	9.688	0.004	0.16	0.15	EOS
3667	Anne-Marie	2024 01/28-02/16	11.6, 16.3	111.7	18.4	12.2813	0.0202	0.09	0.05	TIR
11861	Teruhime	2025 04/30-05/07	5.5, 7.5	206.3	8.6	4.897	0.001	0.95	0.02	MB
26328	Litomysl	2024 11/09-11/20	4.6, 7.0	215.8	1.6	4.6802	0.0038	0.22	0.10	MB
5480	1989 YK8	2025 04/19-04/28	3.5, 5.7	205.6	8.3	15.5437	0.0684	0.13	0.04	MB

Table 2. Observing circumstances and results. The phase angle is given for the first and last date. L_{PAB} and B_{PAB} are the approximate phase angle bisector longitude and latitude at mid-date range (Harris et al., 1984). Grp is the asteroid family/group (Warner et al., 2009).

LIGHTCURVE ANALYSIS FOR TWENTY MAIN-BELT ASTEROIDS

Gonzalo Fornas (J57)
Asocación Valenciana de Astronomía
(Centro Astronómico Alto Turia)
C/ Profesor Blanco 16. 46014 Valencia, SPAIN
gon@iicv.es

Alfonso Carreño (Y76)
Nova Canet Observatory

(Received: 2026 January 5)

From photometric observations for twenty main-belt asteroids we derived the following rotational synodic periods: 147 Protogeneia, 7.8505 ± 0.0009 h; 152 Atala, 6.245 ± 0.003 h; 317 Roxane, 8.1559 ± 0.0013 h; 360 Carlova, 6.1906 ± 0.0001 h; 418 Alemannia, 4.6729 ± 0.0003 h; 427 Galene, 3.7062 ± 0.0001 h; 585 Bilkis, 8.5749 ± 0.0014 h; 670 Ottegebe, 10.0399 ± 0.0002 h; 675 Ludmilla, 7.7141 ± 0.0002 h; 679 Pax, 8.4512 ± 0.0004 h; 757 Portlandia, 6.5810 ± 0.0005 h; 794 Irenaea, 9.1748 ± 0.0018 h; 909 Ulla, 8.7111 ± 0.0012 h; 934 Thuringia, 8.1650 ± 0.0002 h; 1069 Planckia, 8.6611 ± 0.0024 h; 1636 Porter, 2.9660 ± 0.0002 h; 1708 Polit, 7.5087 ± 0.0001 h; 1967 Menzel, 2.84954 ± 0.00015 h; 2019 van Albada, 2.7295 ± 0.0003 h; 2326 Tololo, 9.4914023 ± 0.0000001 h.

We report on the photometric analysis for twenty main-belt asteroids. The data were obtained during 2025. We present graphic results of data analysis, mainly lightcurves, with the plot phased into a given period. We managed to obtain several accurate and complete lightcurves and calculated their rotation periods as accurately as possible.

Observatory	Telescope (meters)	CCD
Y76	SC 9,25"	ATIK 314L+

Table I. List of instruments used for the observations.

The targets were selected from the Collaborative Asteroid Lightcurve Link (CALL) website (*http://www.minorplanet.info/call.html),* the Minor Planet Center (*http://www.minorplanet.net*). The Asteroid Lightcurve Database (LCDB; Warner et al., 2009) was consulted to locate previously published results.

Images were measured using *MPO Canopus* (Bdw. Publishing) with a differential photometry technique. The comparison stars were restricted to near solar color to minimize color dependencies, especially at larger air masses. The lightcurves show the synodic rotation period. The amplitude (peak-to-peak) that is shown is that for the Fourier model curve and not necessarily the true amplitude.

Results

147 Protogeneia. This outer main-belt asteroid was discovered on 1875 July at Vienna by L. Schulhof. We made observations on 2025 July 20 to 28. From our data we derive a synodic rotation period of 7.8505 ± 0.0009 h and an amplitude of 0.15 mag. Behrend (2005web) found a period of 7.85 h. Buchheim (2005) got 7.8528 h and Hanus et al. (2013a) got a sidereal period of 7.85232 h.

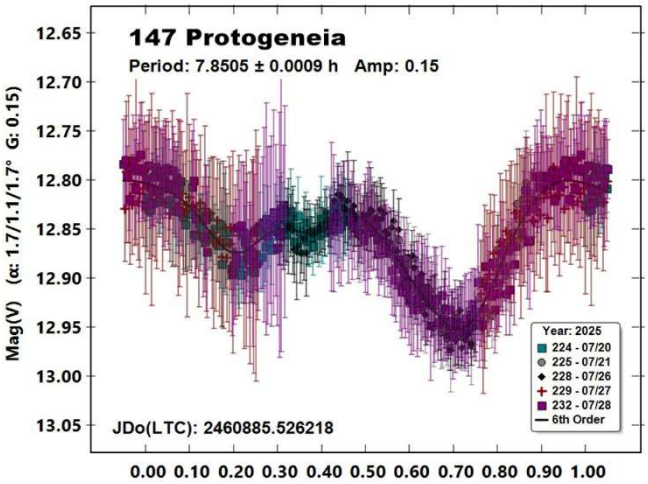

152 Atala. This outer main-belt asteroid was discovered on 1875 November at Paris by P. Henri. We made observations on 2025 November 8 to 9. From our data we derive a synodic rotation period of 6.245 ± 0.003 h and an amplitude of 0.23 mag. Durech (2006), Durech et al. (2009), and Durech et al. (2011) found a period of 6.24472 h, 6.24472 and 6.24472 h, respectively. Behrend (2005web, 2006web) found periods of 6.2443 h and 6.2461 h. Hanus et al. (2011) and Hanus et al. (2013b) found 6.24472 h and 6.24472 h, respectively. Martikainen et al. (2021) found 6.244720 h.

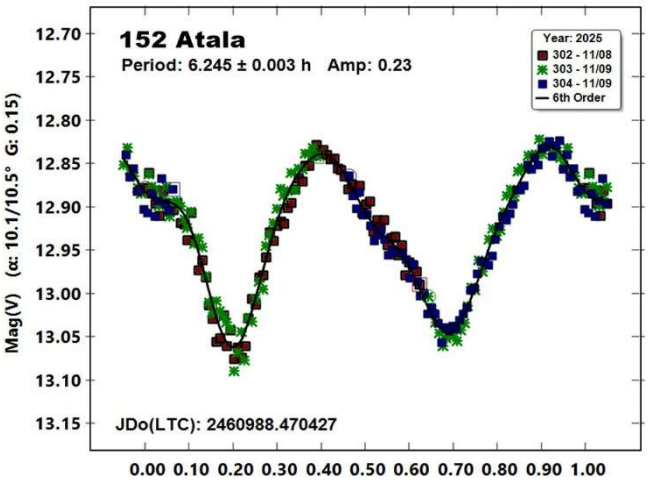

317 Roxane. This inner main-belt asteroid was discovered on 1891 September at Nice by A. Charlois. We made observations on 2025 April 23 to 25. From our data we derive a synodic rotation period of 8.1559 ± 0.0013 h and an amplitude of 0.68 mag. Behrend (2005web, 2007web, 2009web, 2013web, 2019web) found periods of 8.16 h, 8.164 h, 8.172 h, 8.18 h and 8.16942 h, respectively. Lagerkvist and Rickman (1982) found a period of 8.16 h. Harris et al. (1992) got 8.169 h. Stephens (2014) found 8.173 h, and Hanus et al. (2016) found a sidereal period of 8.16961 h.

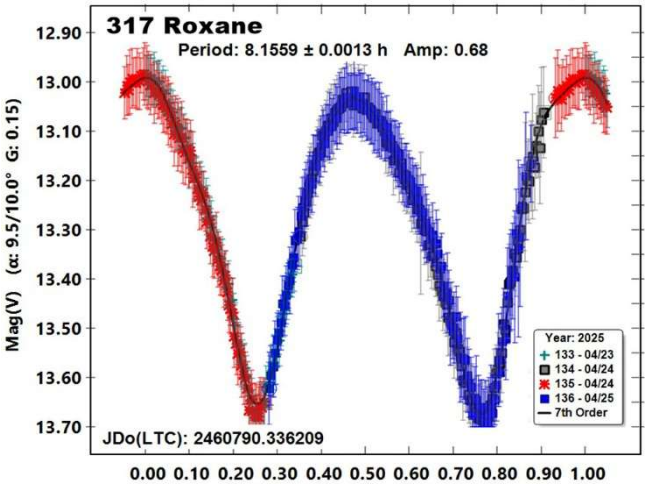

360 Carlova. This outer main-belt asteroid was discovered on 1893 March at Nice by A. Charlois. We made observations on 2025 August 9 to September 10. From our data we derive a synodic rotation period of 6.1906 ± 0.0001 h and an amplitude of 0.39 mag. Behrend (2012web, 2018web) found periods of 6.1904 h and 6.1891 h. Harris and Young (1983) got a period of 6.21 h. Di Martino et al. (1987) found 6.183 h. Michalowski et al. (2000) got a period of 6.188 h. Alton (2012) got 6.1894 h.

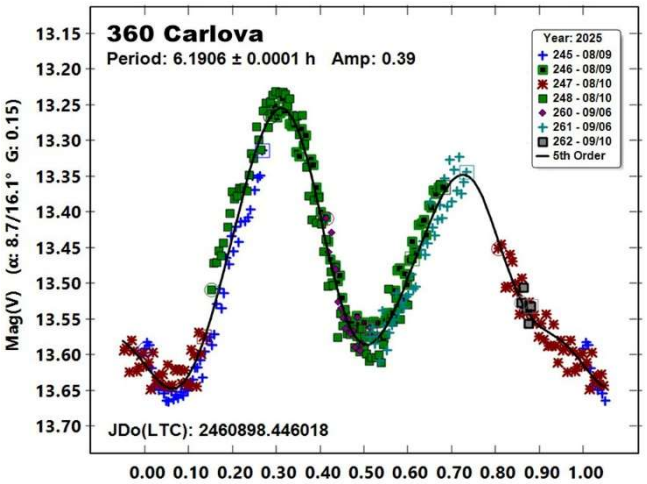

418 Alemannia. This inner main-belt asteroid was discovered on 1896 September at Heidelberg by M.F. Wolf. We made observations on 2025 June 29 to July 1. From our data we derive a synodic rotation period of 4.6729 ± 0.0003 h and an amplitude of 0.20 mag. Behrend (2001web, 2005web, 2007web) found a period of 4.6714 h, 4.67 h and 4.6727 h, respectively. Wetterer et al. (1999) got 4.680 h. Pilcher (2018) got 4.673 h, Klinglesmith and Hendrickx (2018) got 4.672 h, and Gorby et al. (2018) got 4.670 h. Pal et al. (2020) got a period of 4.67226 h.

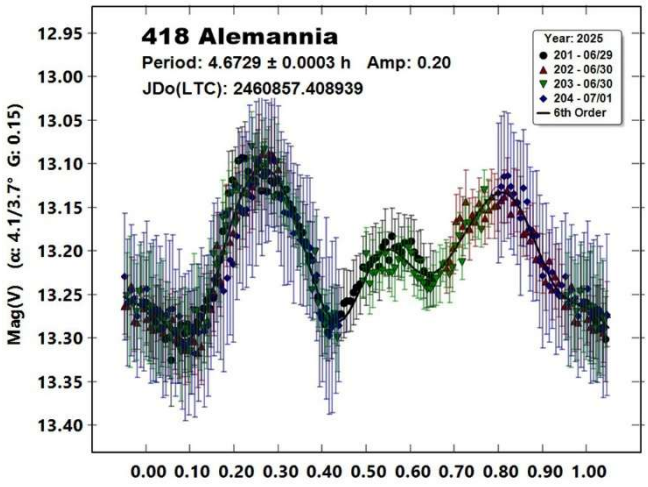

427 Galene. This outer main-belt asteroid was discovered on 1897 August at Nice by A. Charlois. We made observations on 2025 August 11 to September 3. From our data we derive a synodic rotation period of 3.7062 ± 0.0001 h and an amplitude of 0.70 mag. Behrend (2010web, 2020web) found periods of 3.7059 h and 3.7057 h. Caspari (2009) got a period of 3.705 h, and Pal et al. (2020) found 3.70625 h.

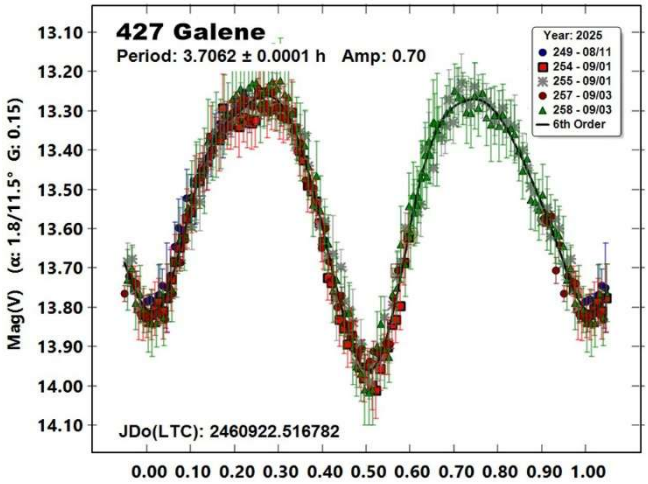

585 Bilkis. This inner main-belt asteroid was discovered on 1906 February at Heidelberg by A. Kopff. We made observations on 2025 September 14 to 16. From our data we derive a synodic rotation period of 8.5749 ± 0.0014 h and an amplitude of 0.14 mag. Behrend (2005web, 2012web) found periods of 8.58 h, 8.5751 h and 8.582 h. Warner (2011) found a period of 8.5742 h. Stephens (2016) got 8.577 h.

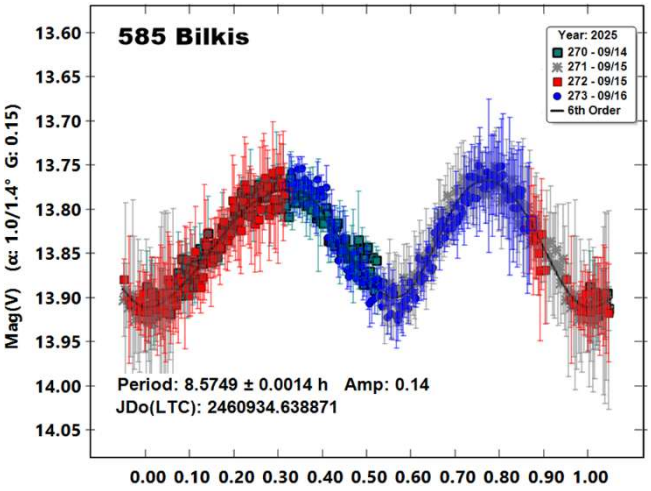

670 Ottegebe. This outer main-belt asteroid was discovered on 1908 August at Heidelberg by A. Kopff. We made observations on 2025 July 13 to 16. From our data we derive a synodic rotation period of 10.0399 ± 0.0002 h and an amplitude of 0.35 mag. We did not find previous information about it.

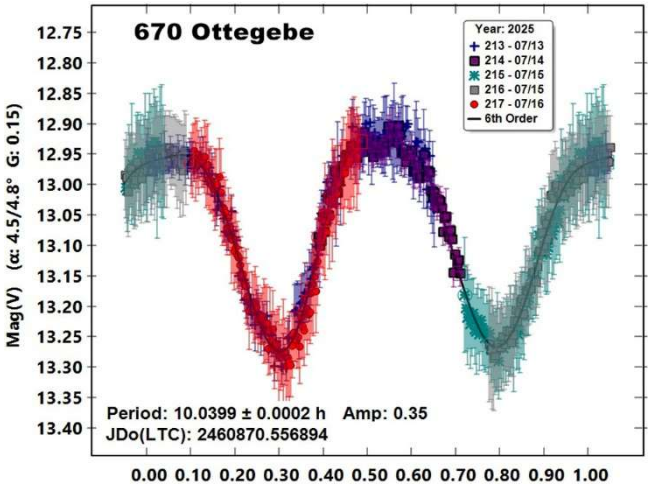

675 Ludmilla. This outer main-belt asteroid was discovered on 1908 August at Taunton by J.H. Metcalf. We made observations on 2025 January 3 to 5. From our data we derive a synodic rotation period of 7.7141 ± 0.0002 h and an amplitude of 0.43 mag. Behrend (2005web, 2021web, 2023web) found periods of 7.713 h, 7.7161 h and 7.71446 h, respectively. Schober and Dvorak. (1975) got 7.717 h, and Velichko et al. (1995) found 7.717 h.

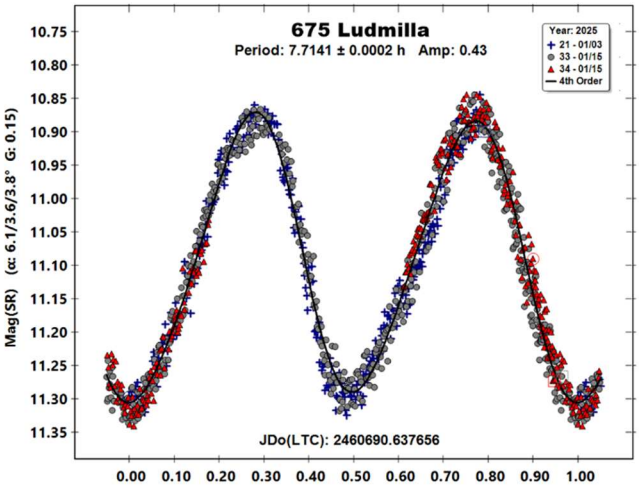

679 Pax. This inner main-belt asteroid was discovered on 1909 January at Heidelberg by A. Kopff. We made observations on 2024 December 28 to 2025 January 14. From our data we derive a synodic rotation period of 8.4512 ± 0.0004 h and an amplitude of 0.27 mag. Behrend (2004web, 2005web, 2023web) found periods of 8.445 h, 8.453 h and 8.4525 h, respectively. Chiorny et al. (2003) got a period of 8.452 h. Schober et al. (1994) got 8.452 h.

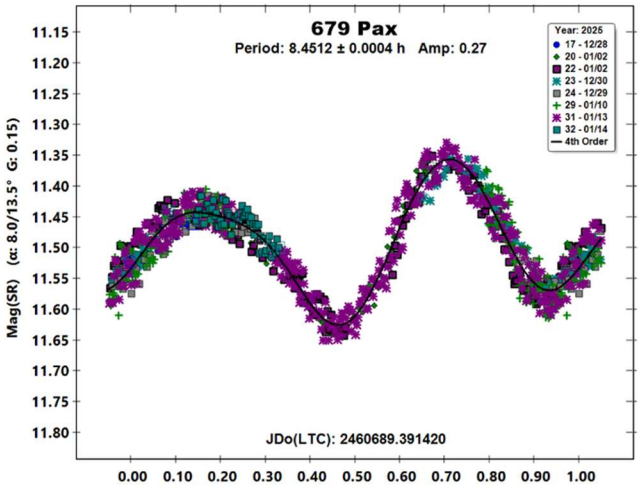

757 Portlandia. This inner main-belt asteroid was discovered on 1908 August at Taunton by J.H. Metcalf. We made observations on 2025 October 23 to 27. From our data we derive a synodic rotation period of 6.5810 ± 0.0005 h and an amplitude of 0.24 mag. Behrend (2005web) found a period of 6.5837 h, Lagerkvist et al. (1988) found 6.58 h. Stephens (2015) got 6.579 h.

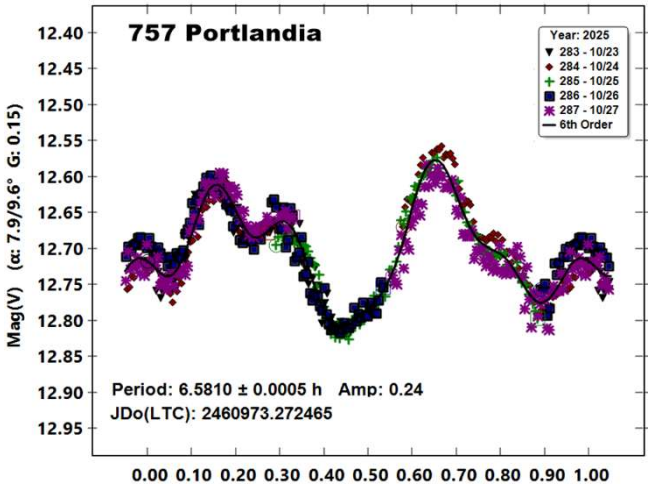

794 Irenaea. This outer main-belt asteroid was discovered on 1914 August at Vienna by J. Palisa. We made observations on 2025 July 31 to August 5. From our data we derive a synodic rotation period of 9.1748 ± 0.0018 h and an amplitude of 0.30 mag. Behrend (2008web) found a period of 9.14 h.

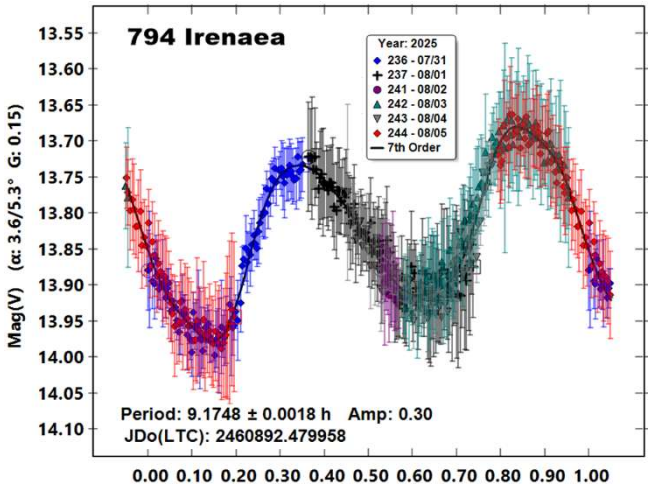

909 Ulla. This outer main-belt asteroid was discovered on 1919 February at Heidelberg by K. Reinmuth. We made observations on 2025 January 19 to 31. From our data we derive a synodic rotation period of 8.7111 ± 0.0012 h and an amplitude of 0.15 mag. Behrend (2002web, 2020web) found periods of 8.72 h and 8.7155 h. Gonano et al. (1991) got a period of 8.71 h. Lagerkvist et al. (2001) got 8.73 h. Franco et al. (2021) found 8.714 h.

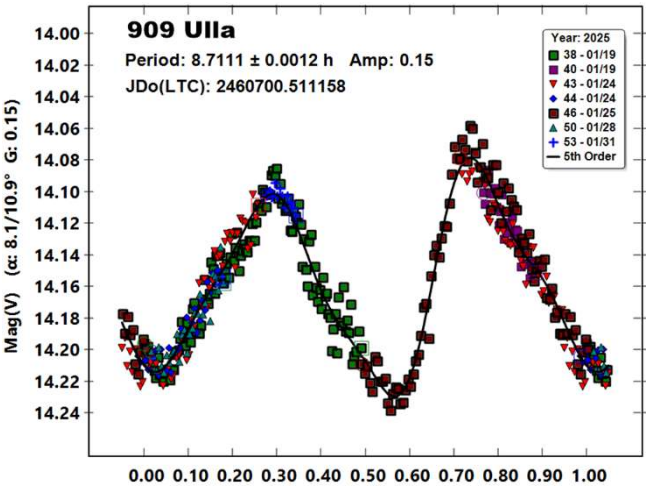

934 Thuringia. This outer main-belt asteroid was discovered on 1920 August at Bergedorf by W. Baade. We made observations on 2025 September 22 to October 2. From our data we derive a synodic rotation period of 8.1650 ± 0.0002 h and an amplitude of 0.34 mag. We did not find previous information about it.

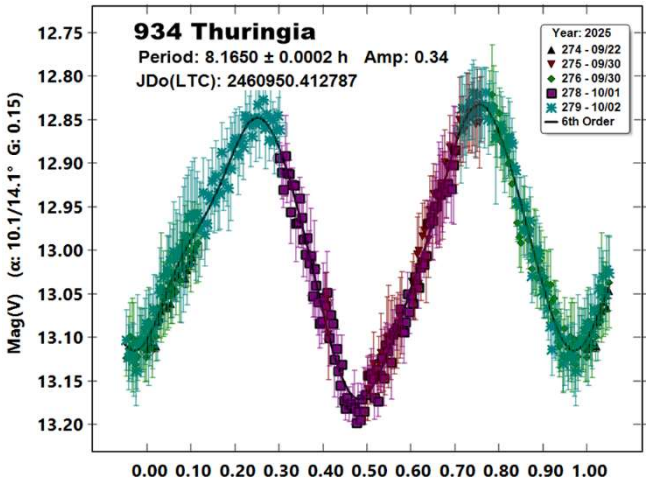

1069 Planckia. This outer main-belt asteroid was discovered on 1927 January at Heidelberg by M.F. Wolf. We made observations on 2025 November 4 to 7. From our data we derive a synodic rotation period of 8.6611 ± 0.0024 h and an amplitude of 0.23 mag. Behrend (2006web, 2011web) found a period 8.66 h and 8.655 h. Warner (2001a, 2010) and Warner et at. (2001b) found 10.58 h, 8.665 h, and 8.5643 h.

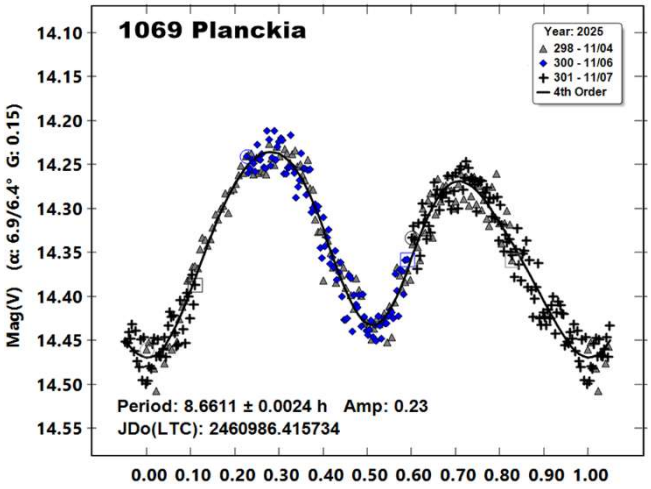

1636 Porter. This inner main-belt asteroid of the Flora family was discovered on 1950 January at Heidelberg by K. Reinmuth. We made observations on 2025 September 2 to 10. From our data we derive a synodic rotation period of 2.9660 ± 0.0002 h and an amplitude of 0.29 mag. Behrend (2014web) found a period 2.9658 h. Albers et al. (2010) got 2.9653 h. Benishek (2023) found a period of 2.9660 h.

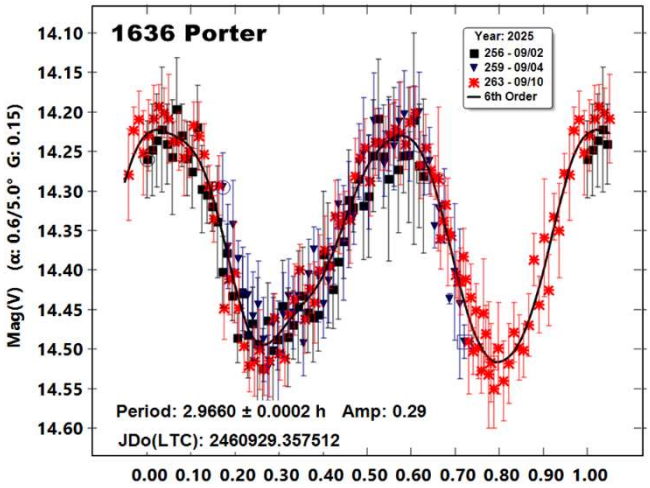

1708 Polit. This outer main-belt asteroid was discovered on 1929 December at Barcelona by J. Comas Sola. We made observations on 2025 February 3 to 22. From our data we derive a synodic rotation period of 7.5087 ± 0.0001 h and an amplitude of 0.32 mag. Behrend (2005web) found a period 7.520 h. Clark (2011, 2015, 2016) got 7.5085 h, 7.507 h, 7.5080 h, 7.5084 and 7.5071 h.

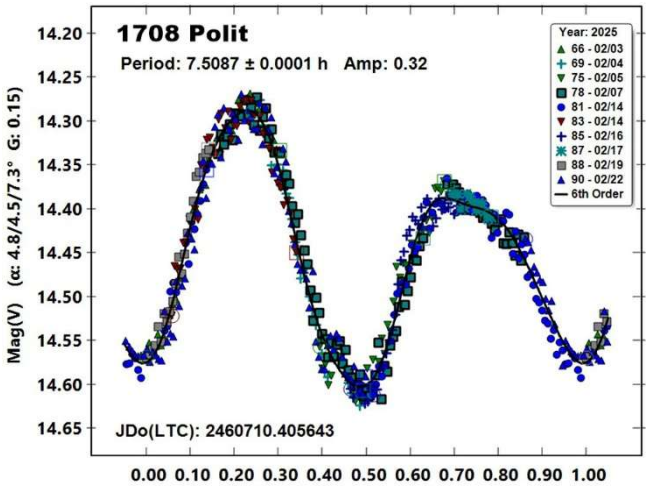

1967 Menzel. This inner main-belt asteroid was discovered on 1905 November at Heidelberg by M.F. Wolf. We made observations on 2025 October 1 to 12. From our data we derive a synodic rotation period of 2.84954 ± 0.00015 h and an amplitude of 0.33 mag. Behrend (2005web, 2015web, 2020web) found periods of 2.83481 h, 2.83497 h and 2.83484 h, respectively. Pravec (2007web, 2010web, 2015web) found 2.8344 h, 2.8343 h and 2.8348 h. Pray (2006) got 2.8350 h. LeCrone et al. (2006) got 2.834 h, and Higgins et al. (2008) found 2.8346 h. Clark (2015) found 2.8364 h. Klinglesmith et al. (2016) and Klinglesmith (2017) got periods of 2.835 h and 2.834 h.

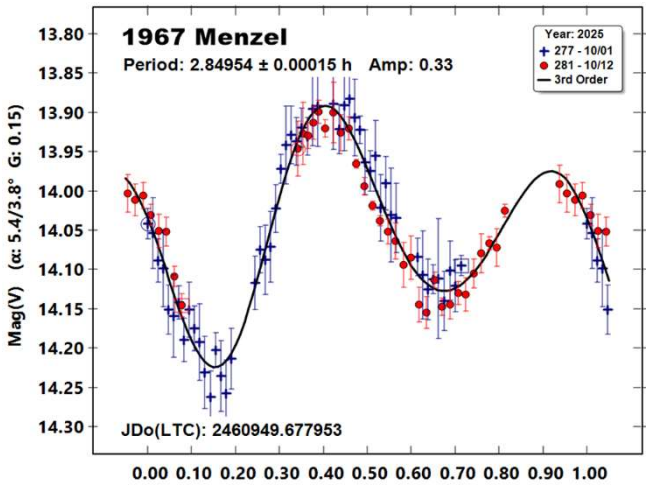

2019 van Albada. This inner main-belt asteroid of the Flora family was discovered on 1935 September at Johannesburg by H. van Hent. We made observations on 2025 May 19 to 25. From our data we derive a synodic rotation period of 2.7295 ± 0.0003 h and an amplitude of 0.16 mag. Behrend (2012web, 2013web, 2019web) found periods of 2.729 h, 2.73 h and 2.73 h, respectively. Waszczak et al. (2015) got 2.583 h and 2.730h. Liu (2015) found 2.729 h, Tan et al. (2018) got 2.295 h and Benishek et al. (2019) got 2.7294 h.

Number	Name	yyyy mm/dd	Phase	L_{PAB}	B_{PAB}	Period(h)	P.E.	Amp	A.E.	Grp
147	Protogeneia	2025/07/20-28	2.0, 1.4	301.9	1.9	7.8505	0.0009	0.15	0.03	MB-O
152	Atala	2025/11/8-9	9.9,10.2	18.9	-4.1	6.245	0.003	0.23	0.05	MB-O
317	Roxane	2025/04/23-25	9.1,10.0	194.9	1.7	8.1559	0.0013	0.68	0.03	MB-I
360	Carlova	2025/08/09-09/10	8.4,16.0	293.4	3.0	6.1906	0.0001	0.39	0.03	MB-O
418	Alemannia	2025/06/29-07/01	4.4, 3.7	284.6	5.0	4.6729	0.0003	0.20	0.05	MB-I
427	Galene	2025/08/11-09/03	1.8,11.1	315.5	2.4	3.7062	0.0001	0.70	0.03	MB-O
585	Bilkis	2025/09/14-16	0.8, 1.4	350.4	1.6	8.5749	0.0014	0.14	0.03	MB-I
670	Ottegebe	2025/07/13-16	4.3, 4.8	288.7	9.0	10.0399	0.0002	0.35	0.05	MB-O
675	Ludmilla	2025/01/03-05	6.1, 5.3	112.7	-6.1	7.7141	0.0002	0.43	0.03	MB-O
679	Pax	2024/12/28-2025/01/14	7.9,13.1	91.1	-10.5	8.4512	0.0004	0.27	0.03	MB-I
757	Portlandia	2025/01/03-05	5.2, 4.8	297.5	-6.9	6.5810	0.0005	0.24	0.05	MB-I
794	Irenaea	2025/07/31-08/05	3.3, 5.2	304.3	4.3	9.1748	0.0018	0.30	0.03	MB-O
909	Ulla	2025/01/19 - 31	8.1,10.7	98.1	-15.4	8.7111	0.0012	0.15	0.02	MB-O
934	Thuringia	2025/09/22-10/02	9.7,14.1	343.4	7.8	8.1650	0.0002	0.34	0.035	MB-O
1069	Planckia	2025/11/4-7	6.9, 6.4	53.1	-16.3	8.6611	0.0024	0.23	0.03	MB-O
1636	Porter	2025/09/2-10	0.6, 4.4	340.0	0.7	2.9660	0.0002	0.29	0.03	MB-I
1708	Polit	2025/02/3-22	5.0, 7.2	140.7	-6.4	7.5087	0.0001	0.32	0.03	MB-O
1967	Menzel	2025/10/1-12	5.4, 3.4	15.0	-4.1	2.84954	0.00015	0.33	0.05	MB-I
2019	van Albada	2025/05/19-25	4.9, 8.5	231.4	-1.8	2.7295	0.0003	0.16	0.03	MB-I
2326	Tololo	2025/01/26-02/04	8.6,11.3	112.2	-12.5	9.4914023	0.0000001	0.29	0.05	MB-O

Table II. Observing circumstances and results. The phase angle is given for the first and last date. If preceded by an asterisk, the phase angle reached an extrema during the period. L_{PAB} and B_{PAB} are the approximate phase angle bisector longitude/latitude at mid-date range (see Harris et al., 1984). Grp is the asteroid family/group (Warner et al., 2009).

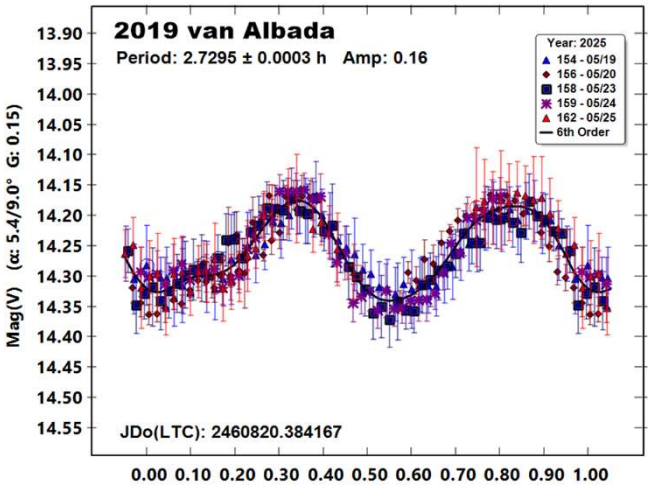

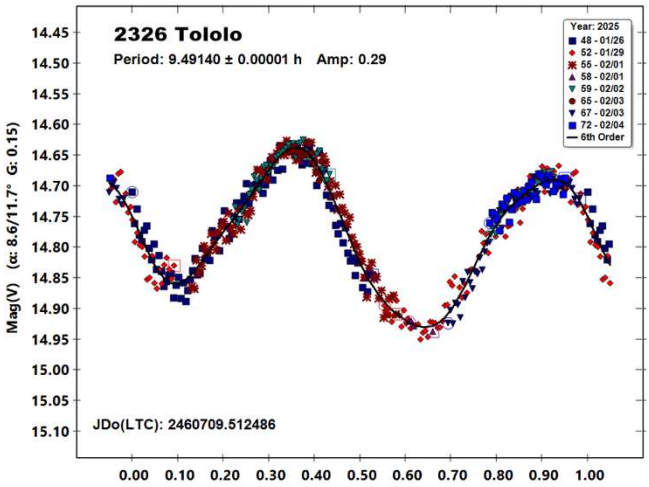

2326 Tololo. This outer main-belt asteroid of the Brasilia family was discovered on 1965 August at Brooklyn by Indiana University. We made observations on 2025 January 26 to February 4. From our data we derive a synodic rotation period of 9.4914023 ± 0.0000001 h and an amplitude of 0.29 mag. Behrend (2022web) found a period of 9.460 h. Percy (2019) found 9.488 h, and Polakis (2020, 2021) got 9.49 h and 9.60 h.

References

Albers, K.; Kragh, K.; Monnier, A.; Pligge, Z.; Stolze, K.; West, J.; Yim, A.; Ditteon, R. (2010). "Asteroid Lightcurve Analysis at the Oakley Southern Sky Observatory: 2009 October thru 2010 April." *Minor Planet Bull.* **37**, 152-158.

Alton, K.B. (2012). "CCD Lightcurves for Asteroids 201 Penelope and 360 Carlova." *Minor Planet Bull.* **39**, 107-108.

Behrend, R. (2001web, 2002web, 2004web, 2005web, 2006web, 2007web, 2008web, 2009web, 2010web, 2011web, 2012web, 2013web, 2014web, 2015web, 2018web, 2019web, 2020web, 2021web, 2022web, 2023web) Observatoire de Geneve web site. *http://obswww.unige.ch/~behrend/page_cou.html*

Benishek, V.; Pravec, P.; Durkee, R.; Husarik, M.; Pikler, M.; Cervak, G.; Tomko, D.; Christmann, B.; Aznar, A.; Pray, D.; Pilcher, F.; Chiorny, V.; Marchini, A.; Papini, R.; Salvaggio, F. (2019). "(2019) Van Albada." CBET 4689.

Benishek, V. (2023). "Lightcurves and Synodic Rotation Periods for 17 Asteroids from Sopot Astronomical Observatory: 2022 June - 2023 January." *Minor Planet Bull.* **50**, 142-147.

Buchheim, R.K. (2005). "Lightcurve of 147 Protogeneia." *Minor Planet Bull.* **32**, 35-36.

Caspari, P. (2009). "Lightcurve Analysis of Minor Planets 427 Galene and 5489 Oberkochen." *Minor Planet Bull.* **36**, 168.

Chiorny, V.G.; Shevchenko, V.G.; Krugly, Yu.N.; Velichko, F.P.; Gaftonyuk, N.M. (2003). Abstracts of Photometry and Polarimetry of Asteroids: Impact on Collaboration, Kharkiv, 9-10.

Clark, M. (2011). "Asteroid Lightcurves from the Preston Gott and McDonald Observatories." *Minor Planet Bull.* **38**, 187-189.

Clark, M. (2015). "Asteroid Photometry from the Preston Gott Observatory." *Minor Planet Bull.* **42**, 163-166.

Clark, M. (2016). "Shape Modelling of Asteriods 1708 Polit, 2036 Sheragul, and 3015 Candy." *Minor Planet Bull.* **43**, 80-86.

Di Martino, M.; Zappala, V.; De Campos, J.A.; Debehogne, H.; Lagerkvist, C.-I. (1987). "Rotational properties and lightcurves of the minor planets 94, 107, 197, 201, 360, 451, 511 and 702." *Astron. Astrophys. Suppl. Ser.* **67**, 95-101.

Durech, J. (2006). IAU 2006, poster paper.

Durech, J.; Kaasalainen, M.; Warner, B.D.; Fauerbach, M.; Marks, S.A.; Fauvaud, S.; Fauvaud, M.; Vugnon, J.-M.; Pilcher, F.; Bernasconi, L.; Behrend, R. (2009). "Asteroid models from combined sparse and dense photometric data." *Astron. Astrophys.* **493**, 291-297.

Durech, J.; Kaasalainen, M.; Herald, D.; Dunham, D.; Timerson, B.; Hanus, J.; Frappa, E.; Talbot, J.; Hayamizu, T. Warner, B.D.; Pilcher, F.; Galad, A. (2011). "Combining asteroid models derived by lightcurve inversion with asteroidal occultation silhouettes." *Icarus* **214**, 652-670.

Franco, L.; Marchini, A.; Cavaglioni, L.; Papini, R.; Privitera, C.A.; Baj, G.; Galli, G.; Scarfi, G.; Aceti, P.; Banfi, M.; Bacci, P.; Maestripieri, M.; Mannucci, M.; Montigiani, N.; Tinelli, L.; Mortari, F. (2021). "Collaborative Asteroid Photometry from UAI: 2021 January - March." *Minor Planet Bull.* **48**, 219-222.

Gonano, M.; Di Martino, M.; Mottola, S.; Neukum, G. (1991). "Physical study of outer belt asteroids." *Adv. Space Res.* **11**, no. 12, 197-200.

Gorby, R.D.; Rengstorf, A.W. Pavel, J. (2018). "Rotation Period Determination for 418 Alemannia and 4911 Rosenzweig." *Minor Planet Bull.* **45**, 319-320.

Hanus, J.; Durech, J.; Broz, M.; Warner, B.D.; Pilcher, F.; Stephens, R.; Oey, J.; Bernasconi, L.; Casulli, S.; Behrend, R.; Polishook, D.; Henych, T.; Lehký, M.; Yoshida, F.; Ito, T. (2011). "A study of asteroid pole-latitude distribution based on an extended set of shape models derived by the lightcurve inversion method." *Astron. Astrophys.* **530**, A134.

Hanus, J.; Durech, J.; Broz, M.; Marciniak, A. and 116 colleagues (2013a). "Asteroids' physical models from combined dense and sparse photometry and scaling of the YORP effect by the observed obliquity distribution." *Astron. Astrophys.* **551**, A67.

Hanus, J.; Marchis, F.; Durech, J. (2013b). "Sizes of main-belt asteroids by combining shape models and Keck adaptive optics observations." *Icarus* **226**, 1045-1057.

Hanus, J.; Durech, J.; Oszkiewicz, D.A.; Behrend, R. and 165 colleagues (2016). "New and updated convex shape models of asteroids based on optical data from a large collaboration network." *Astron. Astrophys.* **586**, A108.

Harris, A.W.; Young, J.W. (1983). "Asteroid rotation IV. 1979 observations." *Icarus* **54**, 59-109.

Harris, A.W.; Young, J.W.; Scaltriti, F.; Zappala, V. (1984). "Lightcurves and phase relations of the asteroids 82 Alkmene and 444 Gyptis." *Icarus* **57**, 251-258.

Harris, A.W.; Young, J.W.; Dockweiler, T.; Gibson, J.; Poutanen, M.; Bowell, E. (1992). "Asteroid lightcurve observations from 1981." *Icarus* **95**, 115-147.

Higgins, D.; Pravec, P.; Kusnirak, P.; Hornoch, K.; Brinsfield, J.W.; Allen, B.; Warner, B.D. (2008). "Asteroid Lightcurve Analysis at Hunters Hill Observatory and Collaborating Stations: November 2007 - March 2008." *Minor Planet Bull.* **35**, 123-126.

Klinglesmith III, D.A.; Hendrickx, S.; Madden, K.; Montgomery, S. (2016). "Lightcurves for Shape/Spin Models." *Minor Planet Bull*. **43**, 123-128.

Klinglesmith III, D.K. (2017). "Asteroids Observed from Estcorn Observatory." *Minor Planet Bull.* **44**, 345-348.

Klinglesmith III, D.A.; Hendrickx, S. (2018). "Asteroid Lightcurves from Etscorn Observatory." *Minor Planet Bull.* **45**, 61-63.

Lagerkvist, C.-I.; Rickman, H. (1982). "On the Rotation of M Asteroids." Sun and Planetary System, W. Fricke, G. Teleki, eds. pp. 289-290.

Lagerkvist, C.I.; Magnusson, P.; Williams, I.P.; Buontempo, M.E.; Gibbs, P. (1988). "Physical studies of asteriods. XVIII - Phase relations and composite lightcurves obtained with the Carlsberg Meridian Circle." *Astron. Astrophys. Suppl. Ser.* **73**, 395-405.

Lagerkvist, C.-I.; Erikson, A.; Lahulla, F.; Di Martino, M.; Nathues, A.; Dahlgren, M. (2001). "A Study of Cybele Asteroids. I. Spin Properties of Ten Asteroids." *Icarus* **149**, 190-197.

LeCrone, C.; Duncan, A.; Hudson, E.; Johnson, J.; Mulvihill, A.; Reichert, C.; Ditteon, R. (2006). "2005-2006 fall observing campaign at Rose-Hulman Institute of Technology." *Minor Planet Bull.* **33**, 66-67.

Liu, J. (2015). "Rotation Period of 2019 van Albada." *Minor Planet Bull.* **42**, 247.

Martikainen, J.; Muinonen, K.; Penttila, A.; Cellino, A.; Wang, X.-B. (2021). "Asteroid absolute magnitudes and phase curve parameters from Gaia photometry." *Astron. Astrophys.* **649**, A98.

Michalowski, T.; Pych, W.; Berthier, J.; Kryszczynska, A.; Kwiatkowski, T.; Boussuge, J.; Fauvaud, S.; Denchev, P.; Baranowski, R. (2000). "CCD photometry, spin and shape models of five asteroids: 225, 360, 416, 516, and 1223." *Astron. Astrophys. Suppl. Ser.* **146**, 471-479.

Pal, A.; Szakats, R.; Kiss, C.; Bodi, A.; Bognár, Z.; Kalup, C.; Kiss, L.L. Marton, G.; Molnár, L.; Plachy, E.; Sárneczky, K.; Szabó, G.M.; Szabó, R. (2020). "Solar System Objects Observed with TESS-First Data Release: Bright Main-belt and Trojan Asteroids from the Southern Survey." *Ap. J. Suppl. Ser.* **247**, id.26.

Percy, S.C. (2019). "Rotation Period for 2326 Tololo." *Minor Planet Bull.* **46**, 13-14.

Pilcher, F. (2018). "Rotation Period Determination for 418 Alemannia, 646 Kastalia and 876 Scott." *Minor Planet Bull.* **45**, 55-56.

Polakis, T. (2020). "Photometric Observations of Thirty Minor Planets." *Minor Planet Bull.* **47**, 177-186.

Polakis, T. (2021). "Lightcurve Analysis for Thirteen Minor Planets."; *Minor Planet Bull.* **48**, 394-398.

Pravec, P.; (2007web, 2010web, 2015web). *http://www.asu.cas.cz/~ppravec/neo.htm*

Pray, D.P. (2006). "Lightcurve analysis of asteroids 326, 329, 426, 619, 1829, 1967, 2453, 10518 and 42267." *Minor Planet Bull.* **33**, 4-5.

Schober, H.J.; Dvorak, R. (1975). "Rotation period and photoelectric light curve of the minor planet 675 Ludmilla." *Astron. Astrophys.* **44**, 81-84.

Schober, H.J.; Erikson, A.; Hahn, G.; Lagerkvist, C.-I.; Albrecht, R.; Ornig, W.; Schroll, A.; Stadler, M. (1994). "Physical studies of asteroids. XXVIII. Lightcurves and photoelectric photometry of asteroids 2, 14, 51, 105, 181, 238, 258, 369, 377, 416, 487, 626, 679, 1048 and 2183." *Astron. Astrophys. Suppl. Ser.* **105**, 281-300.

Stephens, R.D. (2014). "Asteroids Observed from CS3: 2014 January - March." *Minor Planet Bull.* **41**, 171-175.

Stephens, R.D. (2015). "Asteroids Observed from CS3: 2014 October - December." *Minor Planet Bull.* **42**, 104-106.

Stephens, R.D. (2016). "Asteroids Observed from CS3: 2016 April - June." *Minor Planet Bull.* **43**, 336-339.

Tan, H.; Yeh, T.; Li, B.; Gao, X. (2018). "Asteroid Lightcurves from Xingming Observatory: 2017 - 2017 June." *Minor Planet Bull.* **45**, 57-59.

Velichko, F.P.; Michalowski, T.; Erikson, A.; Krugly, Yu.N.; Dahlgren, M.; Kalashnikov, A.V.; Lagerkvist, C.-I. (1995). "Lightcurves, magnitude-phase dependence and spin vector of asteroid 675 Ludmilla." *Astron. Astrophys. Suppl. Ser.* **110**, 125-129.

Warner, B.D. (2001a). "Asteroid Photometry at the Palmer Divide Observatory." *Minor Planet Bull.* **28**, 40-41.

Warner, B.D.; Malcolm, G.; Stephens, R.D. (2001b). "The Lightcurve of 1069 Planckia Revisited." *Minor Planet Bull.* **28**, 71-72.

Warner, B.D.; Harris, A.W.; Pravec, P. (2009); "The Asteroid Lightcurve Database." *Icarus* **202**, 134-146. Updated 2016 Sep. *http://www.minorplanet.info/lightcurvedatabase.html*

Warner, B.D. (2010). "Asteroid Lightcurve Analysis at the Palmer Divide Observatory: 2009 December - 2010 March."*Minor Planet Bull.* **37**, 112-118.

Warner, B.D. (2011). "Upon Further Review: VI. An Examination of Previous Lightcurve Analysis from the Palmer Divide Observatory." *Minor Planet Bull.* **38**, 96-101.

Waszczak, A.; Chang, C.-K.; Ofeck, E.O.; Laher, F.; Masci, F.; Levitan, D.; Surace, J.; Cheng, Y.-C.; Ip, W.-H.; Kinoshita, D.; Helou, G.; Prince, T.A.; Kulkarni, S. (2015). "Asteroid Light Curves from the Palomar Transient Factory Survey: Rotation Periods and Phase Functions from Sparse Photometry." *Astron. J.* **150**, A75.

Wetterer, C.J.; Saffo, C.R.; Majcen, S.; Tompkins, J. (1999). "CCD Photometry of Asteroids at the US Air Force Academy Observatory During 1998." *Minor Planet Bull.* **26**, 30-31.

ASTEROID PHOTOMETRY FOR 15 MAIN-BELT ASTEROIDS

Milagros Colazo
Astronomical Observatory Institute, Faculty of Physics
Adam Mickiewicz University
ul. Słoneczna 36, 60-286 Poznań, POLAND
Grupo de Observadores de Rotaciones de Asteroides (GORA)
ARGENTINA
https://aoacm.com.ar/gora/index.php
milirita.colazovinovo@gmail.com

Víctor Amelotti
Observatorio Astronómico Naos (GORA NAO)
Observatorio Astronómico Naos 2 (GORA NA2)
Observatorio Astronómico Naos 3 (GORA NA3)
Observatorio Astronómico Naos 4 (GORA NA4)
Alta Gracia (Córdoba-ARGENTINA)
Estación Astrofísica Bosque Alegre (MPC 821)
Departamento Punilla (Córdoba-ARGENTINA)

Giuliat Navas
Observatorio Astronómico Nacional Llano del Hato (MPC 303)
Observatorio Astronómico Nacional Llano del Hato (OAN)
Centro de Investigaciones de Astronomía Francisco J. Duarte (CIDA) - Apartaderos (Mérida-VENEZUALA).

Raúl Melia
Observatorio de Raúl Melia Carlos Paz (GORA RMC)
Carlos Paz (Córdoba- ARGENTINA)
Estación Astrofísica Bosque Alegre (MPC 821)
Departamento Punilla (Córdoba- ARGENTINA)

Gerard Tàrtalo
Dark Energy Observatory (DEO)
Dark Energy Observatory 2 (DE2)
Àger (Lleida-ESPAÑA)

Marcos Anzola
Observatorio Astronómico Vuelta por el Universo 2 (GORA OM2) - Córdoba (Córdoba- ARGENTINA)
Estación Astrofísica Bosque Alegre (MPC 821)
Departamento Punilla (Córdoba- ARGENTINA)

Paolo Aldinucci
OsservatorioAstronomico Piero Angela (MPC D42)
Scandicci (Florencia-ITALIA)

Javier Aguilera
Observatorio Protón-Protón (MPC X41)
Longchamps (Buenos Aires- ARGENTINA)

Francisco Santos
Observatorio Astronómico Giordano Bruno (MPC G05)
Piconcillo (Córdoba- ESPAÑA)

José Álvarez
Observatorio Astronómico Corgas (MPC Z65)
Corgas-Taboadela-Ourense (Galicia- ESPAÑA)

Martín Leiva
Estación Astrofísica Bosque Alegre (MPC 821)
Departamento Punilla (Córdoba-ARGENTINA)

Zlatko Orbanic
Osservatorio Explorer (MPC M19)
Pula (Istria-CROACIA)

Alberto García
Observatorio Río Cofio (MPC Z03)
Robledo de Chavela (Madrid- ESPAÑA)

Mario Morales
Observatorio de Sencelles (MPC K14)
Sencelles (Mallorca-Islas Baleares- ESPAÑA)

Carlos Ambrosioni
Observatorio Astronómico de Carlos Ambrosioni 2 (GORA OC2)
Observatorio Astronómico de Carlos Ambrosioni 3 (GORA OC3)
Cañuelas (Buenos Aires-ARGENTINA)

Carlos Colazo
Observatorio Astronómico El Gato Gris (MPC I19)
Tanti (Córdoba-ARGENTINA)

Estación Astrofísica Bosque Alegre (MPC 821)
Departamento Punilla (Córdoba-ARGENTINA)

(Received: 2026 January 11)

Synodic rotation periods and amplitudes are reported for 1068 Nofretete, 1818 Brahms, 1942 Jablunka, 2097 Galle, 2098 Zyskin, 2125 Karl-Ontjes, 3237 Victorplatt, 4583 Lugo, 5256 Farquhar, 7842 Ishitsuka, 8556 Jana, (11564) 1993 FU41, (16009) 1999 CM8, (35539) 1998 FJ91, and (65127) 2002 CG63.

The periods and amplitudes of asteroid lightcurves presented in this paper are the product of collaborative work by the GORA (Grupo de Observadores de Rotaciones de Asteroides) group. In all the studies, we have applied relative photometry assigning V magnitudes to the calibration stars.

The image acquisition was performed without filters and with exposure times of a few minutes. All images used were corrected using dark frames and, in some cases, bias and flat-field corrections were also used. Photometry measurements were performed using *FotoDif* software and for the analysis, we employed *Periodos* software (Mazzone, 2012).

Below, we present the results for each asteroid studied. The lightcurve figures contain the following information: the estimated period and period error and the estimated amplitude and amplitude error. In the reference boxes, the columns represent, respectively, the marker, observatory MPC code, or - failing that - the GORA internal code, session date, session offset, and several data points.

Targets were selected based on the following criteria: 1) those asteroids with magnitudes accessible to the equipment of all participants, 2) those with favorable observation conditions from Argentina, Venezuela, Spain, Italy, or Croatia, i.e. with negative or positive declinations δ, and 3) objects with few periods reported in the literature and/or with Lightcurve Database (LCDB) (Warner et al., 2009) quality codes (U) of less than 3.

1068 Nofretete is a main-belt asteroid discovered in 1926 by E. Delporte with an estimated diameter of 21.346 km. A previously reported rotational period for this asteroid is P = 6.15 h (Binzel, 1987). In this work, we propose a longer period of P = 22.874 ± 0.021 h, with an amplitude of Δm = 0.06 ± 0.03 mag.

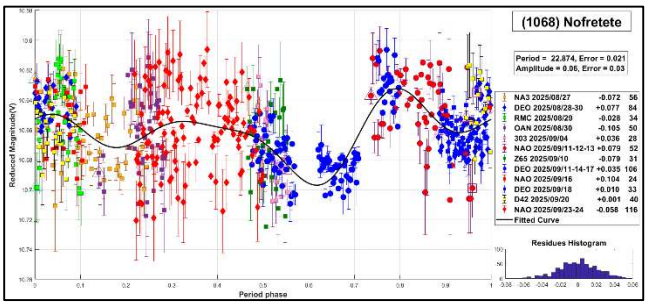

1818 Brahms is a main-belt asteroid with an estimated diameter of 13.747 km. It was discovered in 1939 by K. Reinmuth. We couldn't find a reported period for this object in the literature. In this paper, we present full light curve coverage. We measured a period of P = 5.357 ± 0.044 h with Δm = 0.69 ± 0.06 mag.

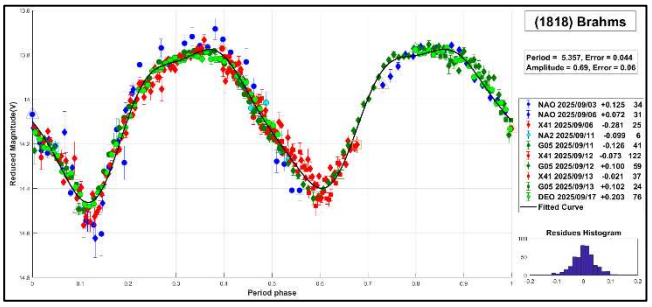

1942 Jablunka is a main-belt asteroid discovered in 1972 by L. Kojoutek. It is a member of the Phocaea family (Nesvorny et al., 2015) with an estimated diameter of 16.766 km. The more recent period published in the literature corresponds to P = 8.91158 h (Ďurech et al., 2016). Our period, P = 8.902 ± 0.020 h, agrees with Ďurech et al.

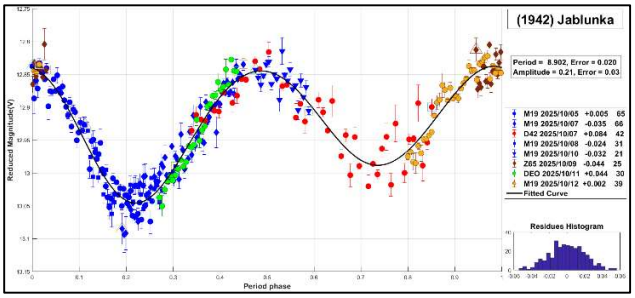

2097 Galle is a main-belt asteroid with an estimated diameter of 26.330 km that was discovered in 1953 by K. Reinmuth. The reported rotational period for this asteroid is P = 26.330 h (Yeh et al., 2020). In this work, we propose a shorter period of P = 7.313 ± 0.025 h with Δm = 0.39 ± 0.04 mag.

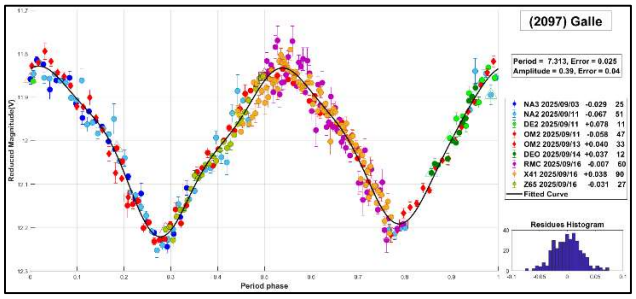

2098 Zyskin is a main-belt asteroid discovered in 1972 by L.V. Zhuravleva. It is a member of the Vesta family (Nesvorny et al., 2015) with an estimated diameter of 12.731 km. The reported rotational period for this asteroid is 3.92 h (Waszczak et al., 2015). We measured a period of P = 3.919 + ± 0.021 h, with Δm = 0.10 ± 0.03 mag.

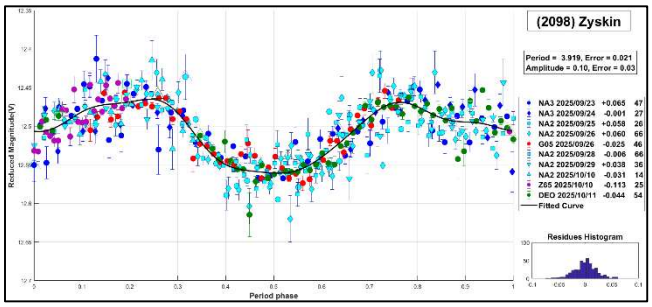

2125 Karl-Ontjes is a main-belt asteroid with an estimated diameter of 11.019 km that was discovered in 1960 at Palomar. No published rotational periods for this asteroid were found in the literature. In this work, we propose a period of P = 106.82 ± 0.43 h with Δm = 0.62 ± 0.04 mag.

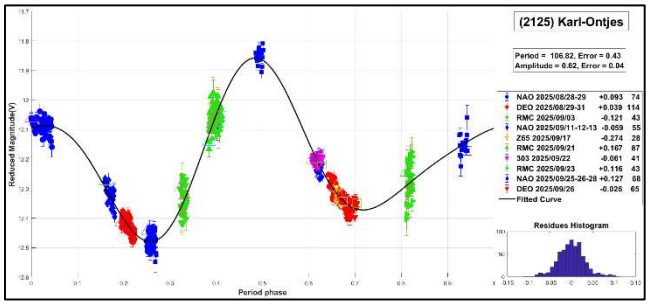

3237 Victorplatt is a main-belt asteroid discovered in 1984 by J. Platt. It belongs to the Eos family (Nesvorny et al., 2015) and has an estimated diameter of 27.751 km. The reported rotational period for this asteroid is P = 10.36 h (Behrend, 2010web). Our observations suggest a longer period, yielding a value of P = 21.000 ± 0.024 h with Δm = 0.18 ± 0.03 mag.

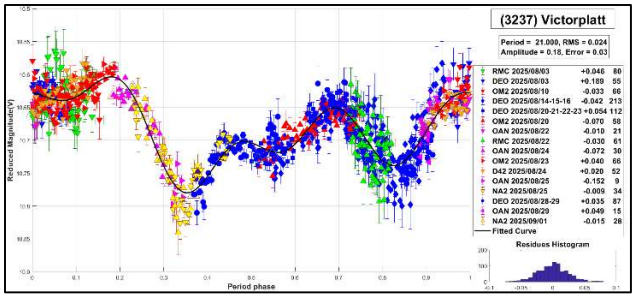

4583 Lugo is a main-belt asteroid discovered in 1989 at Smolyan. It is classified as a X-type asteroid according to the SDSS-based Asteroid Taxonomy (Hasselmann et al., 2012), with a diameter of 13.761 km. A previously reported rotational period for this asteroid is 12 h (Behrend, 2021web). Our measurements indicate a slightly longer period of P = 19.858 ± 0.034 h, with a lightcurve amplitude of Δm = 0.41 ± 0.05 mag.

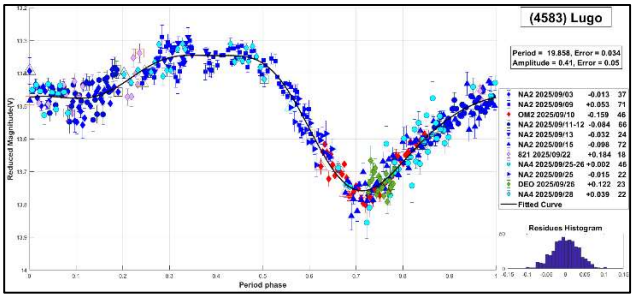

5256 Farquhar is a main-belt asteroid that was discovered in 1988 by Helin-Mikolaj.-Coker and has an estimated diameter of 11.990 km. A rotational period of P = 11.504 h was previously reported for this asteroid (Farfan et al., 2022). Our results are consistent with this rotation period, giving a value of P = 11.514 ± 0.019 h and an amplitude of Δm = 0.12 ± 0.03 mag.

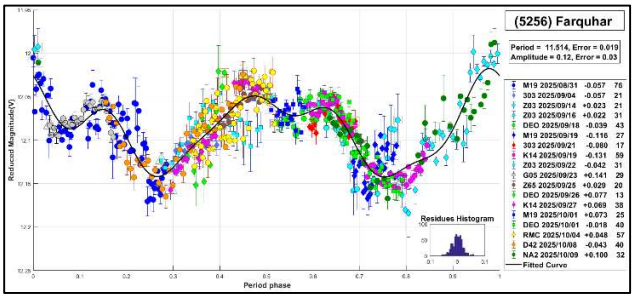

7842 Ishitsuka is a main-belt asteroid that was discovered in 1994 by K. Endate and K. Watanabe, with an estimated diameter of 3.710 km. For this asteroid, we could not find any published rotational periods in the literature. In this work, we propose a period of P = 7.269 ± 0.052 h with Δm = 0.55 ± 0.07 mag.

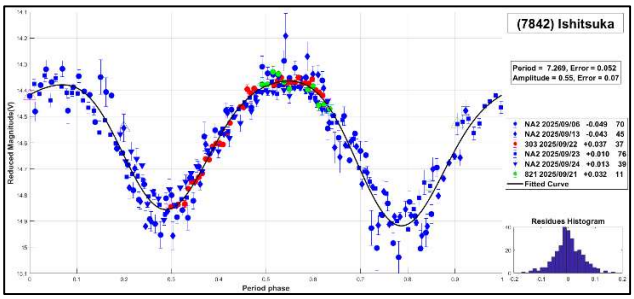

8556 Jana is a main-belt asteroid that was discovered in 1995 by Z. Morave and has an estimated diameter of 7.343 km. For this asteroid as well, we could not find published periods in the literature. In this work, we propose a period of P = 35.496 ± 0.031 h with Δm = 0.38 ± 0.04 mag.

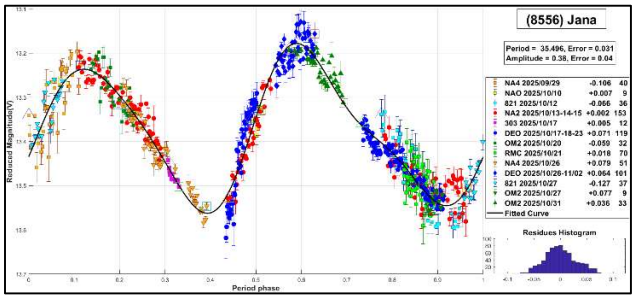

(11564) 1993 FU41 is a main-belt asteroid with an estimated diameter of 4.997 km that was discovered in 1993 by UESAC at La Silla. Based on the SDSS taxonomy (Hasselmann et al., 2012), it is classified as a C-type and belongs to the Flora or Baptistina family (Nesvorny et al., 2015). We couldn't find a reported period for this object in the literature. We measured a period of P = 6.987 ± 0.033 h with Δm = 0.13 ± 0.05 mag.

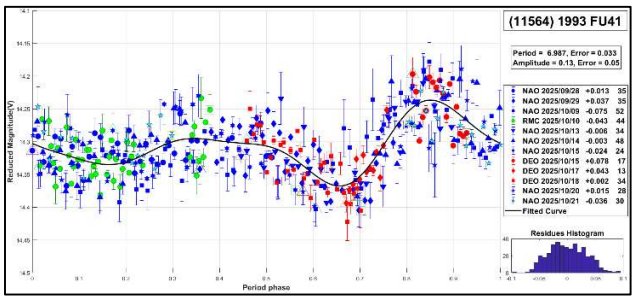

(16009) 1999 CM8 is a main-belt asteroid with an estimated diameter of 10.143 km; it was discovered in 1999 by T. Kobayashi. It is a member of the Maria family (Nesvorny et al., 2015). The more recent period published in the literature corresponds to P = 16.7 h (Waszczak et al., 2015). Our period, P = 16.698 ± 0.024 h, agrees with the one measured by Waszczak et al.

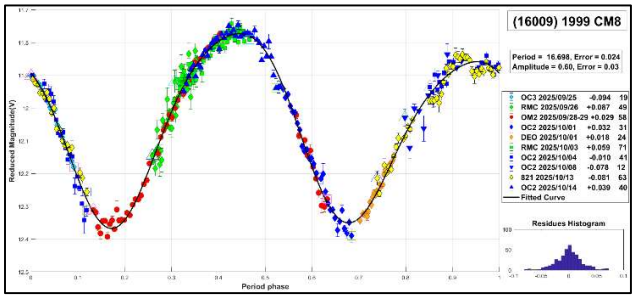

(35539) 1998 FJ91 is a main-belt asteroid with and estimated diameter of 5.877 km. It is classified as an S-type asteroid according to the SDSS-based Asteroid Taxonomy (Hasselmann et al., 2012). It was discovered in 1999 by LINEAR. We couldn't find a reported period for this object in the literature. We propose a period of P = 21.645 ± 0.028 h with Δm = 0.07 ± 0.04 mag.

Number	Name	2025/ mm/dd	Phase	L_{PAB}	B_{PAB}	Period(h)	P.E.	Amp	A.E.	Grp
1068	Nofretete	08/27-09/24	*05.9,05.1	348	3	22.874	0.021	0.06	0.03	MB-O
1818	Brahms	09/03-09/18	13.2,04.6	358	5	5.357	0.044	0.69	0.06	MB-I
1942	Jablunka	10/05-10/12	12.3,13.3	14	18	8.902	0.020	0.21	0.03	Pho
2097	Galle	09/03-09/16	01.2,06.3	341	2	7.313	0.025	0.39	0.04	MB-O
2098	Zyskin	09/23-10/12	*05.8,06.3	9	5	3.919	0.021	0.10	0.03	Vesta
2125	Karl-Ontjes	08/28-09/28	*08.9,05.6	353	1	106.82	0.43	0.62	0.04	MB-O
3237	Victorplatt	08/03-09/02	*03.9,09.4	317	7	21.000	0.024	0.18	0.03	Eos
4583	Lugo	09/03-09/28	*01.3,13.1	343	0	19.858	0.034	0.41	0.05	MB-I
5256	Farquhar	08/31-10/09	*16.6,08.5	5	13	11.514	0.019	0.12	0.03	MB-I
7842	Ishitsuka	09/06-09/24	*10.8,01.3	359	2	7.269	0.052	0.55	0.07	MB-I
8556	Jana	09/29-10/31	*13.0,09.1	25	-8	35.496	0.031	0.38	0.04	MB-O
11564	1993 FU41	08/28-10/21	*04.2,10.5	11	-1	6.987	0.033	0.13	0.05	Levin
16009	1999 CM8	09/25-10/14	*08.4,08.7	9	-11	16.698	0.024	0.60	0.03	Maria
35539	1998 FJ91	08/22-09/21	*04.5,15.0	333	-8	7.313	0.025	0.39	0.04	MB-O
65127	2002 CG63	08/25-09/02	11.2,08.0	340	-10	10.426	0.028	0.33	0.04	MB-M

Table I. Observing circumstances and results. The phase angle is given for the first and last date. If preceded by an asterisk, the phase angle reached an extremum during the period. L_{PAB} and B_{PAB} are the approximate phase angle bisector longitude/latitude at mid-date range (see Harris et al., 1984). Grp is the asteroid family/group (Warner et al., 2009). MB-O: main-belt outer; MB-I: main-belt inner; Pho: 25 Phocaea; Vesta: 4 Vesta; Eos: 221 Eos; Levin: 2076 Levin; Maria: 170 Maria; MB-M: main-belt middle.

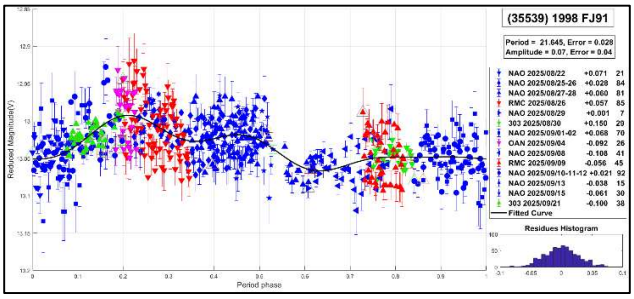

65127 2002 CG63 is a main-belt asteroid with an estimated diameter of 8.813 km. It was discovered in 2002 by LINEAR. We couldn't find a reported period for this object in the literature. We propose a period of P = 10.426 ± 0.028 h with Δm = 0.33 ± 0.04 mag.

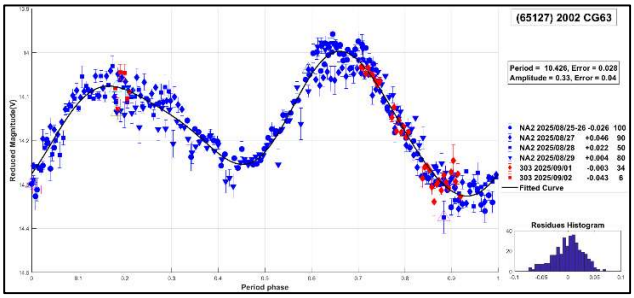

Acknowledgements

We want to thank Julio Castellano as we used his *FotoDif* program for preliminary analyses, Fernando Mazzone for his *Periods* program, which was used in final analyses, and Matías Martini for his *CalculadorMDE_v0.2* used for generating ephemerides used in the planning stage of the observations. We also used *Seqplot* (*https://www.aavso.org/seqplot*), which proved very effective for checking the magnitudes of the calibration stars. This research has made use of the Small Bodies Data Ferret (*https://sbnapps.psi.edu/ferret/*), supported by the NASA Planetary System. This research has made use of data and/or services provided by the International Astronomical Union's Minor Planet Center.

References

Behrend, R. (2010web, 2021web). Observatoire de Geneve web site. *http://obswww.unige.ch/~behrend/page_cou.html*

Binzel, R.P. (1987). "A photoelectric survey of 130 asteroids." *Icarus* **72**, 135-208.

Ďurech, J.; Hanuš, J.; Oszkiewicz, D.; Vančo, R. (2016). "Asteroid models from the Lowell photometric database." *Astronomy & Astrophysics* ***587***, A48.

Farfan, R.G., García de la Cuesta, F., Delgado Casal, J., Reina Lorenz, E., Ruiz Fernández, J., De Elías Cantalapiedra, J.; Naves Nogues, R.; Fernández Andújar, J.M.; González Carballo, J.-L.; Fernández Mañanes, E.; Martínez Morales, R. (2022). "Periods Determinations for Seventeen Asteroids." *Minor Planet Bulletin* **49**, 229-233.

Harris, A.W.; Young, J.W.; Scaltriti, F.; Zappala, V. (1984). "Lightcurves and phase relations of the asteroids 82 Alkmene and 444 Gyptis." *Icarus* **57**, 251-258.

Hasselmann, P.H.; Carvano, J.M.; Lazzaro, D. (2012). "SDSS-based Asteroid Taxonomy V1.1. EAR-A-I0035-5-SDSSTAX-V1.1." NASA Planetary Data System.

Mazzone, F.D. (2012). *Periodos* sotware, version 1.0. *http://www.astrosurf.com/salvador/Programas.html*

Nesvorny, D.; Broz, M.; Carruba, V. (2015). "Identification and dynamical properties of asteroid families." *arXiv*:1502.01628.

Warner, B.D.; Harris, A.W.; Pravec, P. (2009). "The Asteroid Lightcurve Database." *Icarus* **202**, 134-146. *https://minplanobs.org/mpinfo/php/lcdb.php*

Waszczak, A.; Chang, C.-K.; Ofek, E.O.; Laher, R.; Masci, F.; Levitan, D.; Surace, J.; Cheng, Y.-C.; Ip, W.-H.; Kinoshita, D.; Helou, G.; Prince, T.A.; Kulkarni, S. (2015). "Asteroid Light Curves from the Palomar Transient Factory Survey: Rotation Periods and Phase Functions from Sparse Photometry." *Astron. J.* **150**, A75.

Yeh, T.-S.; Li, B.; Chang, C.-K.; Zhao, H.-B.; Ji, J.-H.; Lin, Z.-Yi.; Ip, W.-H. (2020). "The Asteroid Rotation Period Survey Using the China Near-Earth Object Survey Telescope (CNEOST)." *Astron J.* **160**, 73.

Observatory	Telescope	Camera
303 Obs.Astr.Nacional Llano del Hato	Newtonian (D=1000mm; f=5.5)	CCD FLI PL4240
821 Est.Astrof.Bosque Alegre	Newtonian (D=1540mm; f=4.9)	CCD APOGEE Alta U9
D42 OsservatorioAstronomico Piero Angela	SCT (D=300mm; f=6.2)	CMOS ToupTek 2600 KMA
G05 Obs.Astr.Giordano Bruno	SCT (D=203mm; f=6.3)	CCD Atik 420 m
K14 Obs.Astr.de Sencelles	Newtonian (D=250mm; f=4.0)	CCD SBIG ST-7XME
M19 Osservatorio Explorer	RCT (D=304 mm; f=6,5)	CCD Moravian G2 4000
X41 ObservatorioProtón-Protón	Newtonian (D=250mm; f=5.0)	CMOS ZWO ASI120MINI MM
Z03 Obs.Astr.RíoCofio	SCT (D=254mm; f=6.3)	CCD SBIG ST-8XME
Z65 Obs.Astr.Corgas	Newtonian (D=310mm; f=4.8)	CMOS ZWO ASI 294 MM
DEO Dark Energy Observatory	Refractor (D=115mm; f=7.0)	CMOS QHY 294M pro
DE2 Dark Energy Observatory 2	RCT (D=200mm; f=5.4)	CMOS Player One Ares-M
NAO Obs.Astr.Naos	Newtonian (D=250mm; f=4.0)	CMOS ZWO 183
NA2 Obs.Astr.Naos 2	Newtonian (D=200mm; f=5.0)	CMOS ZWO ASI 174
NA3 Obs.Astr.Naos 3	SCT (D=279; f=10)	CMOS QHY 163M
NA4 Obs.Astr.Naos 4	Newtonian (D=200mm; f=5.0)	CMOS ZWO ASI 174
OAN Obs.Astr.Nacional Llano del Hato	Cámara Schmidt (D=1000mm; f=3.0)	CMOS Fujifilm GFX 50R
OC2 Obs.Astr.de Carlos Ambrosioni	SCT (D=150mm; f=6.7)	CCD FLI 8300
OC3 Obs.Astr.de Carlos Ambrosioni	SCT (D=279mm; f=7)	CCD SBIG ST8XME
OM2 Obs.Astr.Vueltaporel Universo 2	Newtonian (D=200mm; f=5.0)	CMOS POA Neptune-M
RMC Obs.Astr.de Raúl Melia Carlos Paz	Newtonian (D=254mm; f=4.7)	CMOS QHY 174M

Table II. List of observatories and equipment.

A POTENTIAL NEW SATELLITE OF (165991) 2001 YL149 DETECTED BY STELLAR OCCULTATION

Victor Bao
Royal Astronomical Society of New Zealand (RASNZ)
victor.bao@rasnz.org.nz

David Gault
Trans-Tasman Occultation Alliance (TTOA)

(Received: 2026 January 15 Revised: 2026 February 14)

We report on observations of (165991) 2001 YL149 occulting TYC 6883-00373-1, a magnitude 10.8 star, on 2025 November 1.351 from a site in New Zealand. The minor planet was ten magnitudes fainter than the star. Bao recorded two consecutive occultations of 180 milliseconds and 40 milliseconds duration. The first drop was more than 2.6 magnitudes followed by a second one-point drop of approximately 1.8 magnitudes. A double star explanation is excluded due to the depth of both occultations. Fresnel analysis is consistent with a satellite explanation; however, the strength of a one-point observation is insufficient to claim satellite discovery. We suggest that anomalies in future rotational light curve observations might provide further evidence for the presence of a satellite.

V. Bao observed asteroid (165991) 2001 YL149 occult TYC 6883-00373-1, a magnitude 10.8 star, from Auckland, New Zealand with a 28-cm Schmidt-Cassegrain telescope equipped with a Complementary Metal-Oxide-Semiconductor (CMOS) astronomy camera, model Player One Ceres 462M. A video recording was made with a time resolution of 40 ms per frame. Video timestamps were accurate to a resolution of 1 ms by synchronizing the computer clock to a GPS 1PPS receiver serial device. Two consecutive photometric events were recorded; an initial occultation drop lasting 180 milliseconds, followed 540 milliseconds later by a single-frame drop of 40 milliseconds. The magnitude drop of the initial occultation was deeper than a comparison star of magnitude 13.6.

For the secondary event, the original recording provided no suitable comparison stars, and recordings with a larger field of view were conducted on a subsequent night with the same equipment and similar air-mass as the occultation. A drop of 1.8 magnitudes was estimated. The combined magnitude drop from both events is too large for a double star explanation where two drops of 0.8 magnitudes each or one drop over 0.8 and one drop under 0.8 magnitudes would be expected.

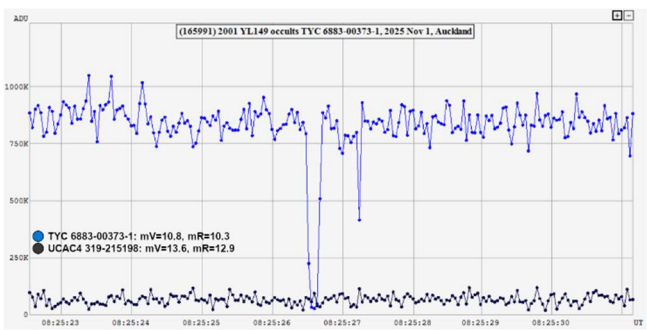

Figure 1. Lightcurve by V. Bao, displaying two occultation events.

Reduction of the Observations

Event times and observation circumstances were entered into *Occult 4* software (D. Herald) and the sky-plane plots are shown in Figure 2. A Fresnel diffraction analysis tool (R. Anderson) was used to extrapolate the magnitude drop of the secondary event to the size of a potential satellite.

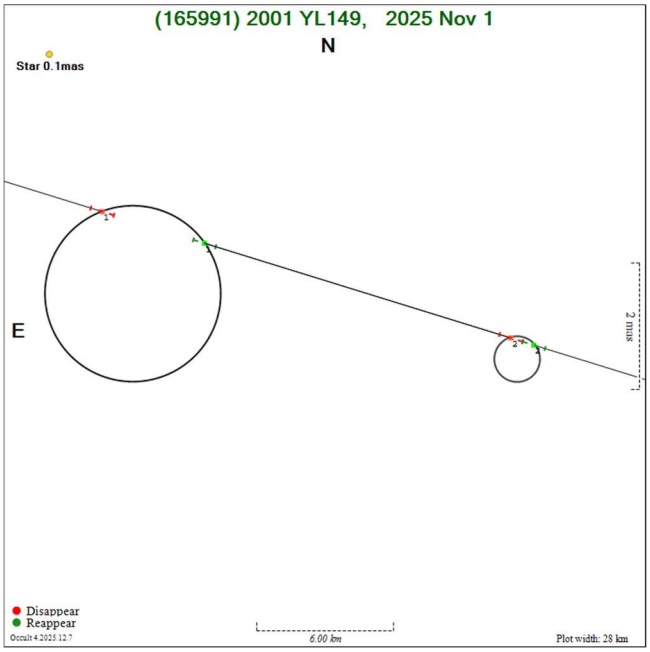

Figure 2. Reduction sky-plane plot, displaying the asteroid and potential satellite.

Main body	7.7 ± 0.8 km (NEOWISE)
Satellite	2.0 ± 2.0km

These diameters were then used to derive a separation of 6.25 ± 0.05 mas and a position angle of 263.0 ± 2.6° or 242.8 ± 2.8°, from the four possible solutions. However, the strength of a one-point observation is insufficient to claim discovery of a satellite.

We are not aware of any rotational lightcurve measurements of this asteroid. We seek those acquainted with rotational lightcurve analysis to check for anomalies in the data for (165991) 2001 YL149 which could be explained by the presence of a satellite.

Acknowledgements

This research used *Occult 4* software, developed by Dave Herald. This research used *Occult Watcher* software for prediction feeds and details, and *TANGRA* for lightcurve reductions, developed by Hristo Pavolv. This research used a Fresnel diffraction analysis tool, developed by Robert Anderson.

LIGHTCURVE ANALYSIS FOR THREE NEAR-EARTH ASTEROIDS OBSERVED BETWEEN OCTOBER AND DECEMBER 2025

Peter Birtwhistle
Great Shefford Observatory
Phlox Cottage, Wantage Road
Great Shefford, Berkshire, RG17 7DA
UNITED KINGDOM
peter@birtwhistle.org.uk

(Received: 2026 January 7)

Lightcurves and amplitudes for three near-Earth asteroids observed from Great Shefford Observatory during close approaches between October and December 2025 are reported. All are small objects (~30 meters or less) with rotation periods significantly shorter than the spin barrier at ~2.2 h. One is identified as having tumbling rotation.

Photometric observations of near-Earth asteroids during close approaches to Earth between October and December 2025 were made at Great Shefford Observatory using a 0.40-m Schmidt-Cassegrain and Apogee Alta U47+ CCD camera. All observations were made unfiltered and with the telescope operating with a focal reducer at f/6. The 1K×1K, 13-micron CCD was binned 2×2 resulting in an image scale of 2.16 arcsec/pix. All the images were calibrated with dark and flat frames and *Astrometrica* (Raab, 2025) was used to measure photometry using G band data from the Gaia DR3 catalogue. *MPO Canopus* (Warner, 2023), incorporating the Fourier algorithm developed by Harris (Harris et al., 1989) was used for lightcurve analysis.

No previously reported results have been found in the Asteroid Lightcurve Database (LCDB) (Warner et al., 2009), from searches via the Astrophysics Data System (ADS, 2025) or from wider searches unless otherwise noted. All size estimates are calculated using H values from the Small-Body Database Lookup (JPL, 2025), using an assumed albedo for NEAs of 0.2 (LCDB readme.pdf file) and are therefore uncertain and offered for relative comparison only.

2025 UT6. The Catalina Sky Survey discovered this Apollo (H = 24.8, D ~32 m) on 2025 Oct 25.36 UTC, 26 hours after it passed Earth at 3 Lunar Distances (LD) (Galli et al., 2025). It was observed for 2.0 h starting at 2025 Oct 26.03 UTC and large variations in brightness were obvious between consecutive exposures taken with a cadence of 10 s.

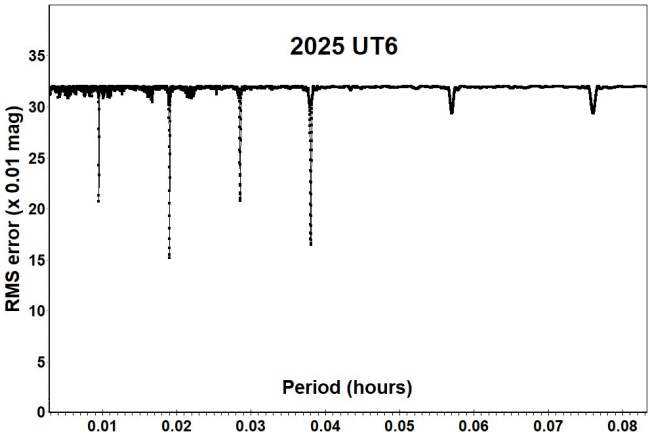

The linearly scaled period spectrum spanning 10 s - 5 min indicates a best-fit period of 0.019025 ± 0.000002 h (~68 s) and that period results in a bimodal, asymmetric phased lightcurve. All other significant minima in the period spectrum are related harmonics, being integer multiples of half the bimodal period. 2025 UT6 completed 105 rotations while under observation.

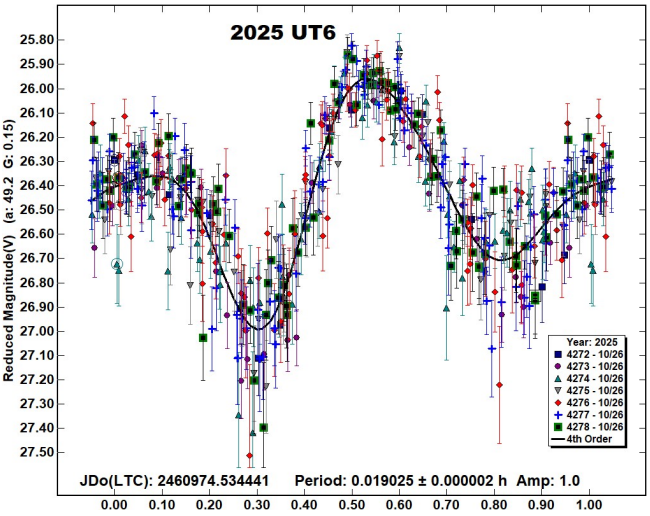

2025 WA. This Apollo (H = 24.9, D ~31 m) was discovered by the ATLAS-HKO, Haleakala station on 2025 Nov 16.3 UTC (Hoegner et al., 2025) and made an approach to within 8 LD of Earth on 2025 Nov 21.5 UTC. Photometry was collected over the nights of 2025 Nov 18, 19 and 20 for 3.0, 5.0 and 3.1 h respectively and independent analysis of all three nights indicated very similar best-fit periods of 0.0340 h (~2.0 min). The 4th order period spectrum combines the data from all three nights, covering periods from 45 s to 10 min.

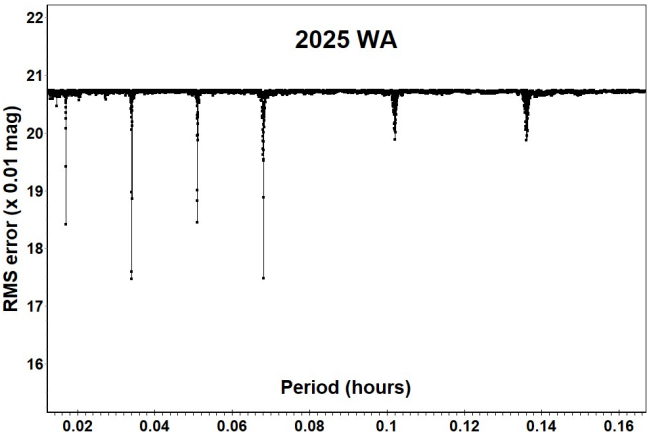

Phased lightcurves are provided for the three nights, each aligned so that the maximum of each curve is at phase = 0. As the phase angle decreased over the three nights from 24° to 16° and then to 9°, as expected, the amplitude reduced, from 0.5 to 0.4 and then to 0.3 mags.

It is noted that there are seven distinct clusters of points evident in the Nov 19 light curve. This pattern arises as a consequence of 9 of the 12 observing sessions used 16 s exposures with an average cadence of 17.6 s, within 1% of one-seventh of the 122.5 s rotation period. In 7 of those 9 sessions, the gap between consecutive sessions was also close to an integer multiple of the cadence. As a

result, 68% of the data points from that night fall into seven discrete regions of the phased light curve. By contrast, the proportion of images taken at that cadence on the other two nights was much smaller, so little or no clustering is visible in those light curves.

During the sessions on Nov 18, 19 and 20, 2025 WA completed 87, 148 and 89 rotations respectively.

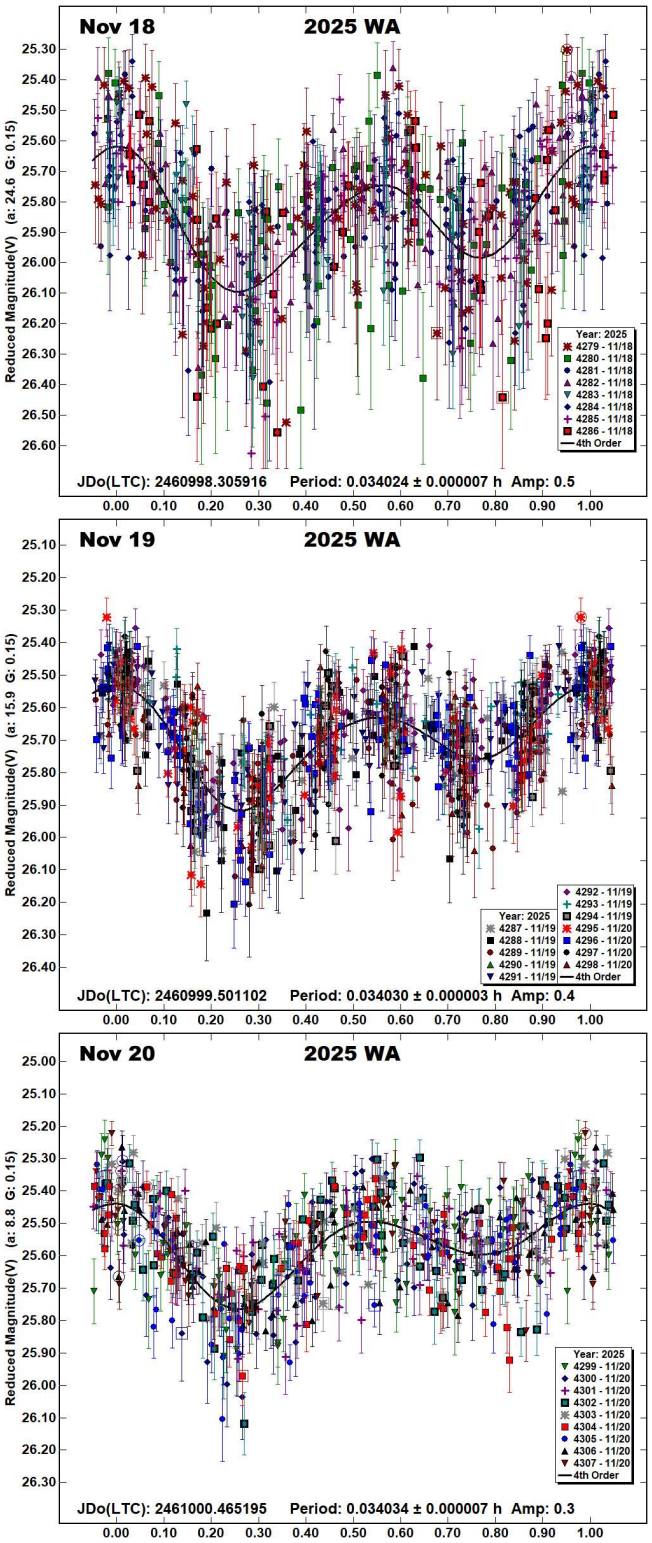

2025 XF1. This was another ATLAS-HKO, Haleakala discovery of an Apollo (H = 28.0, D ~7 m), made on 2025 Dec 8.2 UTC (Hogan et al., 2025). It approached Earth to 0.8 LD on 2025 Dec 13.0 UTC and during its final approach photometry was obtained starting on 2025 Dec 12.75 UTC for 1 h, then after a gap of 1.9 h, for a further 2.4 h. Exposures were limited by the fast apparent motion to 3.6 - 4.7 s and a linearly plotted period spectrum covering periods from 10 s to 75 s reveals two sets of equally spaced minima, the stronger in multiples of 0.0036 h (~12.9 s) and the other at multiples of 0.0048 h (~17.1 s), these two sets being indicative of very fast non-principal axis rotation (NPAR), or tumbling.

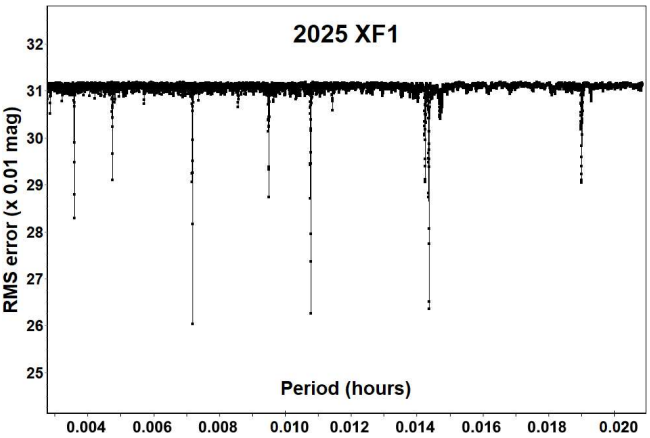

Further analysis with the Dual Period Search function of *MPO Canopus* located the best-fit NPAR periods as:

P1 = 0.0071866 ± 0.0000001 h (~25.9 s)
P2 = 0.0095075 ± 0.0000002 h (~34.2 s)

Lightcurves for these are given, labelled P1 and P2. 2025 XF1 faded by approximately 0.16 mag more than predicted by an ephemeris computed using a value of (G = 0.15) in the H/G system. This systematic trend was removed by applying small zero-point adjustments to each of the 35 observing sessions. The adjustments had an RMS of 0.07 mag and were chosen to minimise the overall scatter in the light curve. The excess fading may be due to changing observing conditions or an incorrect assumed value of (G); however, these zero-point adjustments do not materially affect the determination of the NPAR solution. The strongest minimum in the period spectrum, aside from those at integer multiples of P1/2 and P2/2, occurs at P3 = 0.0147 h; however, the corresponding frequency of P3 is simply a linear combination of the frequencies of P1 and P2, where:

$$2/P1 - 2/P2 = 1/P3$$

and P3 is therefore likely to be just an alias of the stronger P1 and P2 periods.

It is expected that 2025 XF1 may be assigned a rating of PAR = -3 (NPA rotation reliably detected with the two periods resolved) on the PAR scale defined in Pravec et al. (2005). The NPAR solution indicates the full amplitude of the tumbling rotation is 1.0 mag and during the 5.3 h that 2025 XF1 was under observation it completed 736 rotations of the P1 period and 556 of the P2 period.

Number	Name	Integration times	Max intg/Pd	Min a/b	Pts	Flds
	2025 UT6	7.7-11	0.161	1.5[1]	436	7
	2025 WA	12-18	0.147	1.3[2]	1806	29
	2025 XF1	3.6-4.7	0.182[3]	1.4[1]	1083	35

Table I. Ancillary information, listing the integration times used (seconds), the fraction of the period represented by the longest integration time (Pravec et al., 2000), the calculated minimum elongation of the asteroid (Zappala et al., 1990), the number of data points used in the analysis and the number of times the telescope was repositioned to different fields. Note: 1 = Value uncertain, based on phase angle > 40°, 2 = Value calculated for 2025 Nov 20 when phase angle was at a minimum, 3 = Calculated using the shorter of the NPAR periods.

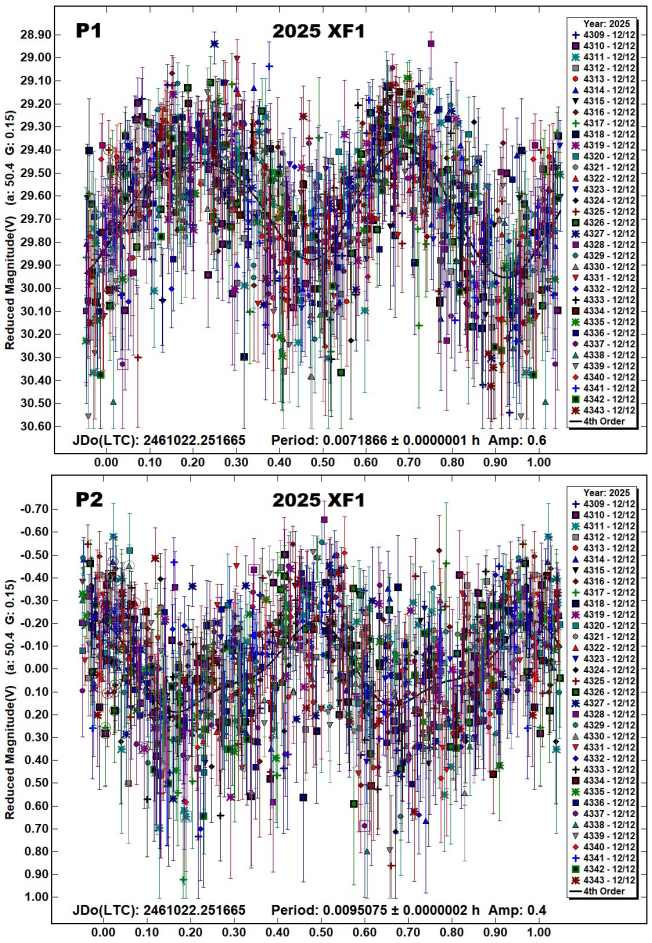

Acknowledgements

The author wishes to thank Petr Pravec, Astronomical Institute, Czech Republic for his review of the solution for tumbler 2025 XF1. The author also gratefully acknowledges a Gene Shoemaker NEO Grant from the Planetary Society (2005) and a Ridley Grant from the British Astronomical Association (2005), both of which facilitated upgrades to observatory equipment used in this study.

This work has made use of data from the European Space Agency (ESA) mission Gaia (*https://www.cosmos.esa.int/gaia*), processed by the Gaia Data Processing and Analysis Consortium (DPAC, *https://www.cosmos.esa.int/web/gaia/dpac/consortium*). Funding for the DPAC has been provided by national institutions, in particular the institutions participating in the Gaia Multilateral Agreement.

References

ADS (2025). Astrophysics Data System. *https://ui.adsabs.harvard.edu/*

Galli, G.; Fumagalli, A.; Testa, A.; Fuls, D.C.; Beuden, T.; Carvajal, V.F.; Fay, D.; Fazekas, J.B.; Gibbs, A.R.; Grauer, A.D.; Groeller, H.; Hogan, J.K.; Kowalski, R.A.; Larson, S.M.; Leonard, G.J. and 32 colleagues (2025). "2025 UT6" MPEC 2025-U224. *https://www.minorplanetcenter.net/mpec/K25/K25UM4.html*

Harris, A.W.; Young, J.W.; Scaltriti, F.; Zappala, V. (1984). "Lightcurves and phase relations of the asteroids 82 Alkmene and 444 Gyptis." *Icarus* **57**, 251-258.

Harris, A.W.; Young, J.W.; Bowell, E.; Martin, L.J.; Millis, R.L.; Poutanen, M.; Scaltriti, F.; Zappala, V.; Schober, H.J.; Debehogne, H.; Zeigler, K. (1989). "Photoelectric Observations of Asteroids 3, 24, 60, 261, and 863." *Icarus* **77**, 171-186.

Hoegner, C.; Ludwig, F.; Hartmann, M.; Stecklum, B.; Gilmore, A.C.; Kilmartin, P.M.; Ikari, Y.; Dupouy, P.; Diepvens, A.; Ivanov, A.; Barcov, A.; Ivanov, V.; Lysenko, V.; Yakovenko, N.; Ivanova, N. and 19 colleagues (2025). "2025 WA" MPEC 2025-W20. *https://www.minorplanetcenter.net/mpec/K25/K25W20.html*

Hogan, J.K.; Carvajal, V.F.; Fay, D.; Fazekas, J.B.; Fuls, D.C.; Gibbs, A.R.; Grauer, A.D.; Groeller, H.; Kowalski, R.A.; Larson, S.M.; Leonard, G.J.; Loewen, C.J.; Rankin, D.; Seaman, R.L.; Shelly, F.C. and 12 colleagues (2025). "2025 XF1" MPEC 2025-X88. *https://www.minorplanetcenter.net/mpec/K25/K25X88.html*

JPL (2025). Small-Body Database Lookup. *https://ssd.jpl.nasa.gov/tools/sbdb_lookup.html*

Number	Name	yyyy mm/dd	Phase	L_{PAB}	B_{PAB}	Period(h)	P.E.	Amp	A.E	PAR	H
	2025 UT6	2025 10/26-10/26	49.2,48.0	48	20	0.019025	0.000002	1.0	0.2		24.8
	2025 WA	2025 11/18-11/18	24.7,23.8	44	2	0.034024	0.000007	0.5	0.3		24.9
		2025 11/19-11/20	16.0,14.3	50	-1	0.034030	0.000003	0.4	0.2		
		2025 11/20-11/20	*8.9, 8.6	56	-3	0.034034	0.000007	0.3	0.2		
	2025 XF1	2025 12/12-12/12	50.1,56.8	65	22	0.0071866	0.0000001	0.6	0.3	-3	28.0
						0.0095075	0.0000002	0.4	0.3		

Table II. Observing circumstances and results. The phase angle is given for the first and last date. If preceded by an asterisk, the phase angle reached an extrema during the period. L_{PAB} and B_{PAB} are the approximate phase angle bisector longitude/latitude at mid-date range (see Harris et al., 1984). Amplitude error (A.E.) is calculated as √2 × (lightcurve RMS residual). PAR is the expected Principal Axis Rotation quality detection code (Pravec et al., 2005) and H is the absolute magnitude at 1 au from Sun and Earth taken from the Small-Body Database Lookup (JPL, 2025).

Pravec, P.; Hergenrother, C.; Whiteley, R.; Sarounova, L.; Kusnirak, P.; Wolf, M. (2000). "Fast Rotating Asteroids 1999 TY2, 1999 SF10, and 1998 WB2" *Icarus* **147**, 477-486.

Pravec, P.; Harris, A.W.; Scheirich, P.; Kušnirák, P.; Šarounová, L.; Hergenrother, C.W.; Mottola, S.; Hicks, M.D.; Masi, G.; Krugly, Yu.N.; Shevchenko, V.G.; Nolan, M.C.; Howell, E.S.; Kaasalainen, M.; Galád, A. and 5 colleagues. (2005). "Tumbling Asteroids." *Icarus* **173**, 108-131.

Raab, H. (2025). *Astrometrica* software, version 4.16.4.468. *http://www.astrometrica.at/*

Warner, B.D.; Harris, A.W.; Pravec, P. (2009). "The Asteroid Lightcurve Database." *Icarus* **202**, 134-146. Updated 2023 Oct. *https://www.minorplanet.info/php/lcdb.php*

Warner, B.D. (2023). *MPO Software*, Canopus version 10.8.6.20, Bdw Publishing, Colorado Springs, CO. *https://minplanobs.org/BdwPub/*

Zappala, V.; Cellini, A.; Barucci, A.M.; Fulchignoni, M.; Lupishko, D.E. (1990). "An analysis of the amplitude-phase relationship among asteroids" *Astron. Astrophys*. **231**, 548-560.

IN THIS ISSUE

This list gives those asteroids in this issue for which physical observations (excluding astrometric only) were made. This includes lightcurves, color index, and H-G determinations, etc. In some cases, no specific results are reported due to a lack of or poor-quality data. The page number is for the first page of the paper mentioning the asteroid. EP is the "go to page" value in the electronic version.

THE MINOR PLANET BULLETIN (ISSN 1052-8091) is the quarterly journal of the Minor Planets Section of the Association of Lunar and Planetary Observers (ALPO, http://www.alpo-astronomy.org). Current and most recent issues of the *MPB* are available on line, free of charge from:

https://mpbulletin.org/

The Minor Planets Section is directed by its Coordinator, Prof. Frederick Pilcher, 4438 Organ Mesa Loop, Las Cruces, NM 88011 USA (fpilcher35@gmail.com). Robert Stephens (rstephens@foxandstephens.com) serves as Associate Coordinator. Dr. Alan W. Harris (MoreData! Inc.; harrisaw@colorado.edu), and Dr. Petr Pravec (Ondrejov Observatory; ppravec@asu.cas.cz) serve as Scientific Advisors. The Asteroid Photometry Coordinator is Brian D. Warner (Center for Solar System Studies), Palmer Divide Observatory, 446 Sycamore Ave., Eaton, CO 80615 USA (brian@MinorPlanetObserver.com).

The Minor Planet Bulletin is edited by Professor Richard P. Binzel, MIT 54-410, 77 Massachusetts Ave, Cambridge, MA 02139 USA (rpb@mit.edu). Brian D. Warner (address above) is Associate Editor. Assistant Editors are Dr. David Polishook, Department of Earth and Planetary Sciences, Weizmann Institute of Science (david.polishook@weizmann.ac.il) and Dr. Melissa Hayes-Gehrke, Department of Astronomy, University of Maryland (mhayesge@umd.edu). The *MPB* is produced by Dr. Pedro A. Valdés Sada (psada2@ix.netcom.com).

Effective with Volume 50, the *Minor Planet Bulletin* is an electronic-only journal; print subscriptions are no longer available. In addition to the free electronic download of the *MPB* as noted above, electronic retrieval of all *Minor Planet Bulletin* articles (back to Volume 1, Issue Number 1) is available through the Astrophysical Data System:

http://www.adsabs.harvard.edu/

Authors should submit their manuscripts by electronic mail (rpb@mit.edu). Author instructions and a Microsoft Word template document are available at the web page given above. All materials must arrive by the deadline for each issue. Visual photometry observations, positional observations, any type of observation not covered above, and general information requests should be sent to the Coordinator.

* * * * *

The deadline for the next issue (53-3) is April 15, 2026. The deadline for issue 53-4 is July 15, 2026.